

International  
Progress Report

**IPR-00-26**

# Äspö Hard Rock Laboratory

## TRUE Block Scale Project

Final report of the detailed  
characterisation stage

Compilation of premisses and  
outline of programme for tracer  
tests in the block scale

Anders Winberg

Conterra AB

February 2000

***Svensk Kärnbränslehantering AB***

Swedish Nuclear Fuel  
and Waste Management Co  
Box 5864  
SE-102 40 Stockholm Sweden  
Tel 08-459 84 00  
+46 8 459 84 00  
Fax 08-661 57 19  
+46 8 661 57 19



**Äspö Hard Rock  
Laboratory**

Report no.	No.
IPR-00-26	F56K
Author	Date
Anders Winberg (ed)	2000-11-15
Checked by	Date
Approved	Date
Olle Olsson	2000-11-22

# Äspö Hard Rock Laboratory

## TRUE Block Scale Project

### Final report of the detailed characterisation stage

### Compilation of premises and outline of programme for tracer tests in the block scale

Anders Winberg (editor)

Conterra AB

February 2000

*Keywords:* block scale, tracer test, hypotheses, retention

This report concerns a study which was conducted for SKB. The conclusions and viewpoints presented in the report are those of the author(s) and do not necessarily coincide with those of the client.

## Foreword

The present report presents the basic results of the Detailed Characterisation Stage characterisation and modelling relevant to planning of block scale tracer tests. Through the definition of issues and hypotheses, design calculations, tentative plans for the Tracer Test Stage are defined.

Important contributions to this report have been provided by;

### **Chapters 1 through 3**

Thomas Doe, Golder Associates

### **Chapter 4**

Peter Andersson, Magnus Holmqvist, Eva Wass, GEOSIGMA

David Holton, AEA Technology

Jan Hermanson, Golder Grundteknik

Thomas Fierz, Solexperts

### **Chapter 5**

Peter Andersson, Eva Wass, Magnus Holmqvist, GEOSIGMA

### **Chapter 6**

Thomas Doe, Aaron Fox, Bill Dershowitz, Thorsten Eiben, Golder Associates

Shinji Takeuchi and Masahiro Uchida, JNC

### **Chapter 7**

Thomas Doe, Golder Associates

Peter Andersson, GEOSIGMA

Jan Hermanson, Golder Grundteknik

### **Chapter 9**

Peter Meier, ANDRA

On the basis of the outcome of the 3<sup>rd</sup> TRUE Block Scale Review Meeting held October 27, 1999, and subsequent discussions, the report has been updated and revised, mainly focused on Chapters 3 and 6.

## **Abstract**

This report presents basic results from the Detailed Characterisation Stage and preliminary plans for the Tracer Test Stage (TTS) of the TRUE Block Scale Project. Premises for the planned tracer tests are presented in terms of formulated hypotheses for the experimental work. In addition a structural model (March'99) substantiated by reconciliation using hydraulic data is presented. Target structures and pathways are visualised and tabulated. The results of the performed tracer pre-tests, the reconciled March'99 structural model and design calculations form the basis for defining the tracer test programme. The results provide arguments for recommending drilling of an additional borehole, and for complementary optimisation of the borehole array.

## **Sammanfattning**

Denna rapport redovisar grundläggande resultat från "Detailed Characterisation Stage" och preliminära planer för "Tracer Test Stage" (TTS) inom ramen för TRUE Block Scale projektet. Förutsättningar för planerade spår försök redovisas, liksom de hypoteser som kommer att ligga till grund för det experimentella arbetet. Vidare redovisas den strukturmodell (Marrs'99) som dessutom understöds av tillgänglig hydrauliska data. Strukturer och flödesvägar som avses att utnyttjas i kommande spår försök redovisas grafiskt och i tabellform. Resultatet från utförda för-försök, den redovisade strukturmodellen, samt utförda designberäkningar utgör plattformen för att definiera det kommande spår försöksprogrammet i blockskala. Resultatet ger argument för att rekommendera borring av ytterligare borrhål och för ytterligare optimering av manschettsystem i existerande borrhål

# Contents

<b>1</b>	<b>Background</b>	<b>1</b>
1.1	General	1
1.2	Organisation of report	1
1.2	Well identified conductors (Type 1)	2
1.3	Less well identified conductors (Type 2)	3
1.4	Identification of suitable conducting networks	3
<b>2.</b>	<b>Practical considerations for performing tracer tests in fracture networks</b>	<b>5</b>
2.1	Effects of background flow	6
2.2	Effects of diffusion in stagnant zones	6
2.3	Effects of pathway complexity	6
2.4	Effects of retention processes	7
<b>3.</b>	<b>Hypotheses</b>	<b>8</b>
3.1	What are hypotheses and how can we test them?	8
3.1.1	Scientific approach	8
3.1.2	Steps in tracer test design	8
3.1.3	Questions, hypotheses, and design tasks	9
3.2	What is the conductive geometry of the TRUE Block Scale volume?	10
3.2.1	Basic question Q1	10
3.3.2	Hypothesis H1	11
3.3.3	Design tasks for Hypothesis H1	12
3.4	What are the properties of the conducting network that affect transport?	12
3.4.1	Basic question Q2	12
3.4.2	Hypothesis H2a – Flow and transport controlled by fracture intersections	13
3.4.3	Hypothesis H2b – Flow and transport controlled by in-plane heterogeneity	14
3.4.4	Design tasks for Hypotheses H2	15
3.5	Which retention processes are important in a network at a block scale?	16
3.5.1	Basic question Q3	16
3.5.3	Hypothesis H3	16
3.5.3	Design tasks for Hypothesis H3	17

<b>4.</b>	<b>Premises for Pre-tests</b>	<b>18</b>
4.1	March'99 structural model	18
4.2	Optimisation of multi-packer array	21
4.3	Catalogue of transport pathways	22
4.4	MAUA analysis of defined pathways	24
4.5	Visualisation of pathways	24
4.6	Development of conservative tracers	28
<b>5.</b>	<b>Pre-tests</b>	<b>33</b>
5.1	Background and objectives	33
5.2	Performance and preliminary results	34
5.2.1	Pressure response matrix	34
5.2.2	Pre-test #1 (PT-1)	36
5.2.3	Pre-Test #2 (PT-2)	38
5.2.4	Pre-test #3 (PT-3)	40
5.2.5	Pre-PT-4 tests	42
5.2.6	Pre-test #4 (PT-4)	44
5.3	Conclusions regarding tracer test array	47
5.3.1	Re-mediation of KI0023B	47
5.3.2	Suggestions for optimisation of the borehole array	48
5.3.3	Need for a new borehole	49
<b>6.</b>	<b>Experimental design and predictions</b>	<b>50</b>
6.1	Background and scope	50
6.2	Study of fracture intersection effects	50
6.2.1	General	50
6.2.2	Generic FIZ study	51
6.2.3	Site-specific FIZ study on Structure #20	55
6.2.3	Site-specific model with sorbing tracers	61
6.2.4	Conclusions	66
6.3	Prediction of pre-tests	67
6.3.1	Model premises and parameters	67
6.3.2	Results of analysis of PT-1 through PT-3	71
6.3.3	Results of PT-4 predictions	72
6.3.4	Conclusions	73

<b>7.</b>	<b>Hydraulic reconciliation of March'99 model</b>	<b>75</b>
7.1	Background	75
7.2	Procedure and results	75
7.3	Conclusions	81
<b>8.</b>	<b>Premises for tracer tests</b>	<b>83</b>
8.1	General	83
8.2	Validity of March'99 Structural model	83
8.3	Feasibility of block scale tracer tests	83
8.4	Feasibility to distinguish intersection effects	84
8.5	Assessment of experimental array	85
8.6	Risks associated with attempted KI0023B salvage	86
<b>9.</b>	<b>Tracer tests</b>	<b>88</b>
9.1	Objectives	88
1)	To assess and quantify the parameters which control radionuclide retention in a fracture network in the block scale	88
9.2	Scope and components	89
9.2.1	Remediation and optimisation phase	89
9.2.2	Tracer tests - Phase A	90
9.2.3	Tracer tests - Phase B	90
9.2.3	Tracer tests - Phase C	91
9.2.4	Evaluation and reporting	91

9.3	Schedule	92
<b>10.</b>	<b>Conclusions</b>	<b>93</b>
10.1	Issues and Hypotheses	93
10.2	Structural-hydraulic model	93
10.2	Instrumented array	94
10.3	Tracer test results	94
10.4	Modelling	94
10.5	Outlook on Tracer Test Stage	95
	<b>REFERENCES</b>	<b>96</b>
	<b>APPENDICES</b>	<b>97</b>
	Appendix A Calculated shortest distances along multi-feature pathways, March '99 Structural Model	98
	Appendix B – Drawdown vs time divided by distance squared for the Pre-tests PT-1 through PT-3	103



# 1 Background

## 1.1 General

The TRUE Block Scale project is an international partnership funded by ANDRA, ENRESA, Nirex, POSIVA, PNC and SKB (Winberg, 1997). The Block Scale project is one part of the Tracer Retention Understanding Experiments (TRUE) conducted at the Äspö Hard Rock Laboratory. The Preliminary Characterisation Stage has been reported (Winberg, 1999). Presently, the third of the defined stages, the Detailed Characterisation Stage, has come to its conclusion. The next stage, the Tracer Test Stage constitutes the final part in the experimental work, where the results of the performed characterisation is used to perform a series of tracer tests on the block scale ( $L=10-50$  m). As a final step in the detailed characterisation a series of Pre-tests have been conducted with the aim of showing the feasibility of performing tracer tests in the block scale.

The present plan presents the latest structural model (March'99), an optimised borehole array for the pre-tests and formulates hypotheses which can be addressed by the planned experiments. The results of the pre-tests, the performed reconciliation of the March'99 structural model and performed design calculations form the basis for defining the actual tracer test programme. These results also form the arguments and recommendations for additional borehole optimisation and the need for an additional borehole.

## 1.2 Organisation of report

Chapter 1 presents our present view of the hydraulically conductive elements which make up the network proposed for future tracer tests. Chapter 2 considers some of the processes and conditions which may impact on the design and interpretation of tracer tests performed in a fracture network.

Chapter 3 presents the key issues identified and questions to be addressed in the planned tracer tests. Different answers to these questions are presented in the form of hypotheses, to be tested by the planned experiments.

Chapter 4 outlines the current understanding before performing the recently completed pre-tests. These include the March'99 update of the structural model. In addition, an account is given of the optimisation of the borehole array which was conducted early Spring 1999. A catalogue of pathways is expressed as a list of combinations of potential sink (abstraction) and source (injection) sections. This list is complemented by a

analysis and ranking of these pathways given available data. Example visualisations of fracture networks, intersection patterns and pathways are also given. Finally, preliminary results of the development of additional conservative tracers is presented, including a test of Helium gas (He-3) as a tracer.

Chapter 5 presents preliminary results of the performed Pre-tests which include 35 tracer dilution tests and 6 transport tests.

Chapter 6 presents preliminary results of a combined generic and site-specific modelling study of the possibility to distinguish the effects of fracture intersections from that of intra-structure heterogeneity. In addition, preliminary predictions of the PT-4 tracer tests (part of Pre-tests) are presented.

Chapter 7 presents a summary of the work performed to reconcile the March '99 structural model with available hydraulic and transport data, including results from the performed Pre-tests.

Chapter 8 condenses the major findings of the work done to support planning and design of the Tracer Test Stage. In addition recommendations are presented with regards to necessary remediation and optimisation work, including drilling of a new borehole.

Chapter 9 outlines the basic elements and components of the Tracer Test Stage, which is further detailed in the supporting Project Plan. This part of the report should be regarded as a dynamic part of the document which will be updated continuously during the upcoming Tracer Test Stage

Chapter 10, finally, provides a review of the main findings of the Detailed Characterisation Stage and summary conclusions.

## **1.2 Well identified conductors (Type 1)**

The characterisation program has identified several major geologic structures that cut across significant portions of the site. These structures have been assigned numbers for identification. For the most part the numbered structures are those, with a high level of confidence, which appear in at least three boreholes. A subset of these structures are hydraulically significant on the basis of pressure interference results during drilling and cross-hole pressure interference tests. These structures, #5, #6, #7, #20, #13, and #19, trend NW and have steep dips. Features in other orientations, both subvertical (eg. #8) and subhorizontal (eg. #18), appear in one or several holes but are not hydraulically conductive, at least not at their intersections in boreholes. Structures #1 through #5 are part of a wide, well connected system of conductors, with portions that required grouting during some of the drilling operations, and are therefore not useable for tracer experiments. Thus the major features that will be the focus of the testing programme will be Structures #13, #20, and #19, cf. Figure 1-1.

### **1.3 Less well identified conductors (Type 2)**

In addition to the major numbered Structures, the TRUE Block Scale volume contains additional geologic features and conductors. These have so far gone un-numbered because they are not sufficiently extensive to appear in more than one or two boreholes. Although the numbered features have been the main focus of testing to date, Type 2 features will be important in forming the networks for tracer testing in the block. In the most recent update of the TRUE Block Scale structural model, two Type 2 features, #21 and #22, have been identified, cf. Figure 1-1. These features will become better identified as the program focuses on a smaller part of the TRUE Block Scale volume.

### **1.4 Identification of suitable conducting networks**

The hydraulic and structural model of the TRUE block area provides a basis for designing the geometry of tests to study tracer transport and retention. The major objective of the TRUE Block Scale experiments is the study of the tracer retention in fracture networks. The tracer tests must therefore include pathways that pass through multiple fractures, or conducting features. In addition to these pathways, the tracer test programme should ideally include some pathways that are entirely within individual conducting features to provide a basis for distinguishing network behaviour from that of single features.

The tracer test designs will need to use both the well-characterised numbered structures of Type 1 and less characterised features of Type 2. The major candidate structures, #13, #19, and #20 are nearly parallel, hence it will be impossible to form a network with these conductive structures, cf. Figure 1-1. At one point in time Structure #9 was considered a potential feature that might provide a connection between the NW trending structures (Winberg, 1999). However, recent tests have confirmed that Structure #9 is not well defined and does not appear to be a conductor. Structure #19 is a well-defined conductive feature, but it appears to be relatively isolated in the upstream part of the investigated rock volume. Hence, the main focus of tracer test design has shifted to structures #13 and #20, which are 10-20 m apart and to the two Type 2 features, #21 and #22, which may provide hydraulic connections between the former two structures. Features #21 and #22 have been investigated during the performed Pre-tests and the subsequent hydraulic reconciliation study, cf. Chapters 5 and 7.

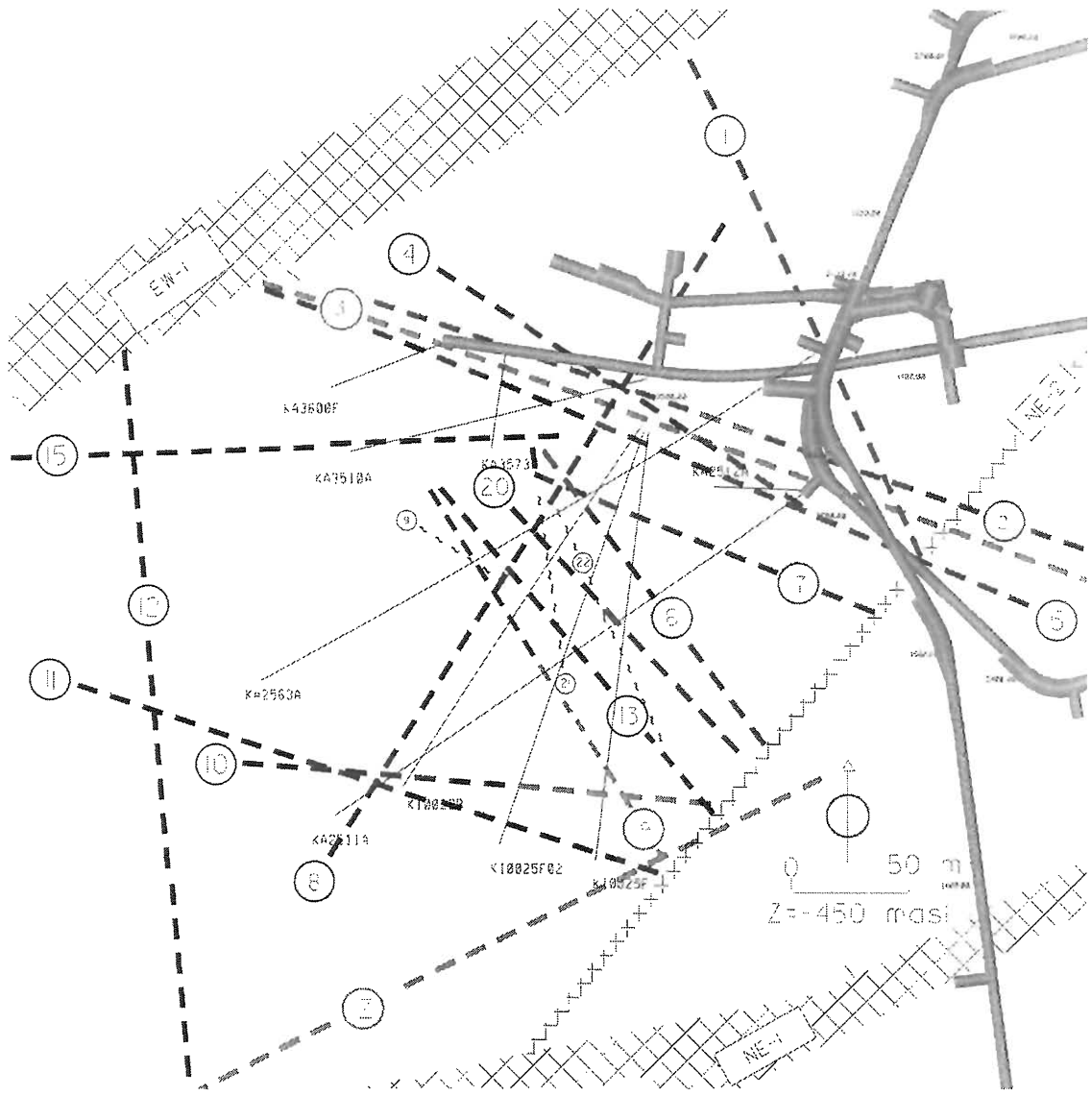


Figure 1-1 March 1999 structural model. Horizontal section at Z=-450 masl..

## **2. Practical considerations for performing tracer tests in fracture networks**

The poor recovery of many tracer tests in fractured rock is a fact. Most numerical models, on the other hand, predict complete recovery, whereas actual tracer tests generally fall short of that goal, or may show no recovery at all.

The poor recovery of tracers may reflect problems in the experiment design, lack of information about hydraulic geometry, or the effects of active fundamental transport processes. It is vital that we learn how to distinguish between these three factors. We wish to eliminate artefacts of the test design and ignorance regarding flow geometry as much as possible so we can concentrate on transport processes.

The question of poor recovery leads to several issues including:

- Tracer recovery is affected by background flow
- Tracer recovery may be affected by accidental injection into stagnant areas of the flow system
- Tracer recovery may reflect multiple complex pathways, such as:
  - Tracers following unexpected, and long pathways
  - Dilution due to intersections providing additional water sources along a tracer transport pathway, making it difficult to actually measure the tracer concentration.
- Tracer recovery may reflect strong matrix interaction effects.

Of these issues the background flow is mainly a design issue. Background flow should be known and understood and compensated for at the design stage - we should not use the tracer test to measure the background flow! The second and third issues are partly design and partly process issues. The complexity of pathways, including the existence of dead-end or stagnant portions of the networks, is important to know in order to completely understand the resulting pathways. However, we should have some idea whether we are likely to encounter simple, complicated, or multiple pathways before tests are run. The performed tracer dilution tests are important in this context.

It should be pointed out, however, that a low tracer recovery, or even the lack of recovery, given a satisfactory understanding of the hydraulic geometry and a good tracer test design, may from the perspective of performance assessment, paradoxically, be a beneficial finding. This conclusion obviously has to be stated in the context of the geological environment in which the test has been performed.

## **2.1 Effects of background flow**

Tracer recovery is significantly affected by background flow in a fracture network. Background flow should be understood before testing by a combination of model simulations and measurements, such as by tracer point dilution measurements. One means of assessing background flow as a factor is to vary pumping rate at the withdrawal section. Clearly recovery should improve with a stronger sink. Background flow will, in conjunction with the transmissivities of the sink and source sections, also affect reciprocity (the change in breakthrough when the source and receiver are reversed).

## **2.2 Effects of diffusion in stagnant zones**

Poor recovery may result when the tracer is accidentally introduced into a stagnant portion of the network, such as along a dead-end fracture. Such a stagnant area may have strong pressure responses to the pumping interval, but will not have a flow response due to the lack of connection to a source of water. The risk of encountering such a situation can be reduced by performing a tracer dilution test prior to the actual tracer injection.

The lack of a water source means that dead-ends will have very low velocities both in tracer dilution measurements and in convergent flow test, where the tracer injection rates are minimal. Tracer breakthrough from a dead-end connection can be enhanced by switching from a convergent flow test (where the tracer is injected with minimal flow rate) to a dipole test (where tracer is injected at the same rate or some significant fraction of the pumping well withdrawal rate). The dipole test should provide a significantly improved breakthrough. Design tasks related to this issue should review existing dilution data and recommend additional tests to support design work. As in the previous tracer tests, preliminary dilution measurements are highly desirable. A review of pressure interference and point dilution behaviours may identify some dead-end zones. Dead-end zones should have very strong drawdown behaviours that are distinctive in pressure interference tests.

## **2.3 Effects of pathway complexity**

Poor recovery may reflect complexities of the pathways. In general, tracer tests that involve only a single fracture or feature may have better recovery than tracer tests in complicated networks, the latter being more prone to involve multiple complicated pathways than the former. Transport along these multiple pathways will have separate and distinctive travel times. In extreme cases, a significant portion of the tracer may be travelling along slow pathways and will not appear during the normal duration of an

experiment. One key to testing this hypothesis may be to understand the detailed geometry of the conductors in the area of tracer test.

Another aspect of the multiple pathways is that multiple water sources will most likely be encountered. Most mathematical solutions to tracer transport only consider transport within a single planar feature. In three-dimensional networks, intersections, which appear along a tracer-transport pathway, may feed additional non-traced water to the stream line/flow path, thus altering the flow field and diluting the tracer concentration.

## **2.4 Effects of retention processes**

Recovery can be affected by retention processes. This issue is closely related to the effects of complicated flow paths discussed above. Matrix diffusion and reversible sorption should only retard transport, not stop it. Breakthrough curve forms should have some distinguishing characteristics, and there should be a dependency of the effect on velocities and pumping rates and the tracer used. ie. breakthrough of dissolved He gas different from that of solutes, cf. Section 4.6. This could be a particularly complicated hypothesis to test if it is combined with the effects of multiple complicated pathways, and especially if the pathways have different matrix interaction effects (mineralogy and chemistry) as well as different advective travel times (transmissivity and porosity).

## **3. Hypotheses**

### **3.1 What are hypotheses and how can we test them?**

#### **3.1.1 Scientific approach**

It is worthwhile to consider what constitutes a hypothesis. Hypotheses are usually derived from our previous experiments and experiences. Some of our previous experiments show that tracer tests have particular kinds of breakthroughs, or have particularly low recoveries, or have no breakthrough at all. We consider these data and wonder "why?"

We also observe fractures in boreholes and underground openings. We develop detailed models of these features in three-dimensions and we wonder, "How does this network geometry affect groundwater movement and solute transport?"

Our observations lead us to a series of "why", "how", and "what if" questions. Hypotheses are possible answers to these questions. As scientists, our job is to develop experiments that test the validity of these hypotheses. We must develop these experiments carefully, because the results of our tests may reflect complicated interactions of flow geometry and flow processes. A valid interpretation of our results may require separating the effects of these interactions.

There are certainly more possible questions, hypotheses, and experiments than we could ever hope to complete within the time frame of the present experimental programme. Therefore, we must prioritise hypotheses and experiments according to their relevance and their feasibility. The experiments we choose must answer questions that are critical to waste disposal issues yet can be accomplished within our available time and budget.

#### **3.1.2 Steps in tracer test design**

We propose the following steps for tracer test design:

1. Formulate a set of important questions about solute transport behaviour in fracture networks and within the TRUE Block Scale volume.
2. For each question suggest possible answers to these questions in the form of hypotheses.



3. Prepare a list of design tasks for each hypothesis – work that must be done to prepare an experiment design or plan.
4. Suggest experiments to test the hypotheses.
5. Prioritise the experiments based on the importance of the hypothesis and the feasibility of the experiment. This step requires a compilation of possible tracer test sites within the block with attributes such as distances, number of features involved, and their hydraulic properties. If a particular test has a very high priority, and no site with appropriate properties is available, then additional drilling or re-configuration of the packer systems may be necessary.
6. Prepare detailed designs of the highest priority experiments.

This section addresses the first three steps – listing of questions, hypotheses, and design tasks. For each hypothesis we list a set of design tasks – information that is needed to develop the tracer test designs. The TRUE Block Scale project involves many technical groups, and the work of the project should be distributed among several of them.

Steps 4 through 6, which involve prioritisation and experiment design, are discussed in the final parts of this report. The current plan takes into full account the results of the planned Pre-tests and performed scoping/design calculations, forming the major output of the final sections of the present report.

### **3.1.3 Questions, hypotheses, and design tasks**

We are proposing three basic questions for future tracer tests. These are:

Q1) "What is the conductive geometry of the defined target volume for tracer tests within the TRUE Block Scale rock volume? Does the most recent structural model reflect this geometry with sufficient accuracy to allow design and interpretation of the planned tracer tests?"

Q2) "What are the properties of fractures and fracture zones that control transport in fracture networks?"

Q3) "Is there a discriminating difference between breakthrough of sorbing tracers in a detailed scale single fracture, as opposed to that observed in a fracture network in the block scale?"

**Comments:**

Possible reasons for the difference related to Q3 could arise as a result of:

- Participating fractures/features being of different fracture types (genetic differences)
- Mineralogy
- Significantly different composition and/or distribution of gouge material
- Anisotropy (arising from shear displacements) in one fracture, and not in another
- Heterogeneity
- Fracture intersections, and intersections of conductive fractures

It is considered important to bring in the question of scale in the formulation of the Q3 to make the correct link between say the TRUE-1 results, and the planned tests of “component single fractures” and the “fracture network” in the block scale.

As discussed above, we propose hypotheses for each of these questions. Furthermore, we discuss in a very general way the type of experiment one might do to test the given hypothesis, and we specify a series of “design tasks”, which are needed to develop the experiments.

The design tasks may take several forms:

- Further characterisation studies at the site, particularly to better determine network geometry
- Geometric analyses of the structural model including visualisation
- Reconciliation of the structural model using available hydraulic data.
- Calculation studies including numerical model simulations, particularly to assess the relative effects of in-plane heterogeneity and intersection properties
- Complementary laboratory studies, generally with reference to diffusion and sorption.

## **3.2 What is the conductive geometry of the TRUE Block Scale volume?**

### **3.2.1 Basic question Q1**

The fundamental question considered in this section is “Is there enough information about the conductive geometry of the TRUE Block Scale volume to successfully design and interpret tracer tests?”.

The March 1999 structural model synthesises the latest results of the exploration work that has been completed in the TRUE Block Scale rock volume. This synthesis constitutes a hypothesis regarding the structural geology of the block.

As discussed above in Section 1, the major conductive features in the TRUE Block Scale rock volume have been identified. The group that is appropriate for tracer testing consists of the Type 1 structures #13, #20, and #19. Because the former two features are subparallel they do not form a network, and additional structures must be identified to complete network connections for experimentation. As of February 1999, the major uncertainty in the structural model was the existence, location, and conductivity of Structure #9, which was required to form a network among the major, numbered features. Subsequent interference tests in KA2563A have confirmed there is no clear conductive structure corresponding to the earlier hypothesised Structure #9. The lack of a major zone to connect the NW structures and complete a network for testing requires a detailed examination of Type 2 features, particularly in the area around structures #13 and #20, where so far two features, #21 and #22, have been identified.

At present, the Type 2 features between and around structures #13 and #20 are known only in one or two boreholes. Candidate fractures may be hypothesised from the POSIVA flow logs and the geologic data obtained by core logging and BIPS borehole television image analysis. Identification of the hydraulic connectivity of these connections will be addressed in cross-hole pressure interference testing and dilution tracer testing as a part of the performed Pre-tests, cf. Chapter 5 and Section 7.1. Dilution testing under ambient "undisturbed" conditions will also indicate the possible magnitudes of background flow that could affect tracer test performance.

### 3.3.2 Hypothesis H1

**H1) "The major conducting structures of the target volume for tracer tests in the TRUE Block Scale rock volume trend northwest and are subvertical. Being subvertical, and subparallel, they do not form a conductive network in the designated target volume. For the purpose of testing fracture network flow and transport effects in the current borehole array, second-order NNW features are required to provide the necessary connectivity between the major conducting NW structures!"**

Comment :

The March'99 structural model consists of NW structures (#20 and #13) which are sub-parallel, and which are likely to intersect within the TRUE Block Scale rock volume. However, for the purpose of studying network effects within the target volume there is a need to take the NNW features (#21, #22, and possible siblings) into account. In the actual treatise of this hypothesis, the experimenters and the individual modelling groups are encouraged to specify the entity of the conductive geometry, ie which structure, they will address, and the property/character addressed (eg. extent, material property etc.).

### 3.3.3 Design tasks for Hypothesis H1

The technical groups should study the following items to design experiments to test Hypothesis H1:

- Review flow log and fracture data from the area around structures #13 and #20 to identify second order fractures that may connect these two zones, cf. Section 7.2.
- Design and perform preliminary Pre-tests to confirm the connectivity of identified Type 2 features with structures #13 and #20. These tests should include dilution tests under pumping conditions to confirm connectivity, cf. Chapter 5 and Section 7.1.
- Reconciliation of March'99 structural model using existing hydraulic and tracer test data, including the Pre-test results. Tabulation of supporting data, identification of weak points, recommendations for further optimisation etc, cf. Section 7.2.
- Data synthesis to assess boundary conditions and their effect on flow in the tracer test target area.
- Numerical simulation and predictions of background fluxes and velocities across proposed tracer test area.

*N.B. It has been decided not to make any revisions of the multi-packer arrays prior to the Pre-tests to improve isolation of the identified structures #21 and #22. The results from the Pre-tests will constitute the basis for a decision as to whether to reposition the packers.*

## 3.4 What are the properties of the conducting network that affect transport?

### 3.4.1 Basic question Q2

Tracer tests provide information on the heterogeneity of flow and transport properties. The primary tool for studying tracer movement and retention is the tracer test. Tracer tests produce breakthrough curves that indicate the distribution of tracer mass among pathways of different velocities. A major purpose of the TRUE programme is to understand how heterogeneity within single conducting features, and in conducting networks of features, influences transport and retention. The aspect of the block scale experiments is to explore heterogeneity within networks of multiple features.

Natural fractures have many forms of heterogeneity that produce pathways with a large range of velocities and retention characteristics. Many of these heterogeneities exist within single conductive features. Within clean, or partially filled fractures, roughness variations lead to channelisation with multiple velocities. In more complex fracture zones or faults, the conducting feature may be a zone of crushed or finely fractured rock that nearly approximates a porous medium. Faults and fracture zones may even have layered structures that reflect zones of varying cataclastic intensity. The heterogeneities furthermore may exhibit a significant degree of anisotropy.

When fractures, fracture zones, or faults form networks there may be the additional effects associated with intersections. Mixing at intersections has been a concern in that intersections may constitute conductors and preferred pathways. There are several reasons why intersections may be preferred pathways. For one, the velocity of the water in a fracture network is controlled in part by friction along the walls of the fractures, which is the basis of parallel plate flow laws. Along a fracture intersection, the friction due to the walls is expected to essentially disappear, and consequently the flow capacity is expected to increase, this discounting any effect of fracture infillings. Second, intersections, or more precisely the edges of rock blocks, are locations of previous stress concentration where rock masses have deformed. Hence one should expect higher levels of fracturing and deformation along intersections. The greater damage should contribute to a larger amount of physical and chemical degradation, hence further enhancing the open space within the intersection area. Alternatively, the deformation may, through movement and degradation, lead to formation of fault gouge which can result in a reduced velocity. On the other hand, gouge material may provide for enhanced retention capacity, see Section 3.5. Another aspect is that variable loads during fracturing/formation and subsequent movements, in combination with a history of exposure to water of different chemistries and flow rates, may result in fracture intersections that exhibit heterogeneous rather than homogeneous characteristics.

A major goal of the TRUE Block Scale experiment is the investigation of the influences of fracture networks on transport and retention. The earlier TRUE detailed scale work was intended to understand transport within a single feature. The current work in the block scale therefore considers multiple features and any special conditions that might exist along the intersections and interfaces.

Two opposing hypotheses that arise from this question are:

- Intersections have distinctive properties; the heterogeneity they introduce is greater than and distinctive from the heterogeneity within features. Intersections may act as preferential conduits, barriers, or a combination of both.
- Transport is dominated by in-plane anisotropy and heterogeneity without regard to network and intersection properties.

### **3.4.2 Hypothesis H2a – Flow and transport controlled by fracture intersections**

**H2a) "Fracture intersections have distinctive properties and have a measurable influence on transport in fracture/feature networks. These distinctive properties may make the intersection a preferential conductor, a barrier, or a combination of both!"**

The structure of these intersections may be more complicated than a simple intersection of parallel plates. Intersections that involve faults or fracture "swarms" may have a very complicated structure. As with fault zones, the intersection region may consist of

combinations of "damage zones", where permeability is enhanced, or gouge zones where permeability is inhibited. Understanding this internal structure of intersections may be important for understanding flow and transport.

We may test hypotheses of intersection behaviours by using multiple pathways that measure flow and transport properties both within features and along pathways that include intersections. This work will require good visualisations of the candidate features and pathways within those features.

An additional design concern for assessing intersections will be the relative values of transmissivity of the target features. The target features for single-feature and intersection tracer tests must have larger transmissivities than surrounding features to avoid loss of tracer to less direct but more transmissive pathways. Thus, careful consideration must be given to the transmissivity data in designing the tests.

### **3.4.3 Hypothesis H2b – Flow and transport controlled by in-plane heterogeneity**

#### **H2b) "In-plane heterogeneity and anisotropy have a measurable influence on transport of solutes in a block scale fracture network!"**

At the JNC research facility in the Kamaishi mine, the reactivation of old fractures by later deformation is thought to have created channels within the fracture planes that introduced a strong anisotropy to flow and transport. This reactivation may also localise filling and fracture healing. This would be tested as part of the same program described for Hypothesis H2a. One should ideally include multiple pathway directions within some features to test in-plane anisotropy. These tests must be carefully designed relative to background flow, as background flow may also introduce directional effects. It is possible to switch sources and sinks in structures with in-plane anisotropy, unlike those cases with structures subject to significant background flow.

Comment :

By the above formulation the stated hypotheses can in principle be disproved if we can not measure the influence for the respective sub-hypotheses! It should be pointed out that we may stand a chance of eventually being in a position where we are unable to measure the influence for either of the effects referred to in the H2 hypotheses! We should also bear in mind that even if we succeeded in disproving of one of the sub-hypotheses this does not imply acceptance of the other!

It should in this context be acknowledged that alternative, more simple and "easy to disprove" hypotheses have also been proposed;

- "The field tracer experiments can be explained with a model of homogeneous parameters!"
- "There is a need to consider fracture intersections in order to explain the field tracer experiments!"

### 3.4.4 Design tasks for Hypotheses H2

Under tracer test design there are four major tasks. The first major task involves developing conceptual models of heterogeneity within fracture planes and along fracture intersections. This task should include a general review of in-plane heterogeneity of structures and a specific review of previous evidence of in-plane heterogeneity of previously studied Äspö fractures.

A second design task is the development of a conceptual model of Type 2 features between Structures #13 and #20. The focus of the future tracer tests will be in the rock volume defined by these structures. There are conductive fractures that connect these two zones (Features #21 and #22), but none have been characterised in detail. The results of the Pre-tests, cf. Section 6.3, and the reconciliation study, cf. Chapter 7, will help define these features as deterministically as possible.

The third design task is numerical simulations. Given a range of conceptual models of in-plane heterogeneity and intersections, numerical simulations may show the effect of heterogeneities on tracer behaviour. The simulations will show whether or not tracer tests can distinguish the effects of intersections from other forms of heterogeneity. The numerical simulations will also show the feasibility of various tracer test geometries as well as help to evaluate uncertainties in the fractures that connect Structures #13 and #20. The results of these studies showing the feasibility to distinguish intersection effects are presented in Section 6.2.

The fourth design task involves cataloguing possible pathways between sources and sinks. At present, the likely sinks will be chosen from several piezometer intervals with significant flow capacities: KI0025F02:P5, KA2563A:T4, and KI0023:P6.

Possible pathway types will have to meet several criteria including:

- Being entirely within a feature at appropriate separation distances.
- Feature pairs should be more transmissive than other nearby features.
- Crossing or following intersections of various types and having appropriate separation distances.

The results of this compilation are presented in Section 4.3.

## 3.5 Which retention processes are important in a network at a block scale?

### 3.5.1 Basic question Q3

The major goal of the TRUE project is the understanding of tracer retention in fractured rock. The experiments proceed from well-characterised single features to a block scale network of features. The important question here is how does retention behaviour change in going from a detailed (single feature) scale ( $L=5-10$  m) to a block scale ( $L=10-50$  m).

The actual retention processes themselves – which are mainly diffusion (either in the matrix or in dead-end fracture pore space) and sorption on fracture or inner matrix surfaces – should not change when moving to a larger scale, or when moving from study of one fracture to a network of fractures. Rather, access to different types of features and larger-scale heterogeneities may be distinctive when taking this step. There may also be some distinctions that one would observe as travel path lengths increase, such as the magnitude of matrix diffusion effects which should become more pronounced over longer path lengths.

Tracer retention will depend on the pore structures, possible infillings, surface mineralogy of fractures and the matrix adjacent to conducting features. These pore structures may vary within the conducting feature depending on the feature type. Faults and shear zones may have various porosity-zonations across their width. Even relatively simple fractures may lie within zones of enhanced matrix porosity, as was observed at the Kamaishi laboratory and also suggested by the results of the TRUE-1 tracer tests (Winberg et al., in prep). If intersections are preferred pathways, they may also be regions of enhanced rock-water interactions that lead to further enhancements in the porosity of the adjacent matrix.

Question Q1 concerns the identification of conductive features. Question Q2 looks at heterogeneity within these features and along intersections. The present Question Q3 considers the tracer retention properties of conducting features, which entails an understanding of the porosity structures and mineralogy of these features and the adjacent matrix. Given the focus of the block scale program, the key features for assessment will be Structures #13 and #20, the Type 2 connecting features, and the intersections among these conductors.

### 3.5.3 Hypothesis H3

**H3) “It is not possible to discriminate between breakthrough curves of sorbing tracers in a single fracture from those obtained in a network of fractures”!**



Comment :

The discussion following the 3<sup>rd</sup> Review Meeting in October 1999 and subsequent discussions have called for the modellers to make use single fracture data in their predictions before the block scale results are released. A number of sub-hypotheses would follow in the case the above basic hypothesis can be negated. The formulated sub-hypotheses would refer to different causes for the observed difference in breakthrough behaviour.

To address Hypothesis H3, tracer tests are designed to look at retention properties by using tracers with different diffusivity and sorption properties and/or by varying the design parameters, such as injection and withdrawal rates, in order to isolate and observe the effects of matrix diffusion. As noted above, Hypothesis H3 has similarities to Hypothesis H2, and it may be tested in a similar manner. Ideally, one observes retention behaviours within conducting features, such as Structures #13 or #20, and compares the breakthrough results with tests that include pathways in both structures and the Type 2 connecting features.

Scoping calculations must consider the optimal distances for such tests. However, tests that address diffusion and sorption may work better with lower velocities and shorter distances than tests aimed at possible determination of the physical properties of intersections.

### **3.5.3 Design tasks for Hypothesis H3**

The following are recommendations for design tasks for Hypothesis 3. In general, these involve developing a conceptual model of the retention properties of conducting features in the target portion of TRUE Block Scale rock volume. Once one has alternative models of the block, one develops of scoping calculations and simulations to assess likely tracer test behaviours.

- Identify features similar to Structures #13 and #20 exposed in the underground workings; examine porosity structures of the features of intersections with Type 2 features.
- Compare the surface mineralogy of the Type 1 structures (#13 and #20) with Type 2 features that provide connections between the Type 1 structures.
- Core studies should be undertaken to describe porosity values associated with various feature types.
- Scoping studies to assess the need for complementary laboratory tests to assess diffusion and sorption behaviours.
- Scoping calculations to determine appropriate velocities to observe diffusion or sorption behaviours. These calculations should consider isolating diffusion effects by using tracers with different free-water diffusivity values (such as He versus Uranine) and by varying the pumping rate.

## **4. Premises for Pre-tests**

This chapter reports the premises for the planned tracer tests as they were manifested prior to performing the planned Pre-tests. This includes a description of the most recent update of the structural model (March'99), a tabulation of geometrical transport pathways within individual structures, and pathways which connect two or more structures. In addition, the resulting borehole multi-packer array after the optimisation of KA2563A and KA2511A is presented. Finally, the conservative tracers planned for use are presented, including preliminary results from field tests of some new tracers at the TRUE-1 site.

### **4.1 March'99 structural model**

The following data has been utilised for the March 1999 structural model update;

- BIPS/Boremap data from KI0025F02
- BIPS/Boremap data from KA3600F and KA3563A
- POSIVA flow log of boreholes KA3510A, KA2563A, KI0025F02 and KA2511A
- Radar reflectors in KI0025F02
- Radar reflectors in KA3573 and KA3600F (Carlsten, 1998)
- Selective pressure build-up tests in KI0023B

The POSIVA flow logging has turned out to be a major achievement in characterising conductive fractures and has increased the ability to select which fractures are conductive with an accuracy of about 0.1 m. This has helped substantially in the interpretation of deterministic structures in the modelled volume. By examining the flow log and identifying conductive fractures it has turned out that most of the previously determined structures can be explained by corresponding anomalies in the flow log. However, A list has been produced of fractures in the TRUE Block Scale boreholes most likely to be conductive based on geological signature. This list has been compared with the conductors identified by the POSIVA flow log and does not always correspond, which is also to be expected. This lack of correlation is subject to further sensitivity analyses, eg. to the threshold value of conductivity/flow used to identify a conductive feature.

Based on the previously presented background data from the POSIVA flow log and the BIPS system, correlation of this material is done with information from the Sep'98 structural model. New information has had the following impact on the previous model, c.f. Figure 4-1.;

- the new borehole KI0025F02 has provided detailed information primarily in the centre of the block.
- boreholes KA3600F and KA3573A have confirmed the orientations and locations of the pack of structures intersected close to the TBM tunnel; #2, #3, #4 and #5.
- the POSIVA flow logging has with its detailed resolution, slightly changed the exact location of Structures #6, #7, #13, #19 and #20
- two new minor north-westerly oriented conductors have been suggested based on observed hydraulic connectivity between Structures #13 and #20
- On the basis of the performed flow logging and interference tests in KA2563A, the extent and significance of Structure #9 as a major connector between Structures #20 and #13 has been significantly reduced.

A systematic control of interpreted intercepts in the Sep'98 structural model showed that with the POSIVA flow log it was possible to identify the specific conductive fracture among many possible fractures in a borehole section. Table 4-1 shows data for the new interpreted intercepts of the defined deterministic structures. The new information, for the most part, introduces minor changes to the geometry of the interpreted structures.

**Table 4-1 March'99 Structural Model – Interpreted Type 1 structures in the TRUE Block Scale borehole array. Numbers marked in bold have changed in relation to the September 1998 model.**

#	KA2563A Ori	KA2511A Ori	KI0025F Ori	KI0023B Ori	KI0025F02 Ori	KA3510A
<b>6</b>	<b>157.2</b> 309/89	89.2 291/84	<b>61.8</b> 342/86	44.2 103/87	<b>52.3</b> 317/89	-
<b>7</b>	153.4 111/73	<b>38</b> 143/87	-(37.1)	-	42.2 338/83	<b>39.9</b> 126/70
<b>9</b>	<b>230</b> 123/88	-	-	-	-	-
<b>13</b>	207 321/86	-	-	-	85.6 318/89	<b>93.9</b> 140/83
<b>19</b>	<b>237.9</b> 243/76	-(156.4)	-	166.4 338/74	111.6 342/87	<b>133</b> 330/76
<b>20</b>	188.7 316/82	122 336/67	87.7 336/77	69.8 157/82	<b>74.7</b> 138/90	-

However, as pointed out, the one major change to the structural model is the limited extent and significance of Structure #9. Structure #9 has been described as a feature intersecting KA2563A and KI0023B (Winberg, 1999). However, the geological characteristics of the two different intercepts as well as the geometry are not coherent. The new borehole KI0025F02 and a series of recent hydraulic tests focused on Structure #9 suggest that connectivity is difficult to explain with the geometry of Structure #9. A structural reinterpretation utilising the new hydraulically active fractures in KA2563A

and KI0025F02, as well as the geological structures that intersect within the sections tested using flow and pressure build-up tests in KI0023B, shows that there exist a number of north-northwesterly structures that appear to be able to connect structures #13, #20 and #6, c.f. Figure 4-1. The interpretation that Structure #9 intersects borehole KI0023B has been revised as well as its actual position in KA2563A.

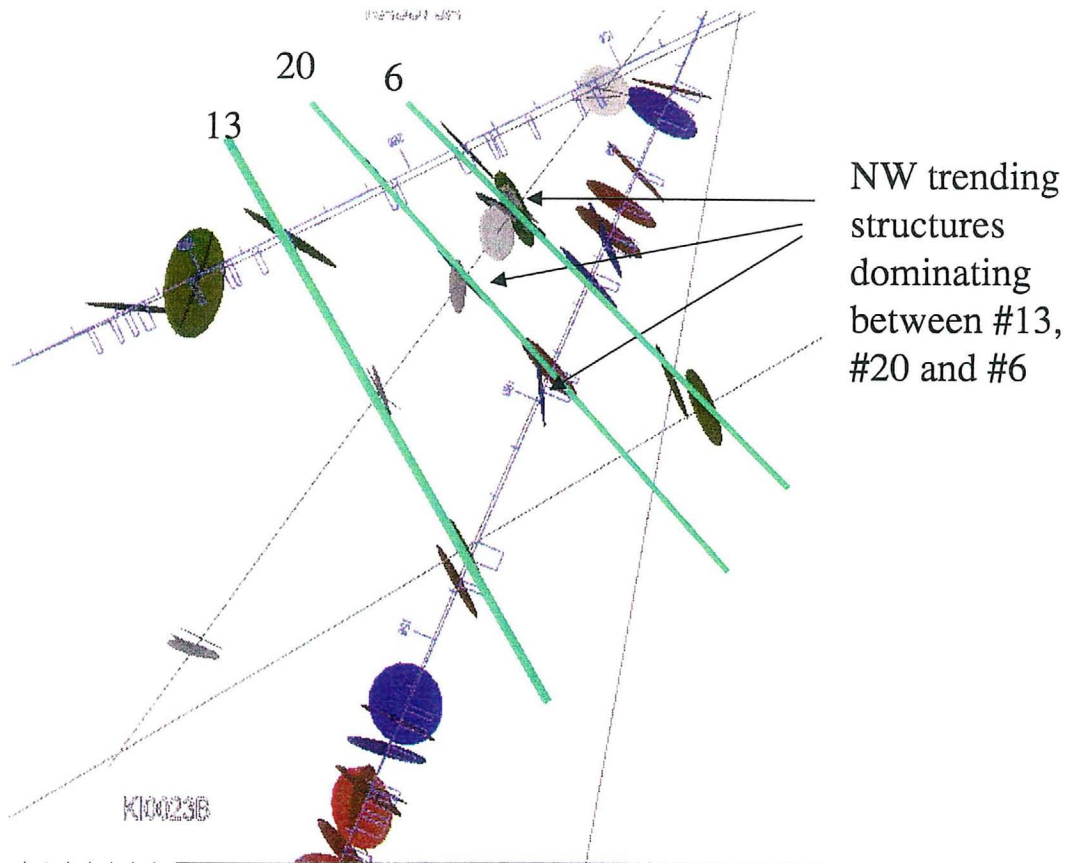


*Figure 4-1 Oblique view of conductive fractures in KA2563A, KI0025F02 and KI0023B. The fractures in KI0023B are derived from the conductive sections tested by using flow and pressure build-up tests. The positions of structures #13, #20 and #6 are only tentatively illustrating their respective geometry.*

Structures #6 has new interpreted intercepts in KA2563A and KI0025F as well as a new intercept in KI0025F02. The new fracture geometry is defined by the positions of conductive fractures in the POSIVA flow log. Structure #7 is interpreted as possibly intersecting KA2511A at L=38 m.

The interpretation of Structures #13 and #20 is the same as in the Sep '98 structural model with the addition of two new intercepts in KI0025F02 at L= 93.9 and L= 74.7 m, respectively. The geological character of both intercepts in KI0025F02 is similar to what is seen in the other boreholes. The two intercepts lead to a slightly different orientations of planes between the intercepts where Structure #13 has an average orientation of 320/78 and Structure #20 an orientation of 317/84.

The north-north-westerly structures between Structures #13, #20 and #6 can be interpreted as two features, #21 and #22, subordinate to Structures #13 and #20. Table 4-2 shows the interpreted intercepts in boreholes KI0025F, KI0023B and KI0025F02. Only planes of intersection of the two features are shown in Figure 4-1. These features are correlated with inflow points as recorded in the POSIVA flow log. Their individual geometry are fairly well constrained and the two structures are steep and oriented 352/80 and 335/78, respectively. Both structures are subordinate in respect of width and geological character and are interpreted as being either splay fractures or belonging to a younger fracture set than the system made up of Structures #13 and #20. The geometry indicates that, at a minimum, these structures connect at least structures #13, #20 and #6.

The complete March'99 structural model is shown in Figure 1-1.

**Table 4-2 Intercepts of the interpreted Type 2 Features #21 and #22.**

#	KI0025F	Strike/dip	KI0023B	Strike/dip	KI0025F02	Strike/dip	Interpreted orientation
21	-(166.4)	-(338/74)	71.1	123/86	97.9	354/77	352/80
22	88.8	340/81	-	-	66.8	337/88	335/78

## 4.2 Optimisation of multi-packer array

On the basis of the results of the complementary hydraulic testing in KA2511A and KA2563A and the verification tests in KA2563A, the multi-packer arrays in these two boreholes have been changed.

Borehole KA2511A has been installed with a packer system with a total of 8 sections for pressure monitoring alone. Borehole KA2563A has been installed with a system that allows pressure monitoring in five sections, but has three sections equipped for circulation (two additional 6/4 mm lines). In the case of KA2563A, the circulating sections are focused on Structures #20, #13 and #19. As a result, the isolation of some of the previously monitored bounding structures (#4, #5 and #10) has been relaxed shifting focus to eg. Structure #13. This is in line with the focus on the part of the TRUE Block Scale volume, the core of which is made up of Structures #13 and #20.

The array available prior to the onset of the Pre-tests is indicated in Figure 5-1.

### 4.3 Catalogue of transport pathways

There are 25 borehole sections equipped for tracer injection/sampling in the TRUE Block Scale array as of March 1999, i.e. prior to performance of the planned Pre-tests. Seven of these are not suitable for tracer injection/sampling due to their large volume, location outside the target area, or low transmissivity. The remaining 18 sections may be used. In the tables below potential pathways for tracer tests are presented. Table 4-3 presents pathways within one structure whereas Table 4-4 presents pathways involving more than one structure. Note that the compilation presented in this section does not include the reappraisal of Structure #9 (reduced importance) and inclusion of the new NNW features #21 and #22.

**Table 4-3. Possible transport pathways within one structure.**

Structure #	Injection section	Sampling section	Distance (m)	T inj E8 (m <sup>2</sup> /s)	T sampl E8 (m <sup>2</sup> /s)	Dilution test *)	Priority
20	2563A:S4	0025F02:P5	35	38	12	Y	1
	0025F:R4	0025F02:P5	24	4	12	Y	2
	0023B:P7	0025F02:P5	26	13	12		5
	0025F:R4	2563A:S4	57	4	38	N	3
	0023B:P7	2563A:S4	16	13	38		4
	0025F:R4	0023B:P7	47	4	13		6
9	0025F02:P8	0023B:P6	23	0.8	13	Y	1
	2563A:S2	0023B:P6	42	3	13		2
	0025F02:P8	2563A:S2	63	0.8	3		3
13	2563A:S3	0025F02:P3	47	3	4		3
	0023B:P4	0025F02:P3	27	3	4		2
	2563A:S3	0023B:P4	21	3	3		1
6	0025F02:P6	0023B:P7	21	10	10		1
19	0023B:P2	0025F:R2	84	10	73		3
	0025F02:P2	0025F:R2	49	10	73		2
	0023B:P2	0025F02:P2	37	10	10		1
7	0025F02:P9	0023B:P8	12	40	150		1

\* Y = Responding section during pumping, N = Non-responding section

A priority index (between 1-6) for each structure has also been introduced based on:

- Results of previous tracer dilution tests
- Local transmissivity of the structures
- Distance (straight line)

The influence of the "natural" gradient has not been considered in assigning the priority index.

In summary Table 4-3 shows:

- It is possible to test six different structures individually, two of them in one flow path only
- In total 17 possible flow paths have been identified
- Geometric distances range from 12 to 84 m
- Local transmissivities range from 0.8 to  $150 \cdot 10^{-8} \text{ m}^2/\text{s}$
- Section KI0023B:P7 contains two structures and may therefore not be suited for tracer tests. In that case the number of possible flow paths will reduce to 13.

**Table 4-4. Possible transport pathways involving two structures.**

Structure #	Injection section	Sampling section	Distance (m)	T inj E8 ( $\text{m}^2/\text{s}$ )	T sampl E8 ( $\text{m}^2/\text{s}$ )	Dilution test*	Priority
9-20	0023B:P6	0025F02:P5	20	13	12	Y	1
	2563A:S2	0025F02:P5	54	3	12		4
	0025F02:P8	0025F02:P5	21	0.8	12		3
	0023B:P6	2563A:S4	16	13	38	Y	Tested
	2563A:S2	2563A:S4	42	3	38		5
	0025F02:P8	2563A:S4	31	0.8	38		2
	0023B:P6	0025F:R4	42	13	4	(Y)	7
	2563A:S2	0025F:R4	72	3	4		8
	0025F02:P8	0025F:R4	38	0.8	4		6
13-20	0023B:P4	0025F02:P5	22	3	12		1
	2563A:S3	0025F02:P5	38	3	12		4
	0025F02:P3	0025F02:P5	24	4	12		7
	0023B:P4	2563A:S4	26	3	38		2
	2563A:S3	2563A:S4	19	3	38		5
	0025F02:P3	2563A:S4	51	4	38		3
	0023B:P4	0025F:R4	41	3	4	(Y)	8
	2563A:S3	0025F:R4	60	3	4		9
	0025F02:P3	0025F:R4	25	4	4		6
13-9	0023B:P4	0023B:P6	15	3	13	N	Tested
	2563A:S3	0023B:P6	21	3	13		1
	0025F02:P3	0023B:P6	36	4	13	Y	2
	0023B:P4	2563A:S2	33	3	3		4
	2563A:S3	2563A:S2	23	3	3		3
	0025F02:P3	2563A:S2	52	4	3		5
20-6	2563A:S4	0025F02:P6	32	38	10		1
	0025F02:P5	0025F02:P6	7	12	10		3
	0025F:R4	0025F02:P6	28	4	10		2
9-6	0023B:P6	0025F02:P6	18	13	10		1
	2563A:S3	0025F02:P6	38	3	10		3
	0025F02:P8	0025F02:P6	14	0.8	10		2
13-6	0023B:P4	0025F02:P6	25	3	10		1
	2563A:S3	0025F02:P6	38	3	10		2
	0025F02:P3	0025F02:P6	31	4	10		3

A number of additional flow paths between structures are not considered in Table 4-4. Those are:

- Flow paths involving Structure #19 which has shown to be hydraulically isolated from the rest of the block
- Flow paths involving Structure #7 (bounding structure)
- Flow paths involving section KI0023B:P7 (two structures intersecting the section in question)

Finally it should also be noted that some of these flow paths may be equally good or better to reverse (shift in sink and source sections for tracer tests) given the direction of the natural gradient and the local transmissivity.

As in the case with the single structure a priority index has been assigned subjectively based on existing dilution test results, local transmissivity values and distance between sink and source sections.

#### **4.4 MAUA analysis of defined pathways**

Multi Attribute Utility Analysis (MAUA) has been employed to formalise the priority assignment and make the assignment less subjective. The basis for MAUA is construction of functions which provide measures of the effects of a particular influence or option. The functions are themselves related to underlying objective performance measures. The utilities and weights are not important in themselves. The weighting of the relevant issues has been designed to draw out the important factors that control the success of performance of a tracer test.

Parameters such as distance, local transmissivity, connectivity, hydraulic gradient and point dilution measurement data are all important to the success of a tracer test. In a first attempt the parameters of transmissivity, connectivity, and dilution were used. The results for the case of multi-structure pathways is shown in Table 4-5. A comparison with Table 4-4 shows that the subjective ranking compares well with the less subjective MAUA results. Only 8 anomalies are identified, marked with the symbol (#). The analysis will be complemented by the inclusion of additional parameters such as hydraulic gradient, source/sink dimension and true geometrical distances.

#### **4.5 Visualisation of pathways**

A number visualisations have been produced as working material for Pre-test planning and planning for subsequent tests. These images are based on in-plane images of the



Table 4-5 Results of MAUA analysis of identified multi-feature pathways in the TRUE Block Scale array

Structure	Priority (PA)	Priority (DH)	Distance (m)	T-inj. $\times 10^{-8}$ (m <sup>2</sup> /s)	T-sampl. $\times 10^{-8}$ (m <sup>2</sup> /s)	Response Interference	Dilution Tests	Measure Sum (pi)	$p_1$	$p_2$	$p_3$	Difference PA vs DH	Total Rank
9 to 20	1	1	20	13	12	1	1	38.35	8.35	20.00	10.00		3
	2	2	31	0.8	38	0.5	0.5	26.30	11.30	10.00	5.00		13
	3	4	21	0.8	12	0.5	0.5	19.20	4.20	10.00	5.00		33
	4	5	54	3	12	0.5	0.5	18.76	3.76	10.00	5.00		35
	5	3	42	3	38	0	0.5	20.97	10.97	10.00	0.00	#	31
	6	6	38	0.8	4	0.5	0.5	16.32	1.32	10.00	5.00		37
	7	8	42	13	4	0	0	4.55	4.55	0.00	0.00	#	47
	8	7	72	3	4	0	0.5	11.64	1.64	10.00	0.00		44
13 to 20	1	3	22	3	12	1	0.5	24.85	4.85	10.00	10.00	#	16
	2	1	26	3	38	1	0.5	32.58	12.58	10.00	10.00		7
	3	2	51	4	38	0.5	0.5	25.68	10.68	10.00	5.00		14
	4	4	38	3	12	1	0.5	24.12	4.12	10.00	10.00		21
	5	5	19	3	38	0	0.5	23.92	13.92	10.00	0.00		24
	6	7	25	4	4	0.5	0.5	17.49	2.49	10.00	5.00	#	36
	7	6	24	4	12	0.5	0.5	20.03	5.03	10.00	5.00		32
	8	9	41	3	4	0	0	1.88	1.88	0.00	0.00	#	48
	9	8	60	3	4	0	0.5	11.71	1.71	10.00	0.00		43
13 to 9	1	1	21	3	13	1	0.5	25.26	5.26	10.00	10.00		15
	2	2	36	4	13	0	1	24.74	4.74	20.00	0.00		17
	3	3	23	3	3	1	0.5	21.91	1.91	10.00	10.00		28
	4	4	33	3	3	1	0.5	21.72	1.72	10.00	10.00		29
	5	5	52	4	3	0	0.5	11.77	1.77	10.00	0.00		42
20 to 6	1	1	32	38	10	1	0.5	33.85	13.85	10.00	10.00		5
	2	3	28	4	10	1	0.5	24.20	4.20	10.00	10.00	#	20
	3	2	7	12	10	0.5	0.5	26.31	11.31	10.00	5.00		12
9 to 6	1	1	18	13	10	1	0.5	27.96	7.96	10.00	10.00		10
	2	2	14	0.8	10	1	0.5	24.09	4.09	10.00	10.00		22
	3	3	38	3	10	1	0.5	23.57	3.57	10.00	10.00		25
13 to 6	1	1	25	3	10	1	0.5	24.04	4.04	10.00	10.00		23
	2	2	38	3	10	1	0.5	23.57	3.57	10.00	10.00		25
	3	3	31	4	10	0.5	0.5	19.08	4.08	10.00	5.00		34

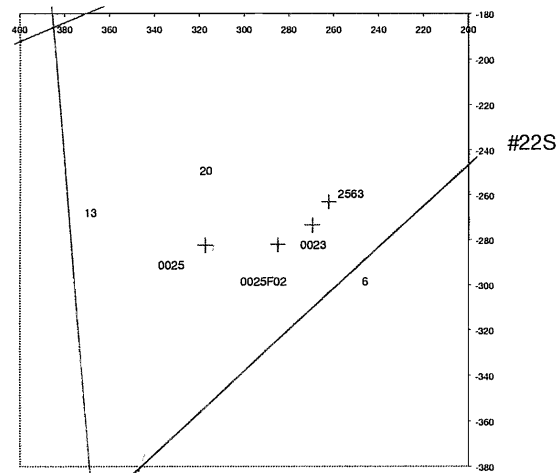
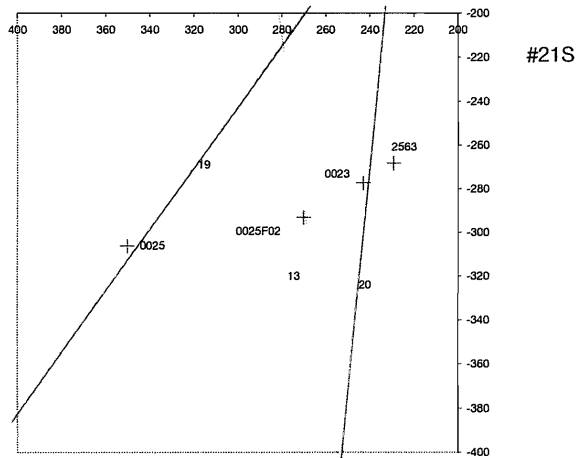
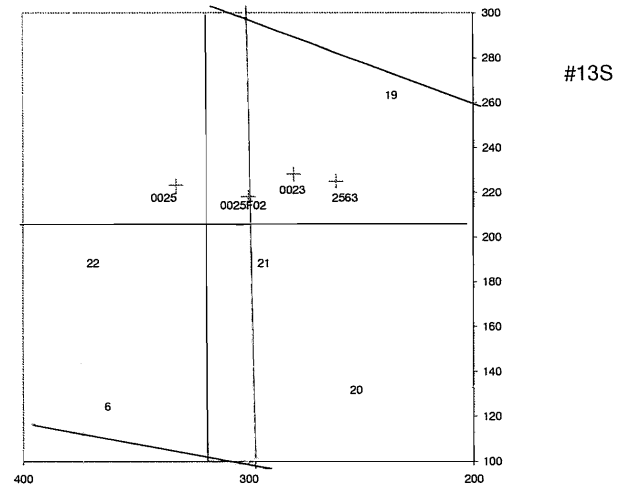
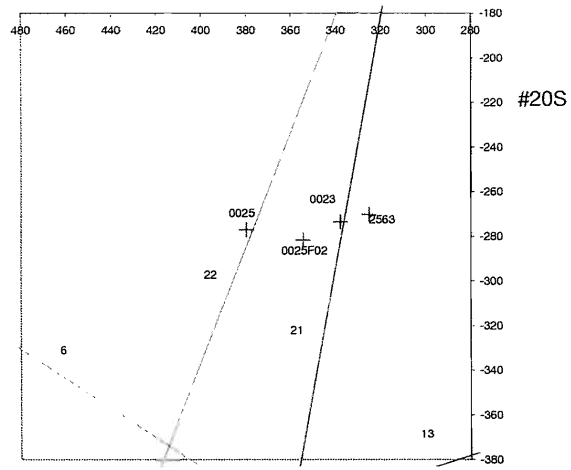


Figure 4-2 In-plane representation (view to the south) of intersections of structures and boreholes for a) #20, b) #13, c) #21, d) #22.

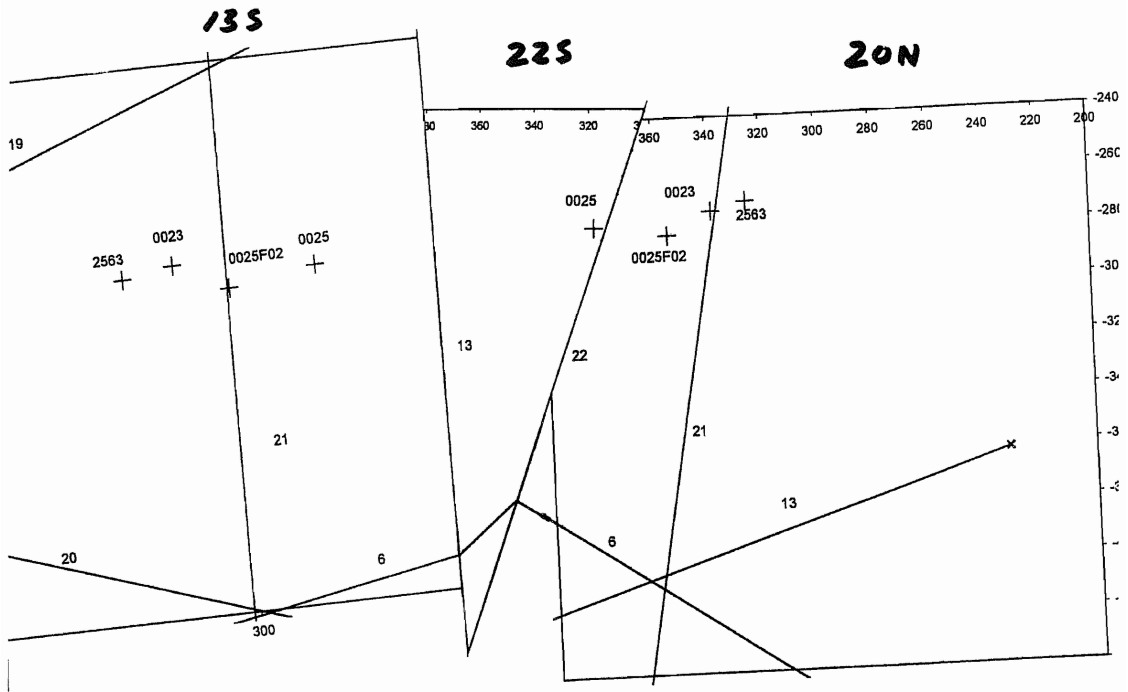


Figure 4-3 Fold-out imaging of flow paths between Structures #13 to #20, by way of Structure #22, cf. Figure 4-2 and Appendix A for details.

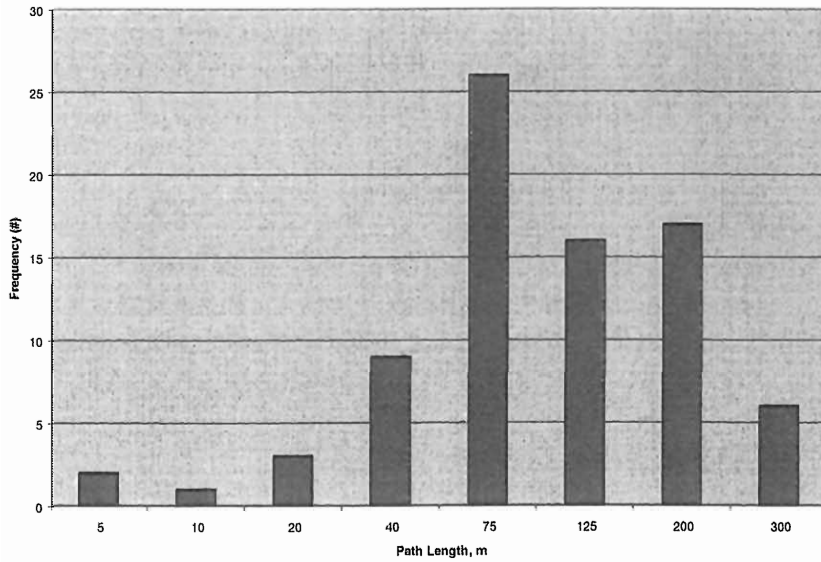


Figure 4-4 Histogram showing results of pathway search in a constructed channel network model based on Structures #13, #20, #21, #22 (and #6).

identified structures and features. Figure 4-2 shows the interpreted intercepts of other structures and existing boreholes in Structures #20 and #13 and Features #21 and #22. These in-plane images have then been combined to produce an image of pathways that involve two or more structures. Figure 4-3 exemplifies such a fold-out image for the pathways from #13 to #20 by #22. Appendix A lists the true shortest travel distances for defined flow paths as measured along the planes of the involved structures, including the length of the different legs in individual structures.

The path lengths given in Appendix A should be compared with the Euclidian distances between sink and source sections given in Table 4-4. The calculated path-way lengths have also been statistically analysed. The results of this analysis are presented as a histogram in Figure 4-4. This figure shows that the short pathways, where tests with sorbing tracers are plausible, only represent a minor fraction of all mapped pathways.

## 4.6 Development of conservative tracers

A series of tracer experiments will be performed within the ongoing TRUE Block Scale Project. The experiments will be performed over distances between 10-50 m in a network of structures. The long distances and complex flow geometry will most probably induce a large dilution of the tracers along the flow path and in the sink section. It is envisioned that these tests will require between 5-10 non-reactive tracers that can be detected in very low concentrations.

**Table 4-6. Non-reactive tracers used in the TRUE-1 experiments.**

Tracer	Type	Test(s)	Comment
Uranin	Fluorescent dye	All	The best
Amino G Acid	Fluorescent dye	RC-1, DP-2,4,5 PDT-1,2	Good but high background and not available any more
Rhodamine WT	Fluorescent dye	RC-1	Weakly sorbing
Eosin Y	Fluorescent dye	RC-1	Solubility problems, less dynamic range
Gd-DTPA	Metal complex	RC-1, DP-1	Irreversible losses, expensive analysis
Eu-DTPA	Metal complex	RC-1	Irreversible losses, expensive analysis
Ho-DTPA	Metal complex	RC-1	Irreversible losses, expensive analysis
Tb-DTPA	Metal complex	RC-1	Irreversible losses, expensive analysis
HTO	Tritiated water	PDT-3, STT-1, STT-1b, STT-2	Good but restrictions may be necessary
<sup>82</sup> Br	Radioisotope	PDT-3,STT-1b, STT-2	Good but restrictions may be needed
<sup>131</sup> I	Radioisotope	STT-1b	Good but restrictions may be necessary

Tracer experiments have also been performed in the detailed scale within the TRUE-1 Project at Äspö HRL. These tests were performed over distances between 2.5 to 10 m in

a single fracture. In all, 11 different non-reactive tracers have been used in the TRUE-1 tests, cf. Table 4-6. However, some of them were found to be weakly sorbing, while others suffered irreversible mass losses, and some of them were radioactive. The latter group (HTO,  $^{82}\text{Br}$ ,  $^{131}\text{I}$ ) will probably not be possible to use other than in a very well controlled experiment where mass losses are unlikely to occur.

The development work comprise a literature survey focused on possible tracers. The tracers addressed are listed in Table 4-7.

The field tracer tests have been performed in two steps. The first step included readily available tracers that have been used in other tests in granitic bedrock. The dye tracer Uranine (Sodium fluorescein) was used as reference in this context. The following tracers were included in the first run:

**Table 4-7. Non-reactive tracers to be studied in the literature study.**

Tracer	Name	Analysis	Dynamic Range	Comment
Gases	He-3	Mass spectrometry	Large	Used by NAGRA
	Ar, Ne, Xe		?	Research needed
Stable isotopes	Deuterium	Mass spectrometry	?	Expensive analysis
	N-15, C-13, O-18		?	
Dyes	Eosin B, Y	Fluorometry	Large	Used in TRUE-1
	Phloxine			Used in Stripa
	Rose Bengal			Used in Stripa
	MTMBA			Solexperts
	UV-1			Hydroisotop
Metal-Complexes	m-EDTA	ICP-MS	Large	Used in Finnsjön, Stripa, TRUE-1
	m-DTPA			
	m-DOTA			
Halogenated hydrocarbons	Many different	Gas chromatography	Large	Used in USA, Hydroisotop has experience
Benzoates	TFMBA and others	HPLC	Large?	Used by SANDIA in USA (WIPP)
Particles		Particle counter	?	Study at CTH Nuclear Chemistry
Others	ReO <sub>4</sub>	ICP-MS	Large	Used in Finnsjön
	CS <sub>2</sub>	?	?	

- In-EDTA, Yb-EDTA, Lu-EDTA
- Gd-DTPA, Ho-DTPA
- Eosin Y
- Phloxine
- Rose Bengal
- $\text{ReO}_4$
- Helium-3

The second included Helium, benzoates and some other tracers identified during the literature study, see below. In the case of Helium the technology used by NAGRA at Grimsel is furnished by ANDRA through Solexperts AG. The second batch of tracers also included stable isotopes (ia. Deuterium):

- Deuterium
- Eosin
- Sulforhodamine G
- Dimethylfluorescein
- Pyranine
- Naphtionate
- UV-1

The field tests have been performed in a radially converging flow field created between borehole sections KXTT4:P4 (sink) and KXTT3:P3 (source). These sections are associated with the geologic structure “Feature B” at the TRUE-1 site (L=2/945 m). This flow path was earlier tested with a tracer test as a part of the characterisation of the site (Winberg, 1996) and found to yield a high recovery (92%).

The tracer injection was performed as a finite pulse injection with a duration (tentative) of one hour. The tracer solution was then replaced by unlabelled water so that approximately 90% of the tracer solution was removed. The remaining tracer solution was circulated and sampled for about one week. Sampling was done both in the injection loop and in the pumped water. Therefore, it was possible to study differences between the tracers both in the injection loop, where the tracer was in contact with tubing material, packer material, dummy material and rock matrix for a relatively long period of time, and also in the sampling borehole where the tracers have been in contact with the minerals along the flow path.

The results of the first test with metal complexes (Figure 4-5) show that most of the complexes behave similar to the reference tracer Uranine. However, two of the injected tracers, Phloxine B and Ni-EDTA, show significant losses (>50%).

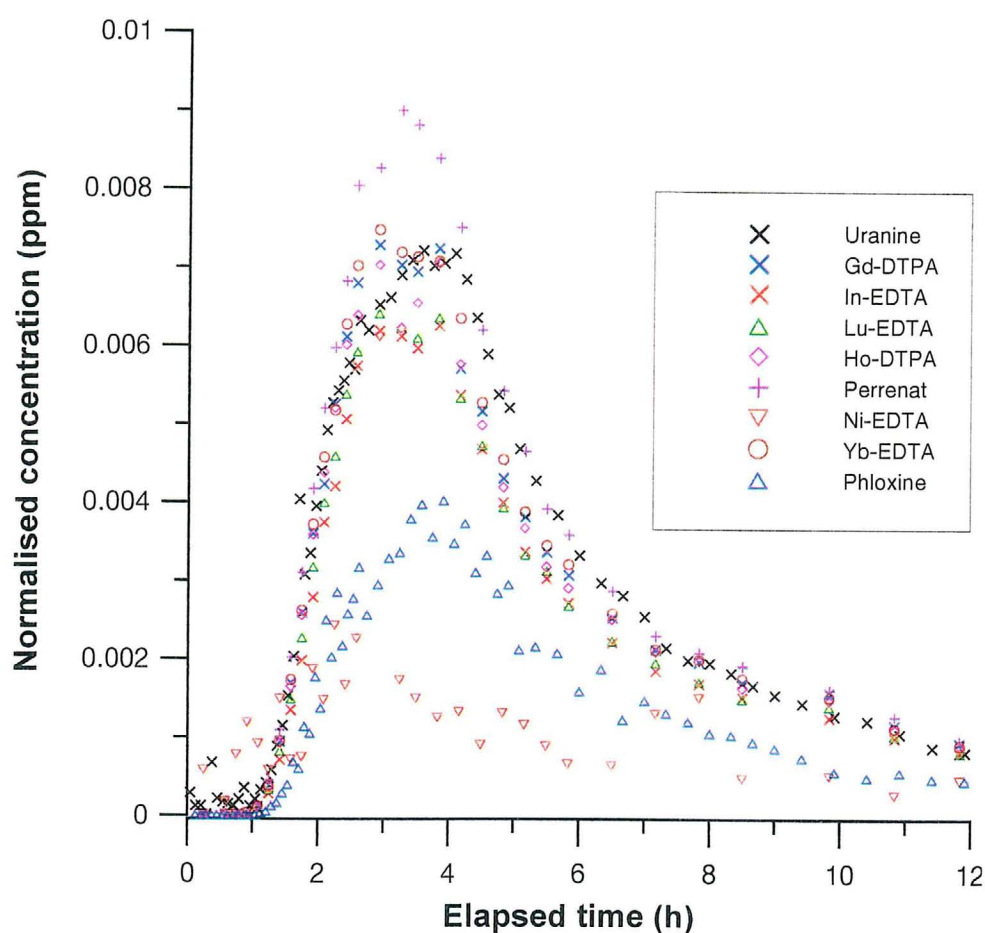


Figure 4-5 Tracer breakthrough curves for the first 12 hours of the first tracer test. The tracer concentrations are normalised to the injection concentrations at  $t=1.99$  hours. Test performed in the Feature B at the TRUE-1 site.

The tracer mass recovery was calculated to 100% for Uranine while recoveries for others are somewhat more uncertain due to the relatively small number of analyses made in the injection loop. Assuming that the same relative mass of metal complexes is injected as for Uranine, mass recoveries are somewhat lower for the metal complexes (81-93%). The analysis is still ongoing.

A closer inspection of the peak of the breakthrough curves shows that the rising part is almost identical for all tracers (except Ni-EDTA and Phloxine) while the peak and the falling part is slightly lower for all metal complexes (Figure 4-5) in particular In-EDTA and Lu-EDTA. The significance of this difference is still under investigation.

In the case of the second batch, not shown in Figure 4-5, including Deuterium, Eosin, Sulforhodamine G, Di-methylflourescein, Pyranine, Naphtionate, UV-1, they all exhibit similar breakthrough curves, with the exception of Sulforhodamine G, the latter finding not surprising. It was possible to analyse 7 of the latter tracers in one sample using the HPLC technique and spectral flourometry.

The on-line detection of Helium compared well with measured samples. Preliminary results from the test with Helium shows equitable first arrival times for Helium and Uranine. Helium has a somewhat shifted peak arrival time (3 minutes) and shows a peak concentration which is 30% less than that of Uranine, cf. Figure 4-6. The tail of Helium is more accentuated. Although portions of the results may be affected by experimental artefacts, preliminary results suggest that use of Helium as a tracer is feasible, and that a small but distinguishable retardation of Helium in relation to Uranine can be measured.

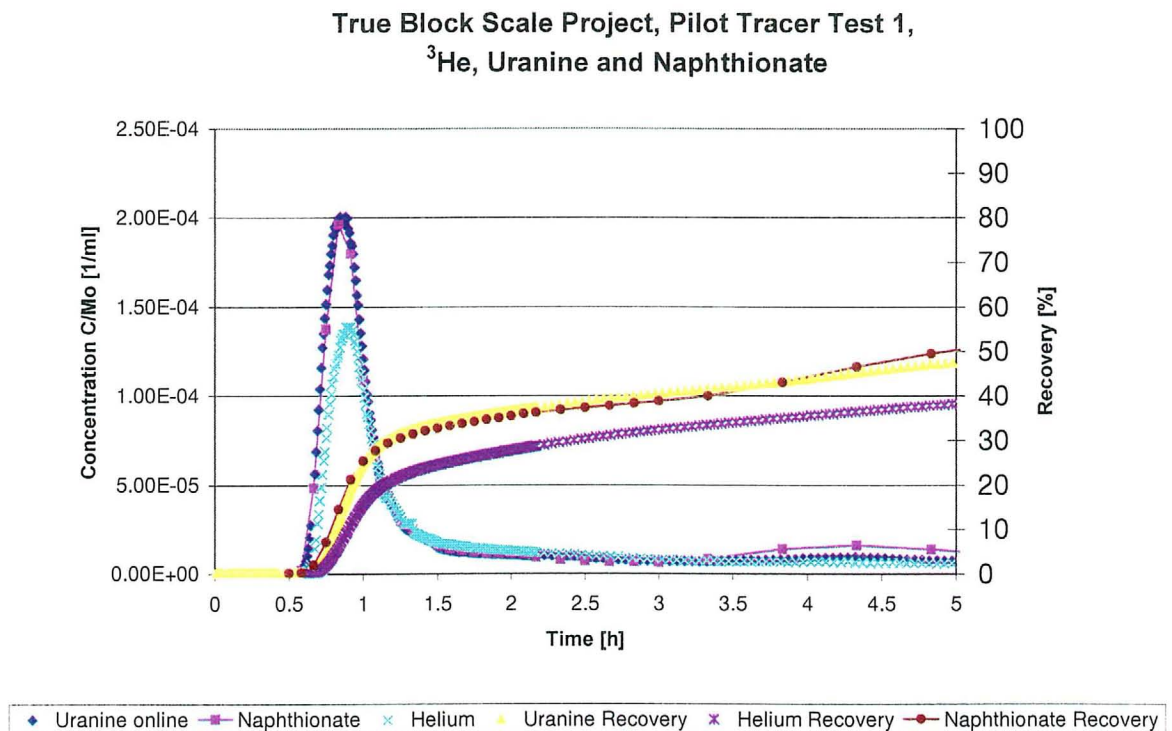


Figure 4-6 Comparison between Helium-3, Uranine and Naphthionate breakthrough obtained from the test performed in the Feature B at the TRUE-1 site, cf. Figure 4-5.



## 5. Pre-tests

### 5.1 Background and objectives

The purpose of the Pre-tests is to assess the possibility of performing quantitative and informative tracer experiments in the current borehole array. The results will serve as a basis for continued planning of the Tracer Test Stage, including the definition of necessary design calculation. The tests will also provide a basis for decisions regarding further optimisation of the multi-packer arrays. The results of the tests will also serve as input as to whether an additional borehole is needed or not.

**Table 5-1. Objectives and performance of pre-tests PT-1 to PT-4. The structural interpretation refers to the March 1999 model.**

Test #	Objective	Performance
PT-1	Test of connectivity within structure #13 and between #13 and #20	Tracer dilution test under natural and pumped conditions. Sink in #13 (KI0023B:P4)
PT-2	Test of connectivity within structure #20 and between #20 and #21, #22, #13, #6 and some minor structures	Tracer dilution test under natural and pumped conditions. Sink in #21 (KI0023B:P6)
PT-3	Test of connectivity within structure #20 and between #20 and #21, #22, #13, #6 and some minor structures	Tracer dilution test under natural and pumped conditions. Sink in #20 (KI0025F02:P5)
PT-4	Test of transport connectivity, assessment of transport properties	Tracer test in radially converging flow geometry. Tracer injection in 3-5 selected sections. Selection of sink and injection sections based on PT-1 to PT-3.

The Pre-tests will include a combination of flow and pressure interference tests similar to the ones performed as part of the Preliminary Characterisation Stage (PCS) (Winberg, 1999). The main difference is the added testing potential introduced by the new borehole KI0025F02, and the introduced changes to the multi-packer systems in KA2563A and KA2511A.

Four pre-tests have now been performed (PT-1 – PT-4) including 35 tracer dilution tests and six tracer transport tests. The preliminary results include PT-1 through PT-3, two tracer injections in KI0023B:P7 (Pre-PT-4) and four tracer injections in PT-4.

The objectives and a listing of involved structures and the used sink (abstraction) sections are listed in Table 5-1.

It should be pointed out that an earlier planned PT-5 focused on Structure #19 has not been performed because of time constraints.

## **5.2 Performance and preliminary results**

### **5.2.1 Pressure response matrix**

The pressure response matrix for PT-1 to PT-3 is shown in Figure 5-1. The matrix is based on the responses during the flow phase. The coding in colours and letters is based on the two defined indexes  $s_p/Q$  (drawdown normalised to pumping rate) and  $t_R/R^2$  (response time normalised to the square of the straight line distance) according to Andersson et al. (1998). For PT-1 and PT-3 the drawdown pattern by the end of the flow phase is shown whereas for test PT-2 the data during the flow phase were truncated at  $t=1140$  minutes due to external disturbances, see below.

Figure 5-1 shows that the pressure responses during PT-1 are restricted to the central area of the block. During PT-2 and -3, most of the monitored borehole sections respond. The response patterns during the latter two tests are similar. The hydraulic responses are discussed in more detail for each test below.


Structure		#13	#21	#20	
Borehole	Interval (m)	PT-1	PT-2	PT-3	Structure
KA2511A:T1	239-293		B	B	#10,11,18
KA2511A:T2	171-238		B	B	#19
KA2511A:T3	139-170		B	B	# ?
KA2511A:T4	111-138		B	B	#20
KA2511A:T5	103-110		B	B	#16
KA2511A:T6	96-102		B	B	#6
KA2511A:T7	65-95		B	B	# ?
KA2511A:T8	6-64		B	B	#4,7
<b>INDEX 1=sp/Q</b> 					
KA2563A:S1	242-246	M	B	B	#19
KA2563A:S2	236-241		B	B	#19
KA2563A:S3	206-208	M	M	G	#13
KA2563A:S4	187-190	M	E	E	#20
KA2563A:S5	146-186	M	G	G	#6,7
<b>INDEX 2=tr/R2</b> E=EXCELLENT G=GOOD M=MEDIUM B=BAD					
KI0025F:R1	169-194		B	B	Z
KI0025F:R2	164-168		B	B	#19
KI0025F:R3	89-163		M	B	?
KI0025F:R4	86-88	M	G	G	# 20
KI0025F:R5	41-85		B	B	#6
KI0025F:R6	3.5-40		B	B	# 5
<b>S=SOURCE</b>					
KI0023B:P1	113.7-200.7		B	B	#10
KI0023B:P2	111.25-112.7		B	B	#19
KI0023B:P3	87.20-110.25	E	E	G	?
KI0023B:P4	84.75-86.20	S	E	M	#13
KI0023B:P5	72.95-83.75	G	G	G	#18
KI0023B:P6	70.95-71.95	B	S	G	#21
KI0023B:P7	43.45-69.95	M	E	E	#6, 20
KI0023B:P8	41.45-42.45		B	M	#7
KI0023B:P9	4.5-40.45			B	#5
KI0025F02:P1	135.15-204		B	B	#?
KI0025F02:P2	100.25-134.15		B	B	#19
KI0025F02:P3	93.40-99.25	B	M	B	#13,21
KI0025F02:P4	78.25-92.4	B	B	B	#?
KI0025F02:P5	73.3-77.25	B	G	S	#20
KI0025F02:P6	64.0-72.3	B	M	M	#22
KI0025F02:P7	56.1-63.0	B	B	M	#?
KI0025F02:P8	51.7-55.1	M	G	G	#6
KI0025F02:P9	38.5-50.7		B	M	#7
KI0025F02:P10	3.4-37.5		B	B	#5
KA3510A:P1	122.02-150				#3,4,5,6,8
KA3510A:P2	114.02-121.02		B	M	#15
KA3510A:P3	4.52-113.02			B	#?
KA3548A01:P1	15-30			B	#?
KA3548A01:P2	10-14			B	#?
KA3573A:P1	18-40		B	B	#15
KA3573A:P2	4.5-17			B	#5
KA3600F:P1	22-50.1			B	#?
KA3600F:P2	4.5-21		B	B	#5, 7?

Figure 5-1. Pressure response matrix for Pre-tests PT-1 to PT-3.

**5.2.2 Pre-test #1 (PT-1)**

The first test, PT-1, performed by pumping Structure #13 in KI0023B:P4, shows pressure responses in 15 borehole sections within the TRUE Block Scale rock volume. The pumping flow rate (at constant head) decreased from 0.89 to 0.68 l/min during the 24-hour pumping period.

In the sink borehole good responses are found in the two sections adjacent to the pumping section (KI0023B:P3 and P5), cf. Figure 5-2. However, both sections have low transmissivity and may be affected by minor changes in the equipment caused by the pressure drop in section P4. It should also be noted that section P3 includes the entire water volume of the (collapsed) central tube. The latter section has therefore been omitted in the diagnostic pressure response plots. Good responses are also found in sections KI0023B:P6 and P7 in the sink borehole. The latter section intersects Structures #6 and #20.

In the receiver boreholes, a very good hydraulic response also occurs in KA2563A:S3 (#13) as expected, cf. Figure 5-2. The remainder of the responding sections are all, except three, interpreted to include structures #6, 7, 13, 20, 21 and 22. The remaining three sections include two low-transmissive sections in KI0025F02 (P4 and P7), and one in structure #19 (KA2563A:S1). Notable also is the slow response in KI0025F02:P3 interpreted to include structure #13. In the latter section the flow rate increased significantly during flowing, cf. Table 5-2.

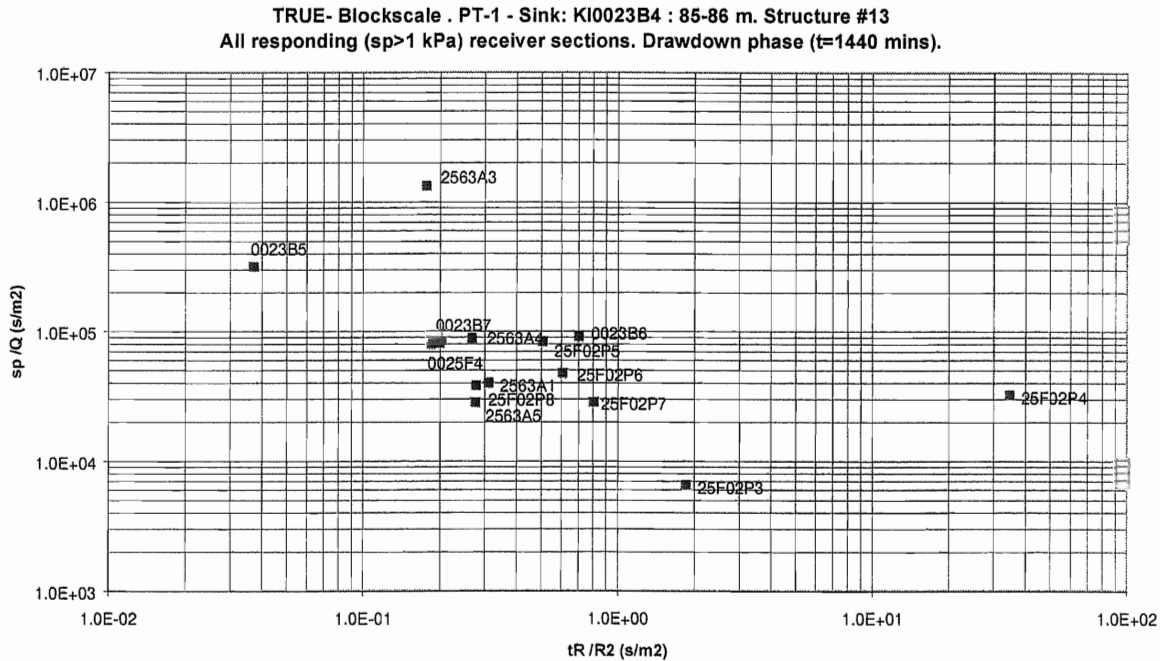


Figure 5-2. Diagnostic response plot for Pre-test PT-1.

The rather strong pressure response in KI0025F02:P8 (Structure #6) may possibly be (partly) explained by the hydraulic short-circuiting in the sink borehole KI0023B. The short-circuit may result in Structure #6 being activated in the former borehole during the flow period via section KI0023B:P7.

PT-1 also included measurements of flow rates using the tracer dilution method in six selected observation sections. The tests were performed both under natural gradient and during pumping in order to study the influence of the pumping. The results presented in Table 5-2 show a distinct influence in three of the selected sections including structures #13, 20 and 21, whereas two sections have a minor and uncertain increase and one section (KI0025F:R4) has no increase at all. The latter section, which is interpreted to contain Structure #20, shows a rather strong pressure response, c.f. Figure 5-2. Notable is that section KA2563A:S4 (formerly R5) has a significantly lower (1/4) natural flow than during the measurements in Spring 1998 (Winberg, 1999). One explanation for this may be the re-instrumentation of KA2563A.

The good flow response in KA2563A:S3 and KI0025F02:P3 confirms the structural interpretation of #13. The response in KA2563A:S4 suggests that Structures #13 and #20 are better interconnected in the NW parts of the block. This is also consistent with the orientation of the two structures.

The most significant pressure response sections (including the tracer dilution sections) during PT-1 are shown in a drawdown versus time/distance squared ( $t_R/R^2$ )-diagram in Appendix B. In a homogenous and isotropic medium all response curves should merge to a common curve. The figure shows that the medium is heterogeneous. The calculated transmissivity and storativity corresponds to the Theis-curve shown and thus mainly represent section KA2563A:S3.

**Table 5-2. Preliminary results of tracer dilution tests during PT-1. Sink in KI0023B:P4 (#13).**

Test section	Structure #	Nat. Flow (ml/h)	Flow during pumping (ml/h)
KA2563A:S3	13	1	16
KA2563A:S4	20	120	280
KI0023B:P6	21	36	40
KI0025F:R4	20	1	1
KI0025F02:P3	13, 21	38	130
KI0025F02:P5	20	49	58
	Increase		
	No increase		
	Uncertain		

### 5.2.3 Pre-Test #2 (PT-2)

The second test, PT-2, performed by pumping Structure #21 in KI0023B:P6, shows pressure responses in 40 of the 47 monitored borehole sections within the TRUE Block Scale array. The pumping flow rate (constant head) decreased from 2.85 to 2.55 l/min during the 48-hour pumping period.

In the diagnostic pressure response plots the data during the flow phase are truncated at  $t=1140$  mins due to external interference after this time. In the sink borehole, strong responses occurred in the adjacent sections KI0023B:P3, P4, P5 and P7 to the flowing section P6 (#21) which results in that several other structures being (indirectly) activated during this test (#6, 13, 18, 20).

In the receiver boreholes, the most prominent responses are found in sections interpreted to include structures #6, 13, 20, 21 and 22, cf. Figure 5-3. The figure shows that the hydraulic connectivity between structures #13, 20, 21 and 22 is very good. The rather strong pressure responses in sections KI0025F02:P8 and KA2563A:S5, located in #6 and 7, may possibly (partly) be explained by the hydraulic short-circuiting in the sink borehole, c.f. above.

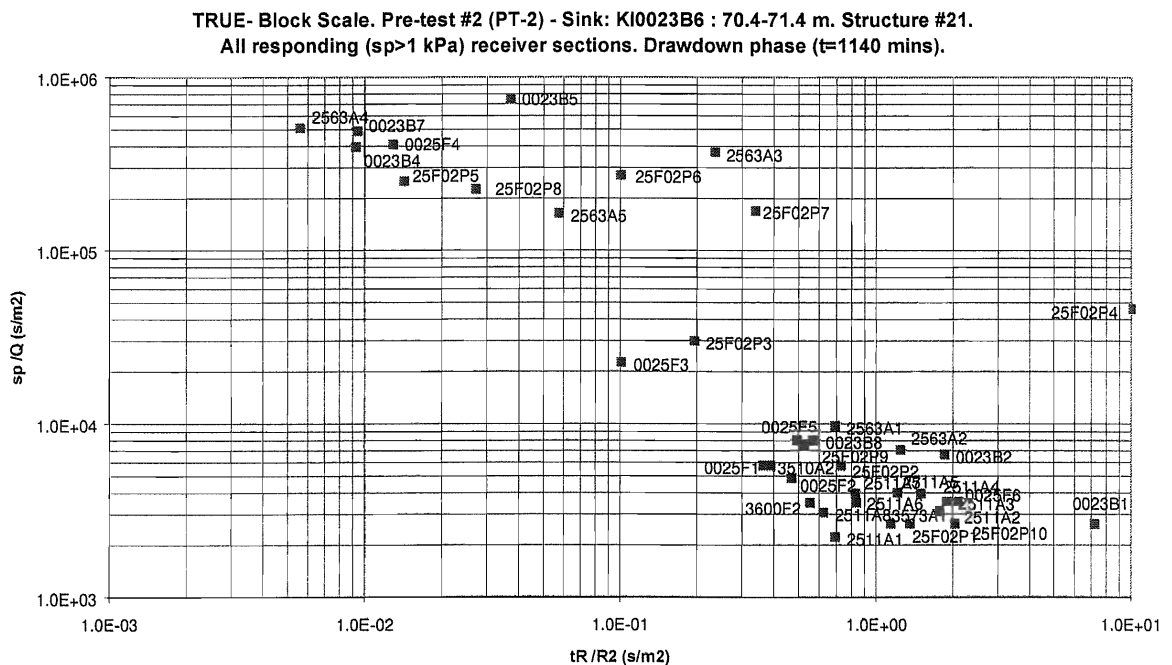


Figure 5-3. Diagnostic response plot for Pre-test PT-2.

The remaining responses are lower and slower. Slow pressure responses are observed in sections KA2563:S1 and S2, indicating that Structure #19 has a certain hydraulic connection to structure #21, cf. Figure 5-3. The non-responding sections are all interpreted to be associated with Structure #5 which seems to be hydraulically well isolated from the system formed by feature #21 and associated structures.

The most significant pressure response sections (including the tracer dilution sections) during PT-2 are shown in a drawdown versus time/distance squared ( $t/R^2$ )-diagram in Appendix C. The calculated transmissivity and storativity corresponds to the limiting Theis'-curve shown and thus mainly represent section KI0025F:R4.

PT-2 included measurements of flow rates using the tracer dilution method in twelve selected observation sections. The test were performed both under natural gradient and during pumping in order to study the influence of the pumping. The results presented in Table 5-3 show a distinct influence in nine of the selected sections including structures #6, 13, 19, 20, 21 and 22 whereas three sections have a minor and uncertain increase/decrease. The two remaining sections measured during PT-2 could not be interpreted to be due to some unknown chemical degradation of the tracer used. In conjunction with PT-4, which uses the same sink as PT-2, some of the uncertainties in the tracer dilution tests were unravelled by repetition of the tests, cf. Table 5-3.

The increases are generally very significant and in one case a decrease is observed from 10100 to 2500 ml/h. This section (KI0023B:P7) is adjacent to the sink and is interpreted to include two structures, #6 and #20. The extremely high flow during natural conditions is likely to be caused by the head difference between structures #6 and #20. When pumping starts in #21, the gradient is reversed, or partly reversed. This is further discussed in Section 5.3.

**Table 5-3. Preliminary results of tracer dilution tests during PT-2. Sink in KI0023B:P6 (#21). Values within brackets are uncertain. The values for these sections are determined from measurements during PT-4 (same flow field).**

Test section	Structure #	Nat. Flow (ml/h)	Pumped flow (ml/h)
KA2563A:S3	13	14	11
KA2563A:S4	20	130	610
KA2563A:S1	19	115	400
KI0023B:P4	13	18	16
KI0023B:P5	?	2	122
KI0023B:P7	6,20	(8800) 10120	(770) 2490
KI0025F:R4	20	3	1
KI0025F02:P3	13,21	25	140
KI0025F02:P5	20	50	111
KI0025F02:P6	22	230	460
KI0025F02:P7	?	(50) 7	(56) 18
KI0025F02:P8	6	(33) 21	(15) 13
	Increase		
	No increase		
	Uncertain		

#### 5.2.4 Pre-test #3 (PT-3)

The third test, PT-3, performed by pumping Structure #20 in KI0025F02:P5, shows pressure responses in 46 of the 47 monitored borehole sections within the TRUE Block Scale array. The pumping flow rate (at constant head) was rather constant throughout the 48-hour pumping period, about 4.8 l/min.

The response pattern for this test is very similar to test PT-2, cf. Figures 5-4 and 5-3. This implies that Structures #20 and #21 have a very good hydraulic connection.

The most prominent responses are found in sections interpreted to include Structures #6, 7, 13, 20, 21 and 22, cf. Figure 5-4. The remaining responses are lower and slower. The same conclusions can be drawn from this test as for the previous test.

The most significant pressure response sections (including the tracer dilution sections) during PT-3 are shown in a drawdown versus time/distance squared ( $t/R^2$ )-diagram in Appendix C. The calculated transmissivity and storativity corresponds to the limiting Theis-curve shown and thus mainly represent section KA2563A:S4.



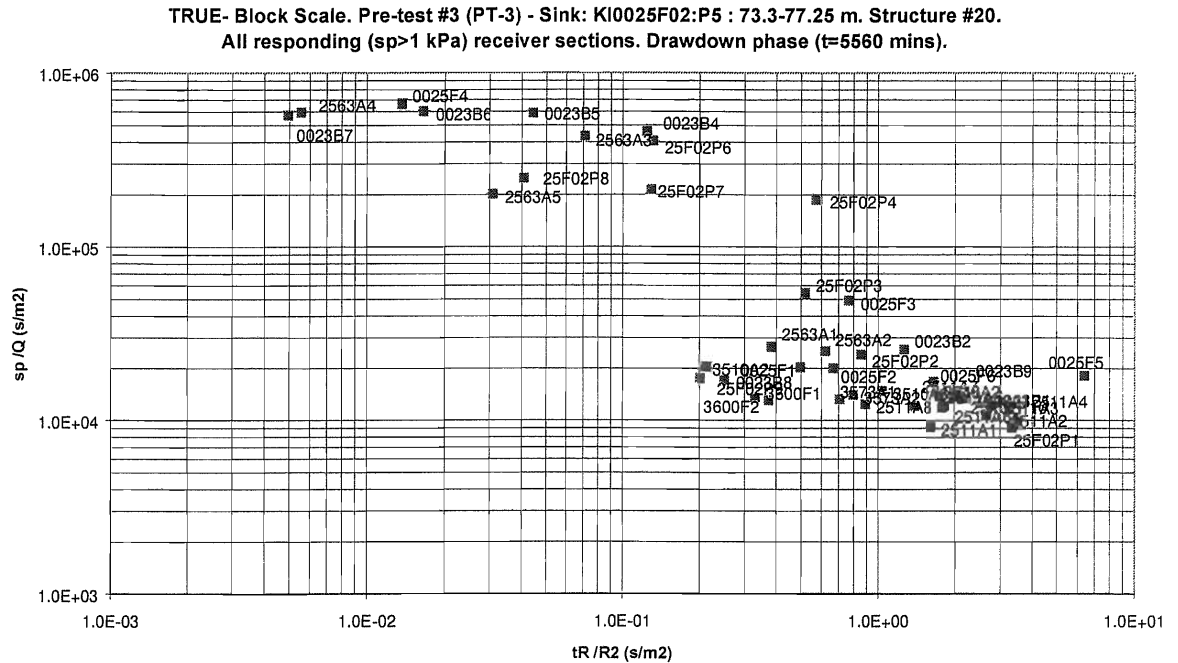


Figure 5-4. Diagnostic response plot for Pre-test PT-3.

PT-3 included measurements of flow rates using the tracer dilution method in twelve selected observation sections. The tests were performed both under natural gradient and during pumping in order to study the influence of the pumping. The results presented in Table 5-4 show a distinct influence in six of the selected sections including Structures #6, 13, 20, 21 and 22 whereas one section (KI0025F02:P8) has a minor and uncertain increase and one (KI0023B:P2) has no increase. The four remaining sections are not yet fully interpreted due to some unknown chemical degradation of the tracer used. Some of these measurements may have to be repeated due to lack of data.

**Table 5-4. Preliminary results of tracer dilution tests during PT-3. Sink in KI0025F02:P5 (#20).**

Test section	Structure #	Nat. Flow (ml/h)	Pumped flow (ml/h)
KA2563A:S3	13	?	15
KA2563A:S4	20	76	950
KI0023B:P2	19	14	14
KI0023B:P4	13	?	?
KI0023B:P5	?	?390	?88
KI0023B:P6	21	3	12
KI0023B:P7	6,20	?	?
KI0025F:R4	20	3	5
KI0025F02:P3	13,21	?	250
KI0025F02:P6	22	100	1500
KI0025F02:P7	?	?	?
KI0025F02:P8	6	33	39
	Increase		
	No increase		
	Uncertain		

### 5.2.5 Pre-PT-4 tests

Prior to the actual tracer injections during PT-4, two tracer injections were performed in KI0023B:P7 with the goal of checking that the pumping in KI0023B:P6 was strong enough to reverse the hydraulic gradient in section P7 caused by the short-circuit between Structures #6 and #20. Figure 5-5 shows a schematic view of borehole KI0023B and the intercepts with different structures.

The first test was performed by injecting a slug of Uranine in the lower part of section P7, close to Structure #20, and the second by injecting a slug of Rhodamine WT close to Structure #6 in the upper part of section P7. The injections were made through the circulation loop.

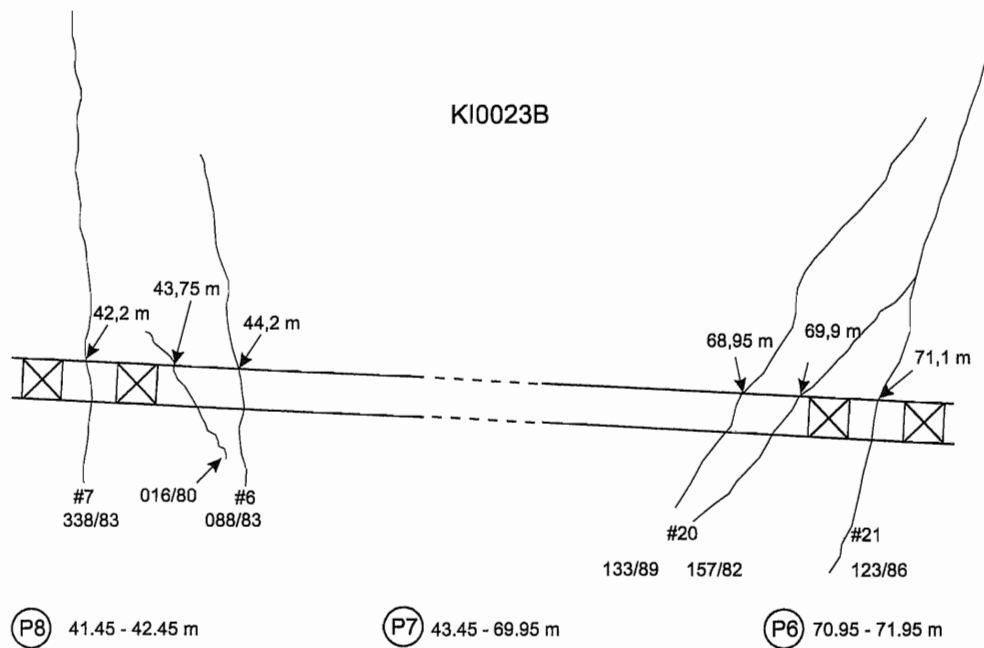


Figure 5-5. Schematic view of borehole KI0023B with fracture intersections in the packed-off sections P6, P7 and P8.

The breakthrough of Uranine (Figure 5-6a) shows a very fast travel time with a first arrival of about 10 minutes. The injection was originally intended to cover the entire length of the section but as breakthrough was clearly visible, the injection was stopped after 25 minutes. The additional small peak after 2 hours results from an unintentional run of the circulation pump creating a short extra pulse. The peak after 4 hours corresponds to the injection of Rhodamine in the upper part of the borehole which was performed by switching the inlet and outlet tubes of the circulation loop. Thus, Uranine remaining in the tube was also injected simultaneously with the Rhodamine pulse. The tracer mass recovery was estimated to 100%.

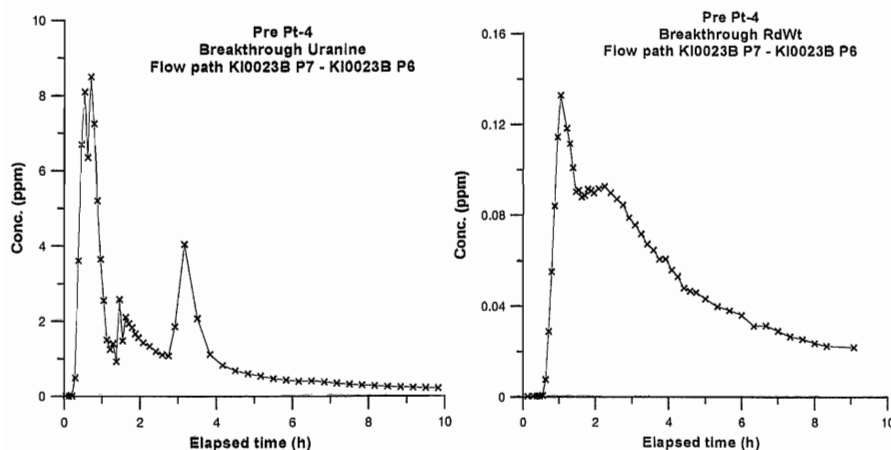


Figure 5-6. Breakthrough of a) Uranine in KI0023B:P6 from injection in the lower part of section P7 and b) of Rhodamine WT in KI0023B:P6 from injection in the upper part of section P7.

The results confirm that Structures #20 and #21 intersect very close to the borehole which also is indicated by the orientation from the BIPS measurement (Figure 5-5).

The breakthrough of Rhodamine WT from the upper part of section P7 (Figure 5-6b) is delayed with about 1-2 hours compared to the Uranine breakthrough which corresponds to the travel time along the 27.5 m long borehole section. The breakthrough confirms that water from Structure #6 flows along the borehole section. However, the tracer mass recovery was estimated to be only about 50%, indicating that some of the tracer mass is lost. Losses could occur either to other fractures intersecting the borehole that are controlled by an even stronger sink than section P6, or by entrapment in poorly mixed parts of the section (no circulation was done).

### 5.2.6 Pre-test #4 (PT-4)

The fourth pre-test, PT-4, was focused on tracer transport. Based on the many good flow responses during PT-2 (Table 5-3) the same set-up was decided for use in PT-4. Pumping was done in KI0023B:P6 with the same pumping rate as PT-2 and four primary injection sections were chosen (Table 5-5). An optional injection section was also selected, but it was decided to limit the number of tracers injected to avoid contamination and also to optimise the analysis efforts. The tracer injection data are presented in Table 5-5.

The injections were performed as decaying pulses. In two of the injections, the tracer solution was exchanged with non-traced water in order to shorten the tail of the breakthrough curve. However, due to the relatively large volume of the circulating system a rather poor efficiency was obtained. The injection concentrations and injection rates given in Table 5-5 are the measured ones.

**Table 5-5. Tracer injection data for PT-4 (measured values).**

Inj #	Section	Structure	Tracer	Max Inj conc(mg/l)	Inj rate (ml/h)*	Vol. of sect. (ml)
1	KA2563A:S4	20	Rhodamine	120	680	6883
2	KA2563A:S1	19	Uranine	420	220	8814
3	KI0025F02:P3	13, 21	Amino G Acid	2200	113	8238
4	KI0025F02:P6	22	Rhodamine	250	350	9717

\*) Calculated from the tracer dilution during injection

The injection functions presented as the logarithm of concentration (Ln C) versus time are shown in Figure 5-7.

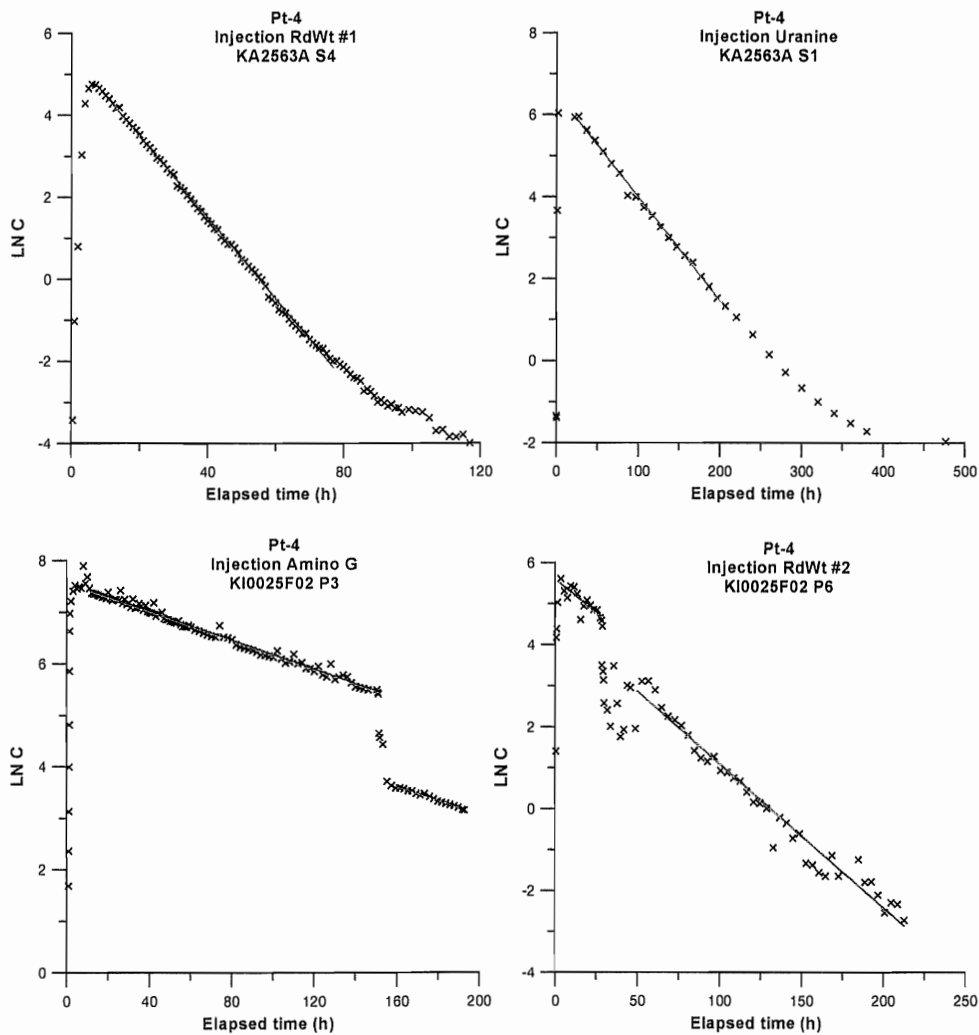


Figure 5-7. Tracer injection functions ( $\ln C$  versus time) including straight-line fits for the four injections during PT-4. Note that the scales of the different axes are different.

The breakthrough of tracer was monitored both in the sink section KI0023B:P6 and also in the adjacent section P7, where the short-circuit between Structures #6 and #20 occurs. Tracer breakthrough was detected from all four injections in section P6. The resulting breakthrough curves are not yet fully analysed but preliminary breakthrough data are presented in Figure 5-8.

The pumping was stopped on June 15<sup>th</sup> after a pumping period of 28 days. The equipment was removed for cleaning and maintenance. No major equipment failure occurred during the test period.

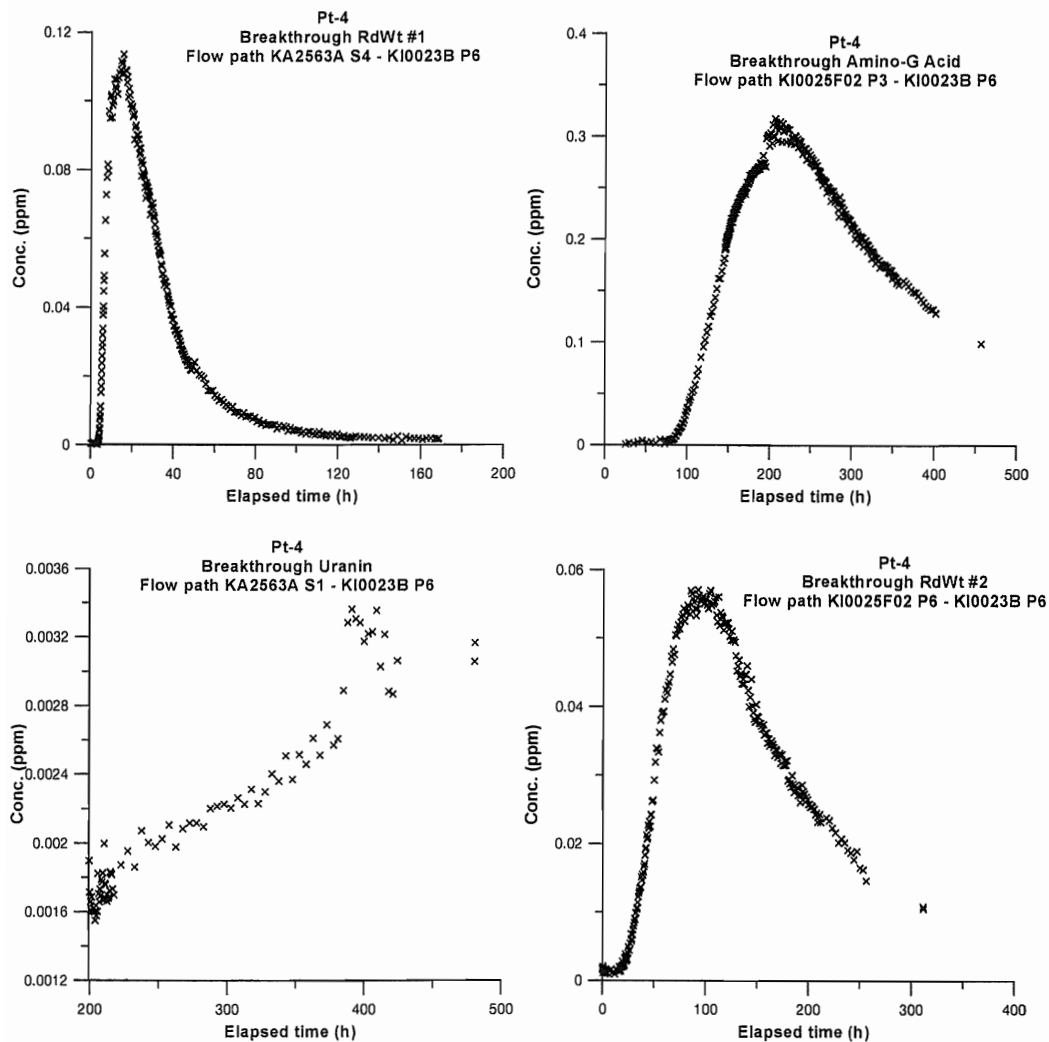


Figure 5-8. Tracer breakthrough in KI0023B:P6 during PT-4. Note that the scales of the axes differ between the plots.

Preliminary calculations of the tracer mass recovery (Table 5-6) shows high mass recovery for two of the flow paths (>75%). A rather large portion of the tail of the breakthrough at the termination of the test still remains to be recovered and it is therefore likely that the mass recovery would have risen to close to 100%. The mass recovery of Rhodamine WT from KA2563A:S4 only reaches about 50%, i.e. only slightly higher than during ESV-1c (Andersson et al., 1998), this despite the fact that the discharge from KI0023B:P6 during PT-4 was 2.5 times higher (2.5 l/min compared to 1.0 l/min during ESV-1c). Finally, the mass recovery of Uranine from Structure #19 in KA2563A:S1 is still less than 1% after 480 hours. It is likely that, in the latter case, the flow path from the injection point to the sink is very long and complicated, as several structures need to be crossed. Preliminary statistics related to the observed breakthrough are presented in Table 5-6.

No tracer breakthrough was observed in KI0023B:P7 during the pumping period.

**Table 5-6. Preliminary tracer mass recoveries from KI0023B:P6 during PT-4.**

Inj #	Section	Structure	Tracer	Mass Recovery (%)	Sampling time (h)
1	KA2563A:S4	20	Rhodamine	51	169
2	KA2563A:S1	19	Uranine	<1	480
3	KI0025F02:P3	13, 21	Amino G Acid	76	456
4	KI0025F02:P6	22	Rhodamine	80	311

**Table 5-6. Preliminary statistical data related to the observed breakthroughs in KI0023B:P6 during PT-4.**

Inj #	Section	T <sub>5</sub>	T <sub>50</sub>	T <sub>95</sub>
1	KA2563A:S4	10	131	N.A.
3	KI0025F02:P3	142	300	N.A.
4	KI0025F02:P6	39	139	N.A.

## 5.3 Conclusions regarding tracer test array

### 5.3.1 Re-mediation of KI0023B

The results of the tracer dilution tests in KI0023B:P7 clearly indicates that there is a major short-circuit between structures #6 and #20 in the borehole section. The measured “natural” flow rate is in the order of 10 l/h in the direction from #20 to #6, i.e. towards the tunnel. This is also consistent with the hydraulic head measurements that indicate a 5-m head difference between the two structures. However, the tracer dilution tests and the pre-PT-4 tests indicate that the gradient in P7 can be reversed by pumping section P6.

This means that tracer tests may be performed when KI0023B:P6 is used as a sink, which is also supported by the results of PT-4. However, if another sink is used it may be more difficult to control the head field and avoid tracer loss. A brief study of the head distribution during PT-3 (KI0025F02:P5 as sink) shows that the head in section P6 still is somewhat lower than in section P7 (about 20 kPa) during pumping. Thus, the gradient should still be directed towards P6. A different choice of sink than in PT-4 would most

probably require further pre-tests to assess the possibility of performing successful tracer tests.

Another uncertainty related to KI0023B is the unknown structure in section P5 which is located in between structures #13 and #21. The results of PT-1 to PT-3 and also the previous tests (Winberg, 1999) shows that section P5 is well connected to the neighbouring structures. This is a potentially interesting tracer injection point but the exact location is not known from the 5-m packer logging. This also implies that the packers need to be re-arranged.

In summary, it is possible to perform tracer tests without re-mediation of KI0023B, but the consequences of choosing another sink need to be explored further. The flowing structure in section P5 cannot be used as a potential injection point without removing and re-arranging the packer system.

### **5.3.2 Suggestions for optimisation of the borehole array**

#### *KI0025F*

The latest update of the structural model (March'99) includes a feature (#22) that is currently located beneath the packer between section R4 and R3 at 88.8 m borehole length in borehole KI0025F. During flow logging in 5-m intervals a flow rate of 1.08 l/min was measured in the interval 87-92 m. Later, during the pressure buildup tests, a localisation of this flowing structure was made, with the main flow located to the section 87.0-87.75 m. However, the detailed localisation was stopped at 88.75 m, i.e. very close to the interpreted intercept of Feature #22. The flow was also measured at 0.72 l/min at a pressure drop of 42 bars. The flow rates may be somewhat difficult to compare, as boundary conditions are different, but there is a possibility that the flow difference is associated with the interpreted Feature #22.

One way of exploring this would be to simply push the entire instrumentation in KI0025F in two steps of one metre and measure the resulting flow. That means that the packers are moved from the original position at 86-88 m, involving only Structure #20, to 87-89 m involving both structures, and finally to 88-90 m involving only Feature #22. If Feature #22 is located, a short-term interference test should be done.

#### *KI0025F02*

The last update of the March-99 model also includes a dual intercept of Feature #21 and Structure #13 in borehole section KI0025F02:P3. The structures are relatively well-separated (4 m) and are easily identified in the detailed POSIVA flow log. Based on the results of the tracer dilution tests and the tracer test during PT-4 it is clear that this section is very interesting for future tracer tests. A separation of the two structures



would possibly further increase the understanding of the structures and maybe also increase the number of possible tracer injection points.

Another observation is that the “natural” flow rate measured in this section (25-40 ml/h) is relatively high in comparison with other structures with similar transmissivity. This may indicate that a short-circuit between the structures induces a gradient, resulting in increased flow rates. However, it should be noted that the head difference between the structure probably is much less than in KI0023B:P7.

In summary, the instrumentation of KI0025F02 seems to be well optimised, with the exception of the section mentioned above. It should also be noted that the structure at 93.9 m (#13) has about one order of magnitude lower transmissivity than Feature #21 at 97.9 m. Thus, it is likely that the main part of the transport occurs in Feature #21. The orientation of the two structures also indicates that they intersect not far from the borehole. This may entail that a separation would not result in a significant gain.

### **5.3.3 Need for a new borehole**

The tracer tests performed during PT-4 and the dilution tests performed during PT-1 to PT-3 clearly shows that there are several potential tracer injection points in the current array. From this point of view there is a limited need for a new borehole. There are, however, a number of arguments in favour of drilling a new borehole. These are:

- The inter-distances between injection and sinks are rather long, from 16 metres and upwards in the current array. This may limit the number of possible pathways for injection of sorbing tracers,
- The borehole intercepts with the target structures line up more or less at the same depth in the array. This means that anisotropy in the system cannot be studied.

## **6. Experimental design and predictions**

### **6.1 Background and scope**

A number of numerical models of the TRUE Block Scale rock volume have been developed on a 500 m scale. These include a stochastic continuum model (SC), a discrete feature network model (DFN), and a channel network model (CN). In addition, a site-scale DFN model has been constructed which can be used to generate boundary conditions for the smaller compartment models. At the time of the TC#9 in mid April it was decided, a) given the pending possible imminent update of the March'99 model resulting from the hydraulic reconciliation study, and b) the fact that updating of DFN and SC models is quite time consuming (models presently in line with Sep'98 structural model), and c) the fact that the channel network model was more or less up to date with the March'99 structural model as a consequence of its use for generic studies of the effects of fracture intersections, to use the latter model to produce predictions of the PT-4 tracer tests;

In the following an account is given of the use of the channel network model for;

- 1) Generic and site-specific studies of the possibility to capture the effects of fracture intersection zones (FIZ) in the planned tracer tests
- 2) Blind predictions of the PT-4 tracer tests

The former task has implications for the practical possibility to address hypotheses 2a and 2b fully, cf. Section 3.3. The latter task provides a test of our present capability to predict tracer transport in the investigated rock volume. The predictive work is preceded by calibration of the model to the hydraulic and tracer dilution data from Pre-tests PT-1 through PT-3.

### **6.2 Study of fracture intersection effects**

#### **6.2.1 General**

In a fracture network, the area on a fracture where another fracture intersects has the potential of having either enhanced or reduced permeability and porosity when compared with the rest of the fracture. Depending on the effects that fracturing has on existing fractures the fracture intersection zone (FIZ) can be developed as a highly

permeable flow channel or as a flow barrier. Alternatively, the result is a mixture of both, or the effects are minimal, making it distinction difficult from the heterogeneity in individual structures.

The locations of the flow channels on any fracture surface are normally not known. In the case of large fractures, however, whose positions in space are known, the location of the FIZ can be determined. This provides the opportunity to design hydraulic tests in a way that the FIZ will be part of the flow channel network that is affected by the tests.

The purpose of this study is to evaluate the possible tracer test designs and the feasibility of identifying network or fracture intersection zones (FIZ) effects within those tracer tests.

In order to achieve this, a generic pattern of channels was distributed on a “generic” fracture plane, cf. Section 6.2.2, and on a fracture plane representing “Structure #20”, cf. Section 6.2.3. These generic patterns of channels are designed to represent the heterogeneity of aperture on fracture surfaces. Future extensions of this study will consider more realistic patterns of roughness based eg. on measurement on actual fracture surfaces, based on resin injection. For this study we are focusing on tracer experiments in the immediate vicinity of a FIZ. As a result, we are concentrating the modelling effort on the fracture of interest as a single plane with intersections and channels.

### **6.2.2 Generic FIZ study**

The basic model used for the generic study consists of two fractures that intersect each other, cf. Figure 6-1a. Both fractures contain a number of random flow channels. At the intersection of the two fractures a FIZ exists, which builds a deterministic flow channel. Both fractures are also intersected by two wells. The intersections are isolated with packers, so they can be used as test intervals.

If tracer is released at the source location it will travel through the flow channel network on the first fracture towards one of the sink intervals. If the sink interval is on the second fracture the tracer will travel a certain distance along the flow channel built by the FIZ before entering the flow channel network on the second fracture. The exact pathway, and therefore the portion of the pathway within the FIZ, is a function of the (random) location of the flow channels and of the packer interval configuration.

If gravity effects are ignored, the flow channel network built by the two fractures shown in Figure 6-1a can be modelled in two dimensions. The resulting conceptual model is shown in Figure 6-1b and the rectangular grid representation in Figure 6-1c.

The channel network model used in this study combines, cf. Figure 6-1c;

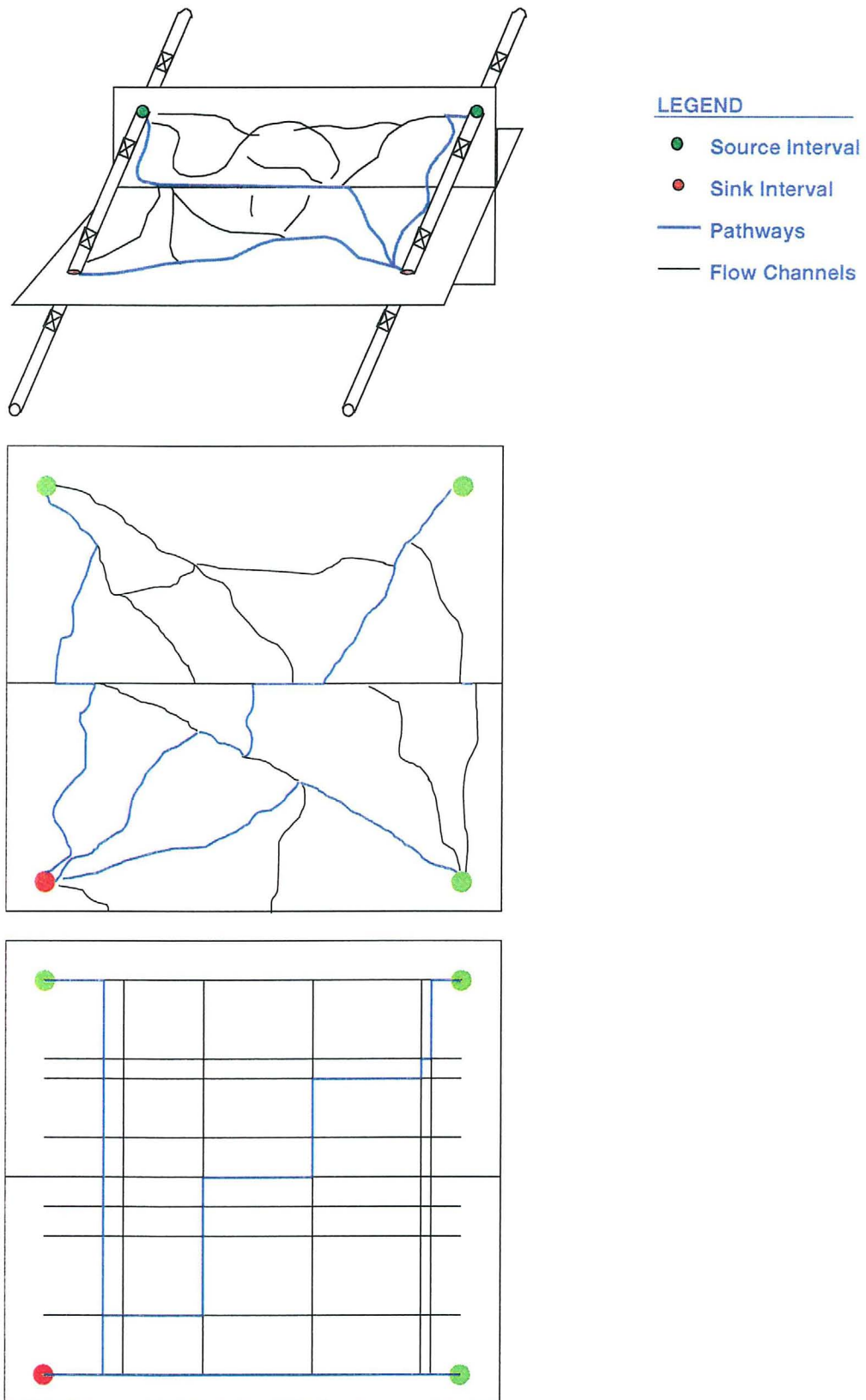


Figure 6-1a) Conceptual model of two fracture intersection, b) Two-dimensional representation of model, c) Rectangular grid based on 2D representation, red=sink.

- deterministic elements (the fractures, the FIZ and the packer intervals)
- stochastic elements (the channels).

### *Channel Network Model*

The model region is 100 x 100 m. The transmissivities of the channels are assigned stochastically based on the defined transmissivity distribution. Ten realisations of the fracture network were generated. Channel apertures were calculated using the following equation:  $2b = 2 T^{0.5}$  (Uchida, et al, 1994). The simulated tracer test was designed as an equal strength dipole test. The model contains one source zone, which is injecting water at a constant head of 10m, and a sink zone, which is withdrawing water at a constant head of -10m. All intervals are at a distance of 48.5 m from the FIZ.

### *Simulation strategy*

The main purpose of the simulations was to investigate under which circumstances the FIZ can be ‘seen’ by tracer tests. As mentioned above, the properties of the FIZ can not be measured directly by *in-situ* experiments, but only in combination with the properties of the overall fracture network. Thus a single tracer test is not sufficient to assess the properties of the FIZ.

However, the simulations allow us to test the hypothesis by comparing results from multiple simulations. By locating well pairs in a certain way, it is possible to generate pathways between well pairs with very different portions of the total pathway length affected by the FIZ. To assess the effect of the FIZ, the minimum travel time for these three different well pairs was computed for:

- Pair 1: Parallel to FIZ
- Pair 2: Perpendicular to FIZ
- Pair 3: Diagonally across the FIZ

For pair 1 the shortest pathway lies completely outside the FIZ. The flow field during a dipole test (and with it the tracer travel time), however, will be affected by the FIZ. For pair 2, the tracer travel time will be affected the least by the FIZ, because all the flow lines will cross the FIZ perpendicularly. For well pair 3, the flow field will be affected by the FIZ, and a large portion of the pathway falls within the FIZ.

### *Transmissivity Models*

The ability to “capture” the FIZ will largely depend on the transmissivity contrast between the FIZ and the surrounding flow channel network. To study this aspect the following four different pipe network cases were generated and analysed:

- Case 1: Homogeneous pipe network, where all pipes including the FIZ have the same transmissivity ( $1 \cdot 10^{-8} \text{ m}^2/\text{s}$ )
- Case 2: Homogeneous pipe network with increased transmissivity for the FIZ ( $1 \cdot 10^{-3} \text{ m}^2/\text{s}$ ), ie. a five order of magnitude difference.
- Case 3: Heterogeneous pipe network, where the pipe transmissivities are random (Normal or Log distribution) except for the FIZ. Transmissivity for the FIZ equals mean of transmissivity distribution ( $1 \cdot 10^{-8} \text{ m}^2/\text{s}$ )
- Case 4: Heterogeneous pipe network, where the pipe transmissivities are random except for the FIZ. Transmissivity for the FIZ is greater than mean of the transmissivity distribution ( $1 \cdot 10^{-3} \text{ m}^2/\text{s}$ )

Cases 1 and 2 assume a homogeneous flow channel network. In Case 1, it is also assumed that the FIZ does not have an increased transmissivity with respect to flow channels in other areas of the fracture. In Case 2 the FIZ transmissivity is increased in comparison with the transmissivity of the flow channels.

For Cases 3 and 4 it is assumed that the transmissivity along the flow channels varies significantly (Normal or Log distribution with standard deviation of  $1 \cdot 10^{-2} \text{ m}^2/\text{s}$ ). In Case 3 the assumption is that the FIZ has no increased transmissivity compared to the flow channels in other areas of the fracture, while Case 4 assumes an increased transmissivity along the FIZ.

### *Results*

The simulations include a pathway search which minimises the overall travel time between the source and the sink interval. The search was carried out for all 10 generated realisations for each case. Table 6-1 shows the results for the four cases modelled and the three assumed well pair setups.

**Table 6-1 Calculated shortest travel time pathways (base cases 1-4)**

<b>Model</b>	<b>Travel Time (hours)</b>		
	<b>Diagonal</b>	<b>Perpendicular</b>	<b>Parallel</b>
Case 1: Homogeneous	5500	1053	1467
Case 2: Homogeneous with increased T for FIZ	6750	1064	1681
Case 3: Heterogeneous	5333	2481	2805
Case 4: Heterogeneous with increased T for FIZ	10278	2742	5861

Table 6-1 shows that an increased transmissivity in the FIZ causes an increase in the smallest travel time for all well pairs. This is probably caused by the larger fracture aperture that is assumed in the model for fractures with an increased transmissivity. The larger aperture causes a slower flow velocity and thus, a longer travel time.

Surprisingly, a FIZ with a higher transmissivity is almost 'invisible' in a homogeneous channel network. The travel times are similar for both cases, with and without the increased transmissivity in the FIZ.

For a heterogeneous channel network, the effects of the increased transmissivity in the FIZ is more apparent. The smallest travel time doubles for the parallel and the diagonal well pairs. Only the perpendicular well pair (which was not expected to be influenced by the FIZ, anyway) shows similar travel times.

#### *Model variations and sensitivity studies*

The above model cases were rerun with a situation where the test sections are located 15 m from the FIZ (compared to 48.5 m in the modelled base cases). The results indicate that a shorter distance will increase the possibility to 'capture' the FIZ.

The homogeneous base cases were rerun with a factor 2.5 higher density of flow channels (50 fractures compared to 20 in the base cases). No significant difference compared to the base cases was observed.

The cases with a 15 m distance between the test intervals and the FIZ were rerun with increased and decreased transmissivity contrast. No significant differences were observed compared to the results of the above variation runs.

### **6.2.3 Site-specific FIZ study on Structure #20**

Structure #20 of the TRUE Block Scale rock block is the current focus of tracer test design, together with hypothesised intersecting Type 2 Features #21 and #22. A plan view of Structure #20 depicting the geometry of these intersections is shown in Figure 6-2.

Structure #20 is currently intersected by four boreholes (KA2563A, KI0023B, KI0025F02, KI0025F). The locations of these intersections are shown in Figure 6-2. In addition to these existing intersections two additional hypothesised intersections (new\_1 and new\_2), representing new boreholes, were included in the model so that various well pairs for the tracer tests could be investigated.

It is assumed that Structure #20 contains a number of random flow channels. Their locations are not known. At the intersections of Features #21 and #22 with Structure #20

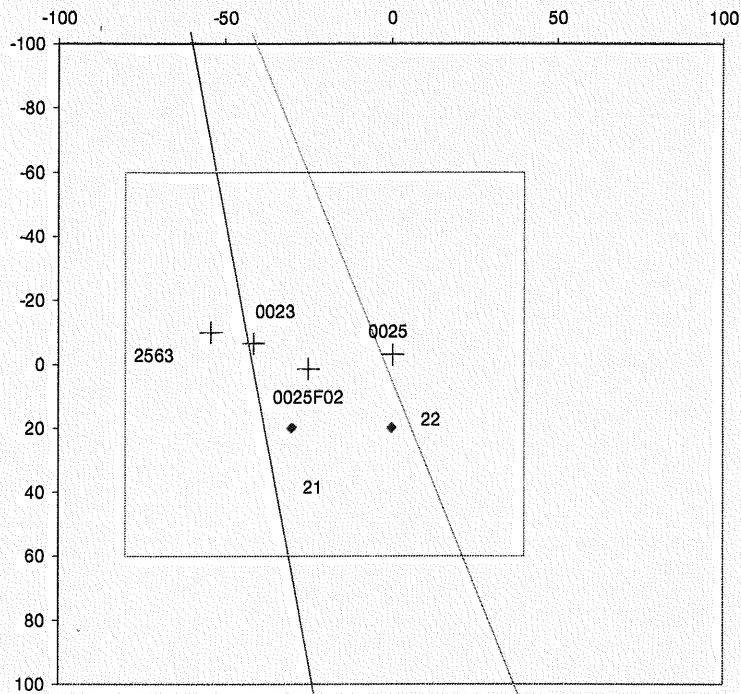


Figure 6-2 Intersections in the plane of Structure #20 with Type 2 Features #21 and #22 and existing and hypothesised new exploration boreholes.

two FIZs are assumed, both of which form deterministic flow channels with known locations.

#### *Channel network model*

The channel network model for this study contains deterministic elements (Structure #20, Type 2 Features #21 and #22, and the packer intervals) as well as stochastic elements (the random flow channels). The model region is 120 x 120 m. Channels are located by a Poisson line process, with transmissivity according to a defined transmissivity distribution.

Five to twenty realisations of the channel network pattern were generated on each fracture plane. The locations and transmissivities of all channels except for the FIZ follow a Poisson line process. Transport apertures were calculated using the following equation:  $2b = 2 \cdot T^{1/2}$  (Uchida, et al, 1994).

#### *Simulation strategy*

The tracer tests were simulated as radially converging tests. The model contains one sink zone, which is located in one of the new borehole locations. The sink zone is withdrawing water at a constant rate of 1 l/min. No active injection takes place at the source locations. The respective head field was calculated using MAFIC1D.



The previous generic model used a dipole test configuration. The dipole test is penetrating a larger region, so that effect of the FIZ was diluted, cf. Section 6.2.2. Radially converging tests typically affect smaller regions. Therefore it is hoped that a radially converging test gives a better resolution of the FIZ than what was seen in the generic FIZ model. To assess the effect of the FIZ the tracer breakthrough time was computed for the following three well pairs:

- Pair 1: KA2563A to new\_1 (across the FIZ)
- Pair 2: KI0023B to new\_1 (parallel to FIZ)
- Pair 3: KI0025F02 to new\_1 (not affected by the FIZ)
- Pair 4 : KI0025F to new\_2 (across FIZ)

Tracer is added at the respective borehole locations by dilution. Tracer breakthrough at the sink locations was calculated using a Laplace Transform Galerkin solver (LTG) (Dershowitz et al., 1998).

### *Transmissivity models*

The ‘visibility’ of the FIZ will largely depend on the transmissivity in the FIZ and in the surrounding flow channel network. To study this aspect these three different pipe network cases were generated:

- Case 1: Homogeneous pipe network, where all pipes including the FIZ have the same transmissivity ( $1 \cdot 10^{-6} \text{ m}^2/\text{s}$ )
- Case 2: Homogeneous pipe network with increased transmissivity for the FIZ ( $1 \cdot 10^{-4} \text{ m}^2/\text{s}$ )
- Case 3 : Heterogeneous pipe network, where the pipe transmissivities are random (Normal or Log distribution) except for the FIZ, transmissivity for the FIZ equals mean of transmissivity distribution ( $1 \cdot 10^{-6} \text{ m}^2/\text{s}$ )
- Case 4: Heterogeneous pipe network, where the pipe transmissivities are random (Normal or Log distribution) except for the FIZ, transmissivity for the FIZ equals mean of transmissivity distribution ( $1 \cdot 10^{-5} \text{ m}^2/\text{s}$ )
- Case 5: Heterogeneous pipe network, where the pipe transmissivities are random (Normal or Log distribution) except for the FIZ, transmissivity for the FIZ equals mean of transmissivity distribution ( $1 \cdot 10^{-4} \text{ m}^2/\text{s}$ )
- Case 6: Heterogeneous pipe network, where the pipe transmissivities are random (Normal or Log distribution) except for the FIZ, transmissivity for the FIZ equals mean of transmissivity distribution ( $1 \cdot 10^{-2} \text{ m}^2/\text{s}$ )

Cases 1 and 2 assume a homogeneous flow channel network. In Case 1, it is also assumed that the FIZ has no increased transmissivity compared to the flow channels in other areas of the fracture. In Case 2 the FIZ transmissivity is increased in comparison with the transmissivity of the flow channels.

For Case 3 through 6 it is assumed that the transmissivity along the flow channels varies significantly (Normal or Log distribution with standard deviation of one order of magnitude). For Case 3, the FIZ has no increased transmissivity, ie. its transmissivity equals the mean of the Normal or Log distribution. In Cases 4, 5 and 6 the FIZ transmissivity is  $10^{-5}$ ,  $10^{-4}$ ,  $10^{-2}$  m<sup>2</sup>/s, respectively. These cases are used to study whether it is possible to distinguish between a homogeneous flow channel network with an FIZ and a heterogeneous network without an FIZ.

### Results

Breakthrough curves were generated and the median breakthrough time was calculated ( $t_{50}$ ) for the four cases and for four different well pairs, cf. Table 6-2. An example suite of breakthrough curves is shown in Figure 6-3.

**Table 6-2 Calculated median breakthrough time  $t_{50}$  for the hypothesised new sink sections in New\_1 and New\_2, cf. Figure 6-2.**

Source interval	Median Breakthrough Time $T_{50}$ (h)			
	KA2563A	KI0023B	KI0025F02	KI0025F
Sink interval	new_1	new_1	new_1	new_2
Case 1: Homogeneous	81	52	28	27
Case 2: Homogeneous with increased T for FIZ ( $1e^{-4}$ m/s)	161	94	27	59
Case 3: Heterogeneous	347	188	62	51
Case 4: Heterogeneous with increased T for FIZ ( $1e^{-5}$ m/s).	376	185	58	46
Case 5: Heterogeneous with increased T for FIZ ( $1e^{-4}$ m/s).	446	166	95	113
Case 6: Heterogeneous with increased T for FIZ ( $1e^{-2}$ m/s).	835	564	87	642

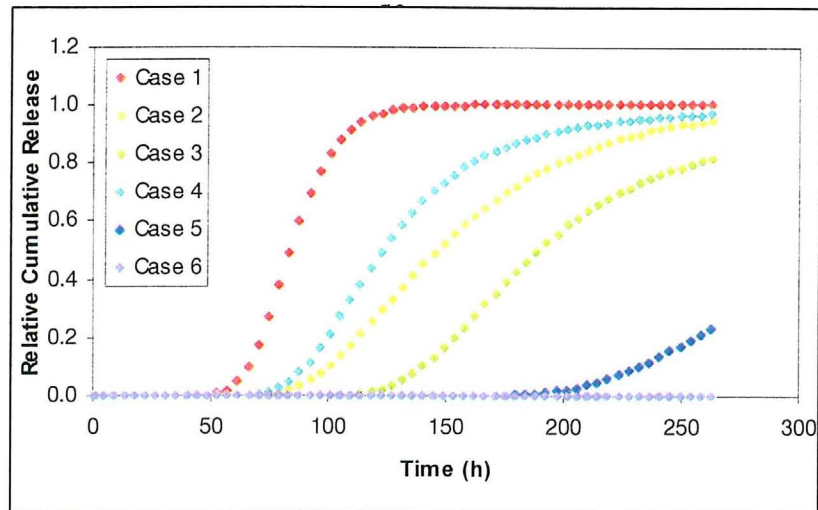


Figure 6-3 Example suite of breakthrough times for injection in KA2563A and pumping in fictive borehole New\_1.

It can be seen in Table 4-1 that for the source intervals KA2563A, KI0023B and KI0025F, an increased transmissivity in the FIZ causes a doubling of the breakthrough time. This is caused by the larger fracture aperture that is assumed in the model for fractures with an increased transmissivity. The larger aperture causes a slower flow velocity and thus, a longer travel time.

Surprisingly, tracer released in KI0023B is affected as much by the FIZ as tracer released in KA2563A although tracer does not have to travel directly through the FIZ. Obviously the FIZ changes the overall flow field and changes the flow velocity in the flow channels in its vicinity.

As expected, tracer released at source interval KI0025F02 is not effected by the FIZ. Hence, the breakthrough times for Cases 1 and 2 are identical. This trend is maintained also for the heterogeneous cases.

For the heterogeneous channel networks, the effects of varying the channel and intersection transmissivities are evident in the large range of breakthrough times for the different realizations. For example, in Case 3, the tracer released in zone KI0025F02 had breakthrough times that range from 18.5 hours to 494 hours. Overall, the existence of slower sections in the pathway causes most realizations to have longer breakthrough times. Hence, the majority of the median breakthrough times for Case 3 are approximately twice as large as the median breakthrough times for Case 2.

The large increase in transmissivity in Cases 5 and 6 generally seem to result in correspondingly higher breakthrough times. However, there is an exception with the source interval KI0023B. The breakthrough time for this interval decreases. The reason for this unexpected result has not been determined.

### *Identification of FIZ in a field situation*

In reality, if the existence of an FIZ is to be investigated, it is obviously not possible to compare test results for cases with and without an increased transmissivity in the FIZ. Instead only one of the cases discussed above, or a combination of them exists, and the goal is to unveil the actual situation. A comparison of possible test results can only be made for the three different well pairs.

As shown before, the velocity for tracer released in zones KA2563A and KI0023B should be affected, if a higher transmissivity exists within the FIZ. In opposition to that, the velocity for tracer released in zone KI0025F02 should not be effected. Hence, a comparison of the tracer velocities should reveal the existence of an FIZ.

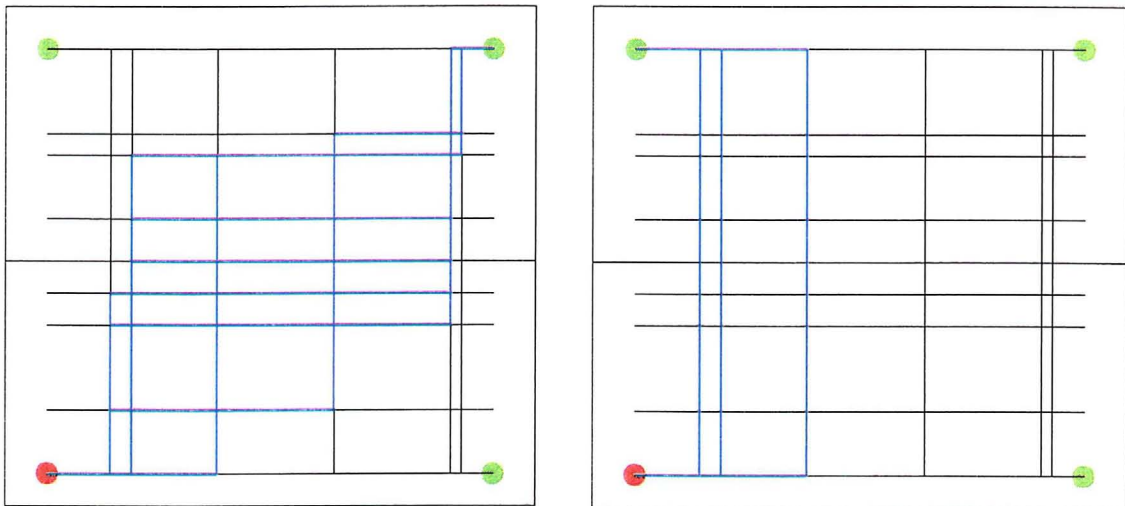


*Figure 6-4. Area affected by diagonal and perpendicular well pairs, respectively.*

However, as shown in the generic FIZ model, the tracer velocity will also be effected by the pipe network geometry. Generally, flow velocity is a function of the flow rate and the flow cross sectional area. In this case the area is the sum of the single pipe cross-sectional areas weighted by flow fraction.

In the previous model in the case of the diagonal well pair the cross sectional area was significantly larger than in the case of the perpendicular well pair, cf. Figure 6.4. Hence, the flow velocities for the diagonal well pair were always slower than for the perpendicular well pair.

In order to eliminate this effect the test configuration was changed to a radially converging flow, where mainly a series of flow channels or different geometry are affected, rather than a set of channels parallel to the flow direction. Furthermore the well pairs are all similarly oriented compared to the pipe network (diagonal flow pattern). Therefore all well pairs should be effected in a similar way.

### 6.2.3 Site-specific model with sorbing tracers

The study described in the previous chapter of this report illustrates the difficulty of identifying FIZ effects for transport based on conservative tracers. This is in part due to the balancing effects of aperture on flux (transmissivity) and cross sectional area on advective transport velocities.

For transport of sorbing tracers, however, the FIZ can be expected to have more pronounced effects due to the smaller surface area available for sorption and diffusion along FIZ pathways. This section describes a series of numerical studies carried out to characterize the possibilities for detection of FIZ effects using sorbing tracers in the fracture network of Structures #20, #21, and #22.

#### *Channel network model*

The channel network model for this study contains deterministic elements (Structure #20, #21, #22 and packer intervals) as well as stochastic elements (random flow channels). The model region is 200m x 200m. Channels are located by a Poisson line process with a constant transmissivity of  $5 \times 10^{-6} \text{ m}^2/\text{s}$ , the assumed transmissivity of Structure #20.

Approximately thirty realizations of both a high and low-density channel networks were generated on the fracture plane. The low-density network contains a set of 100 channels while the high-density network contains 200 channels. Transport apertures were based on the equation  $2b=2T^{1/2}$  (Uchida, et al, 1994). The widths of the channels and FIZ were set at 0.5 m and 0.005 m, respectively. Figures 6-5 and 6-6 show examples of the low and high-density models along with the FIZ and borehole locations.

#### *Simulation strategy*

The simulated tracer test was designed as a radially converging test. Each simulation contains one sink and one source. The sink zone is withdrawing water at a constant rate of 1 l/min. No active injection takes place at the source locations. Simulations were conducted using numerous source and sink combinations with non-sorbing and sorbing tracers. Helium-3 and Barium-133 were used as tracers. Table 6-3 contains the properties of Helium-3 and Barium-133 used, where Ba-133 is considered more sorbing compared with the Helium.

**Table 6-3. Properties of Barium-133 and Helium-3 used in simulations.**

Property	Parameter/unit	Barium-133	Helium-3
Sorption coefficient	$K_d$ ( $m^3/kg$ )	1.3E-03	0.0
Diffusivity	$D_w$ ( $m^2/s$ )	8.24E-10	1.0E-12
Half-life	$\lambda$ (1/yr)	0.0952	9E-09

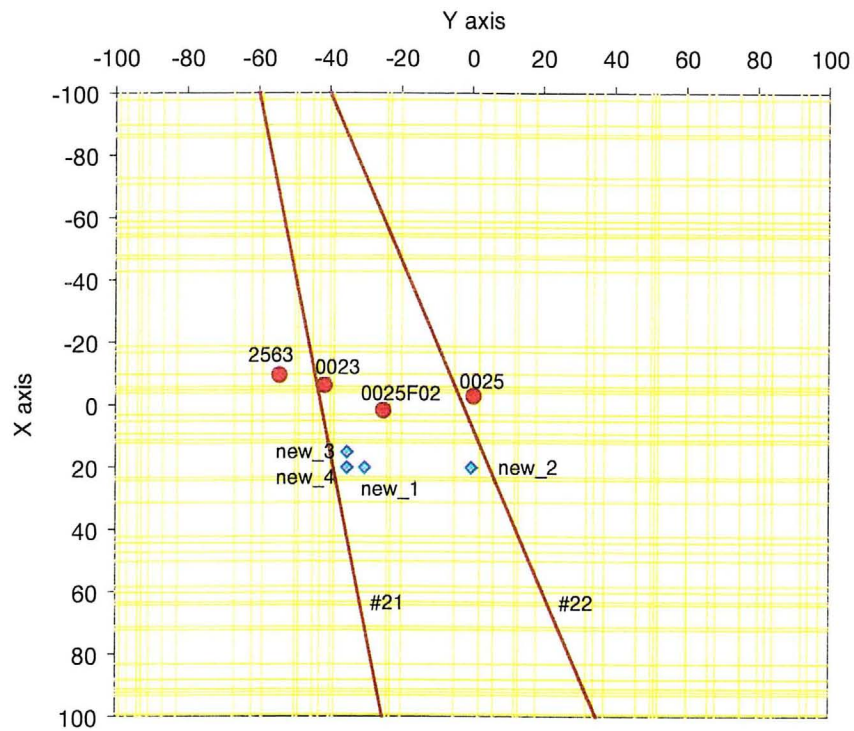


*Figure 6-5 Illustration of Low Density Channel Network Model*

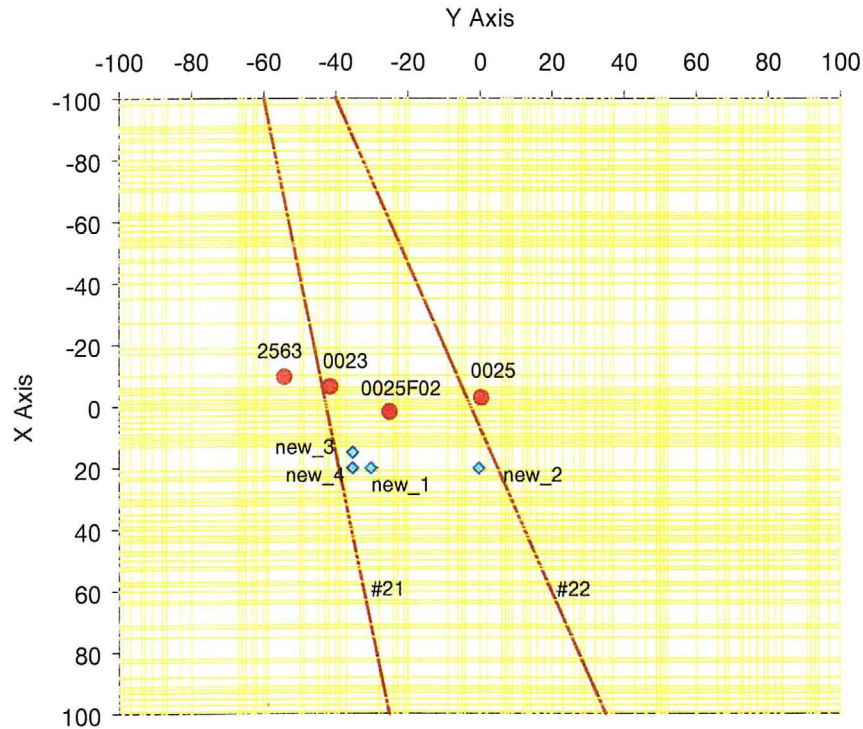


Figure 6-6 Illustration of High Density Channel Network

To assess the effect of the FIZ, the tracer breakthrough time was computed for numerous well pairs with varying channel and FIZ properties. The tracer breakthrough time was set to be the time when half of the tracer mass reach the source well ( $T_{50}$ ). The well pairs were chosen to represent flow parallel, perpendicular, and diagonal to the FIZ. One well pair was chosen to show the anisotropic effects of flow away from the FIZ and as a comparison with the other well pairs. The well pairs are:

- Perpendicular Flow – KA2563A to KI0023B
- Parallel Flow – KI0025F02 to KI0023
- Diagonal Flow – KA2563A to new\_3 or new\_4
- “Anisotropic Flow” – KI0025F02 to new\_3 or new\_4

Tracer is added at the respective borehole locations by dilution due to pumping in the sink section. Tracer breakthrough at the sink locations was calculated using the developed Laplace Transform Galerkin solver (LTG).

#### *Transmissivity and Transport Width Models*

The “visibility” of the FIZ will largely depend on the transmissivity in the FIZ and in the surrounding flow channel network. To study this aspect simulations were run using FIZ transmissivity values that were three and five orders of magnitude larger than the transmissivity of the channel network ( $5 \times 10^{-3} \text{ m}^2/\text{s}$  and  $5 \times 10^{-1} \text{ m}^2/\text{s}$ ).

The transport widths of the FIZ and channel network are also important factors in observing the effects of the FIZ. In the first simulations, the pipe width for the channel and FIZ was set at 0.5m and 0.005m respectively. Simulations were then run using a FIZ transport width at 0.001 m and 0.01 m and a channel network transport width of 0.3 m. The transport width models were designated as shown in Table 6-4:

**Table 6-4 Transport width models for reference in Tables**

Model Name	FIZ transport width	Channel transport width
W1	0.005 m	0.5 m
W2	0.01 m	0.3 m
W3	0.001 m	0.3 m

### *Simulation Results*

Tables 6-5 through 6-10 contain the  $T_{50}$  breakthrough times for each of the simulation runs. Each  $T_{50}$  is recorded as an average of the completed realisations for each simulation. Due to the randomly generated flow channels, occasionally a channel will not intersect with the desired source or sink. Therefore, the simulation of the realisation cannot be completed. On average, approximately fifteen to twenty-five of the thirty realisations are completed. The  $T_{50}$  values are recorded in units of hours. For the cases with high FIZ transmissivity and sorption, the effect of the FIZ significantly decreases breakthrough times. This makes it possible to distinguish FIZ effects from other factors such as fracture roughness.

**Table 6-5 Average  $T_{50}$  Breakthrough Times (hrs) for Low Density Model (W1)**

FIZ Transmissivity	$T=5 \times 10^{-3} \text{ m}^2/\text{s}$		$T=5 \times 10^{-1} \text{ m}^2/\text{s}$	
	No	Yes	No	Yes
<b>Perpendicular</b> (KA2563A-KI0023B)	30	855	642	18606
<b>Parallel</b> (KI0025F02-KI0023B)	60	1789	162	4444
<b>Diagonal</b> (KA2563A-new_3)	105	3033	683	43060
<b>“Anisotropy”</b> (KI0025F02-new_3)	37	1430	78	1990



**Table 6-6 Average T<sub>50</sub> Breakthrough Times (hrs) for High Density Model (W1)**

FIZ Transmissivity	T=5x10 <sup>-3</sup> m <sup>2</sup> /s		T=5x10 <sup>-1</sup> m <sup>2</sup> /s	
	No	Yes	No	Yes
Tracer (Ba-133)				
<b>Perpendicular</b> (KA2563A-KI0023B)	47	1367	681	24592
<b>Parallel</b> (KI0025F02-KI0023B)	102	3042	354	9676
<b>Diagonal</b> (KA2563A-new_3)	188	5263	2840	61434
<b>“Anisotropy”</b> (KI0025F02-new_3)	71	2054	120	3551

**Table 6-7 Average T<sub>50</sub> Breakthrough Times (hrs) for New\_4 Borehole (W1)**

FIZ Transmissivity	T=5x10 <sup>-3</sup> m <sup>2</sup> /s		T=5x10 <sup>-1</sup> m <sup>2</sup> /s	
	No	Yes	No	Yes
Tracer (Ba-133)				
<b>Diagonal</b> (Low Density) (KA2563A-new_4)	125	3596	4331	51361
<b>Anisotropy</b> (Low Density) (KI0025F02-new_4)	70	1876	134	3697
<b>Diagonal</b> (High Density) (KA2563A-new_4)	241	6724	5811	53984
<b>“Anisotropy”</b> (High Density) (KI0025F02-new_4)	116	3440	293	7533

**Table 6-8 Average T<sub>50</sub> Breakthrough Times (hrs) for He-3 Tracer (W1)**

FIZ Transmissivity	T=5x10 <sup>-3</sup> m <sup>2</sup> /s		T=5x10 <sup>-1</sup> m <sup>2</sup> /s	
	Low	High	Low	High
Fracture Density				
<b>Perpendicular</b> (KA2563A-KI0023B)	33	47	611	662
<b>Parallel</b> (KI0025F02-KI0023B)	68	108	175	320
<b>Diagonal</b> (KA2563A-new_4)	125	229	1595	1652
<b>“Anisotropy”</b> (KI0025F02-new_4)	62	117	123	240

**Table 6-9 Average  $T_{50}$  Breakthrough Times (hrs) for High Density Model (W2)**

FIZ Transmissivity	$T=5 \times 10^{-3} \text{ m}^2/\text{s}$		$T=5 \times 10^{-1} \text{ m}^2/\text{s}$	
	No	Yes	No	Yes
Tracer (He-3)				
<b>Perpendicular</b> (KA2563A-KI0023B)	44	44	2479	1315
<b>Parallel</b> (KI0025F02-KI0023B)	80	81	244	236
<b>Diagonal</b> (KA2563A-new_4)	144	145	3651	2708
<b>“Anisotropy”</b> (KI0025F02-new_4)	86	88	160	164

**Table 6-10 Average  $T_{50}$  Breakthrough Times (hrs) for High Density Model (W3)**

FIZ Transmissivity	$T=5 \times 10^{-3} \text{ m}^2/\text{s}$		$T=5 \times 10^{-1} \text{ m}^2/\text{s}$	
	No	Yes	No	Yes
Tracer (He-3)				
<b>Perpendicular</b> (KA2563A-KI0023B)	23	28	200	185
<b>Parallel</b> (KI0025F02-KI0023B)	56	58	150	151
<b>Diagonal</b> (KA2563A-new_4)	146	152	500	408
<b>“Anisotropy”</b> (KI0025F02-new_4)	62	64	135	136

## 6.2.4 Conclusions

### *Generic FIZ study*

Based on the simulations carried out for generic borehole locations and channel properties, a tracer test that is carried out parallel to the FIZ would be affected most by an increased transmissivity in the FIZ. Although the pathway between source and sink interval may not go directly through the FIZ, the higher transmissivity changes the overall flow field and slows down the tracer.

This effect is increased for packer intervals closer to the FIZ, which implies that tracer tests can be improved by placing the packer intervals for new boreholes closer to expected FIZ locations. In this case also a well pair at locations diagonally across the FIZ would be significantly affected by a higher transmissivity within the FIZ.

The generic FIZ study also indicates that it is likely that any effect of a higher transmissivity in the FIZ could be concealed by heterogeneities in the properties of the channels formed on the fracture planes.

#### *Site-specific FIZ study on Structure #20*

A range of tracer test simulations has been carried out to evaluate the design of tracer tests in the fracture network of Structure #20 and Features #21, and #22. In these simulations, fracture intersection zones (FIZ) with one, two and four orders of magnitude enhanced transmissivity significantly affected travel times and breakthrough curves when compared with networks defined by homogeneous channels.

However, the effect of the FIZ was masked by that of heterogeneous channels, for the assumed 1 order of magnitude standard deviation on channel transmissivity.

#### *Site-specific FIZ study on Structure #20 using sorbing tracers*

Sensitivity studies carried out using sorbing tracers clearly showed the effect of FIZ on transport times, even for cases where it was difficult to see these effects using conservative tracers. This is a direct consequence of the smaller channel width, and hence greater sorption and diffusion along pathways defined by FIZ.

The simulations carried out in Structure #20 using the existing borehole array indicate that it may in fact be possible to detect FIZ effects through a comparison of sorbing and conservative tracers. The borehole array including the “new borehole” locations will provide a variety of pathways that cross and run parallel to significant FIZ, as is necessary for these studies.

## **6.3 Prediction of pre-tests**

### **6.3.1 Model premises and parameters**

Pre-tests PT-1 through PT-4, cf. Chapter 5, were modelled utilising the latest structural model revision represented in the constructed channel network model (Fox et al., in prep). This model includes two new Type 2 fractures (#21 and #22) to allow for pathways connecting Structures #13 and #20. A set of conditionally generated background fractures were added to provide for additional connectivity within the TRUE Block Scale volume. Table 6-3 presents a summary of the model parameters, while Figure 6-5 illustrates the current structural model in 3-D. Figure 6-6 is a trace map view of the March 1999 Structural model at the centre of the block at  $Z = -450$  m).

A fracture transmissivity distribution for background fracturing is derived from flow logging results in the TRUE Block Scale rock volume. Results from the 5m double-packer logs are entered into the Oxfilet module of FracMan, which then calculates transmissivity distributions (Dershowitz et al, 1998). Background fracture intensity was derived from the September 1998 structural model. A procedure for estimating the conductive fracture intensity  $P_{32}$  from  $P_{10}$  is described in Winberg (1996).

**Table 6-3 Description of features and parameters of current structural model**

<b>Large-scale Features</b>	27 fractures: (22 Primary structures, 5 bounding structures) March'99 Äspo Structural Model	
<b>Background Fractures</b>	Derived from drill logs, BIPS, POSIVA flow logs and borehole radar measurements in the following TRUE Block Scale boreholes (KA2511A, KA3510A, KA2563A, KI0025F, KI0023B, KA3573A, KA3600F, KI0025F02)	
	<i>Fracture Model</i>	Enhanced Baecher
	<i>Orientation Model</i>	Bootstrap: Dispersion (K) = 200
	<i>Size Model</i>	LogNormal distribution Mean = 6 m Std Deviation = 2
	<i>Termination %</i>	25
	<i>Intensity (P32c)</i>	$0.293232 \text{ m}^{-1}$
	<i>Transmissivity Distribution: Truncated LogNormal</i>	Mean (arithmetic) : $10^{-7} \text{ m}^2/\text{s}$ Std. Dev. (arithmetic) : $8 \cdot 10^{-6} \text{ m}^2/\text{s}$ Max: $1 \text{ m}^2/\text{s}$ Min: $10^{-10} \text{ m}^2/\text{s}$
	<i># of Fractures</i>	18699

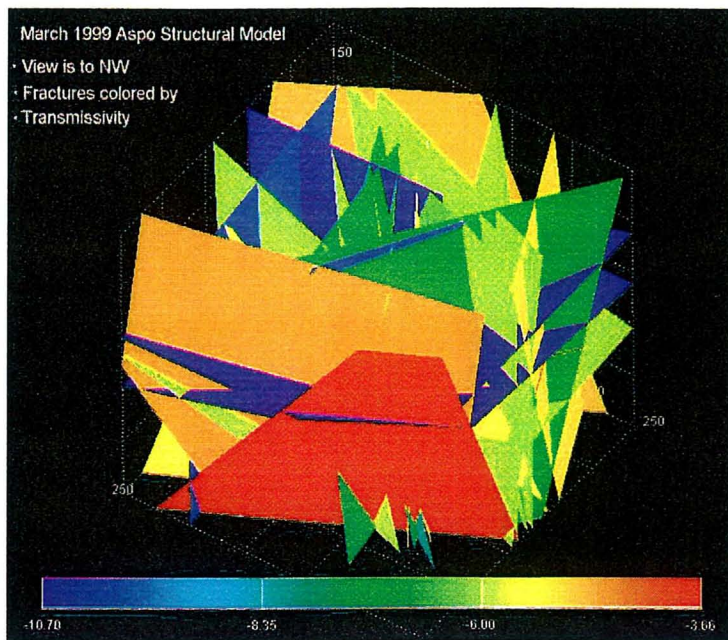


Figure 6-5 3D view of March '99 Structural model. Structures coloured by transmissivity. Birds-eye view towards northwest.

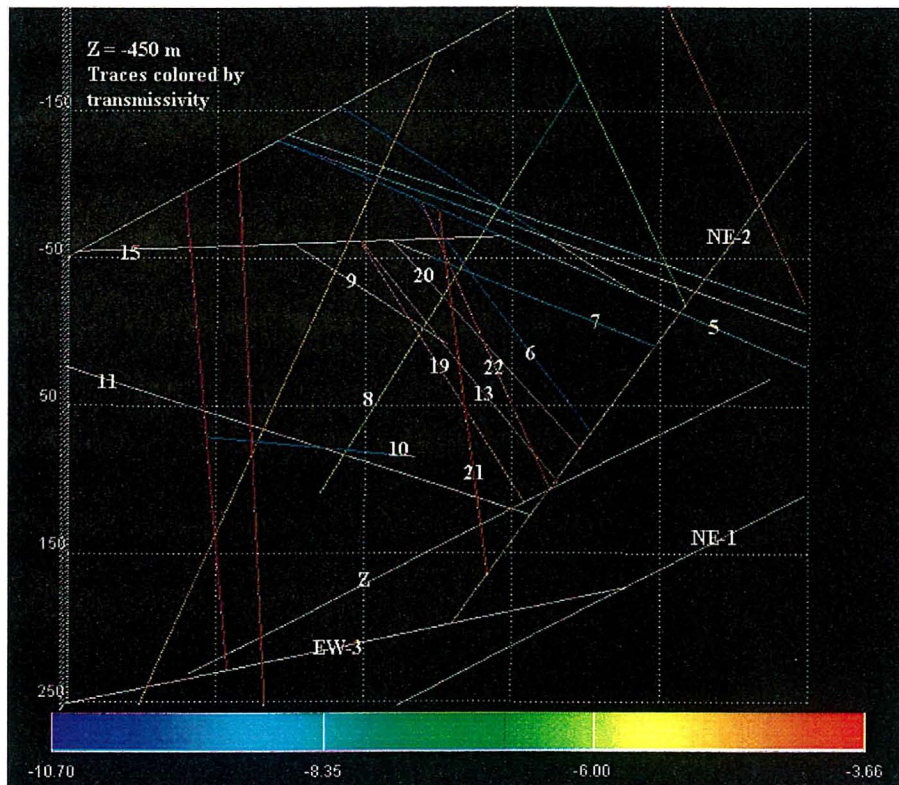


Figure 6-6 Horizontal section through March '99 structural model at Z=-450 masl. Structures coloured by log of transmissivity.

Structure 9 was left in the model, even though its significance as a conductor is now in doubt, cf. Section 4.1. A 500mx500mx500 m cube was modelled, with background fracturing present only within an inner 200m x 200m x 200m block.

All simulations were run using a set of external boundary conditions provided by the developed site scale DFN model. Freshwater head boundary conditions were used at all external boundaries, with no corrections for density or salinity. Simulations were run only for the specified duration of the respective test. Table 6-4 presents the specific testing parameters used for each test. PT-1 through PT-3 were run as transient flow simulations, while PT-4 was run solely as a steady-state simulation.

For PT-4, an ideal conservative tracer was used, with  $K_d = 0$ , free-water diffusivity =  $0.032 \text{ m}^2/\text{s}$ , and  $D_e = 9.39 \times 10^{-15} \text{ m}^2/\text{s}$ . The tests were simulated as four different radially converging tracer tests in a steady-state system.

**Table 6-4 Parameters used for simulation of Pre-tests PT-1 through PT-4, cf. Chapter 5 for details on Pre-Tests.**

Parameter	Values
<b>PT-1</b>	
Pumping Rates (minutes   l/min)	+ .001 min : 0.89 l/min + 50 min : 0.75 l/min +100 min : 0.7125 l/min +200 min : 0.695 l/min +400 min : 0.6875 l/min +1440 min : 0.68 l/min
Output Times	Same as pumping times
Test Duration	24 hours (1440 min)
<b>PT-2</b>	
Pumping Rates	+0.001 min : 2.85 l/min +100 min : 2.75 l/min +275 min : 2.75 l/min +1250 min : 2.6 l/min +2000 min : 2.575 l/min +2700 min : 2.55 l/min +2880 min : 2.55 l/min
Output Times	Same as pumping times
Test Duration	48 hours (2880 min)
<b>PT-3</b>	
Pumping Rates	+0.0001 min : 4.8 l/min +2880 min : 4.8 l/min
Output Times (min)	.001, 166.67, 416.67, 1250, 2500, 2880, 2881
Test Duration	48 hours (2880 minutes)

<b>PT-4</b>	
Injection Rate	Constant Flow KA2563A: S4 -- 600 ml/hr KA2563A: S1 -- 400 ml/hr KI0025F02: S3 -- 140 ml/hr KI0025F02: S6 -- 460 ml/hr
Injection Duration	KA2563A: S4 --- 11.57 hrs KA2563A: S1 --- 22.12 hrs KI0025F02: S3 --- 58.66 hrs KI0025F02: S6 --- 21.2 hrs
Test Duration (how long observations were taken)	KA2563A: S4 --- 24.0 hrs KA2563A: S1 --- 36.0 hrs KI0025F02: S3 --- 60.0 hrs KI0025F02: S6 --- 36.0 hrs
Pumping Rates	KI0023B: P6 Constant Flow: 2.5 l/min

### 6.3.2 Results of analysis of PT-1 through PT-3

Results for PT-1 through PT-3 were obtained as head and head drops at individual borehole segments (sections). The results were then loaded into an Excel spreadsheet, where distance-drawdown plots were computed. These graphs plot absolute drawdown for the entire test (in kPa) versus time divided by real distance squared ( $t/R^2$ ). Distances are from packer interval midpoints. All points were plotted assuming the late-time drawdown value used in the hydraulic analysis of PT1 through PT3, cf. Chapter 7.

Figure 6-7 shows a sample distance-drawdown plot. As in the case with the field data analysis, cf. Chapter 7, the data tend to define groupings of data which appear to identify individual conductors or groups of conductors.

In general, pre-test simulations agreed with the analysis of the actual test data. However, there are several discrepancies.

#### 1. Drawdown

Many of the calculated drawdowns are much smaller than what field data show. This is most evident in the results of PT-3, where analysis of field data shows that about 50% of the observation sections show drawdowns greater than 100 kPa. The simulation results for PT-3 show only two sections with drawdowns larger than 100 kPa.

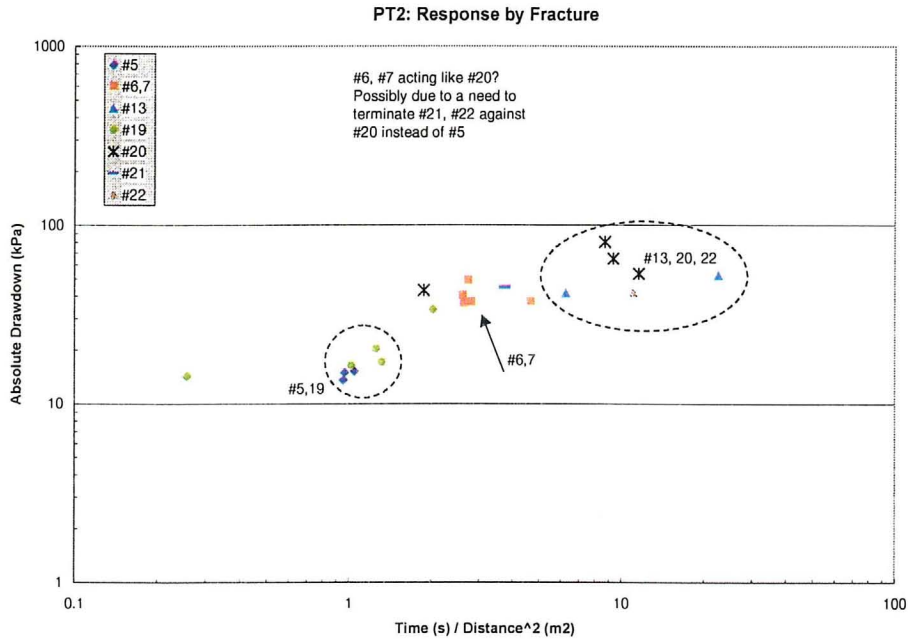


Figure 6-7 Simulated distance-drawdown plot for Pre-test PT-3 (calibrated data).

## 2. Structures #6 and #7

An analysis of data from PT-2 and, to a lesser degree, PT-3, indicates that Structures #6 and #7 exhibit a hydraulic response much lower in magnitude than that of other interconnected structures (#19, #20).

However, simulation data tends to show a much larger drawdown in sections connected via #6 and #7. This would suggest over-connection within the investigated block. Possible sources of this discrepancy include the Type 2 Features #21 and #22. In the March 1999 Structural model (Hermanson, in prep) these two structures terminate against Structure #15. It seems more likely that Features #21 and #22 do not extend that far north, and instead terminate at, or just beyond Structure #20. This would provide for maintained Structure #13-#20 connectivity, and would result in a reduction of responses in packer sections intersecting Structures #6 and #7.

### 6.3.3 Results of PT-4 predictions

The analysis of Pre-Test PT-4 consisted of four simulations of a simple radially converging dipole tracer test using conservative tracers. Identical tracers were used in all four simulations; injection location was the only variation in test parameters. The only changes made to the existing CN model were to the Type 2 Feature #21, in which transmissivity was adjusted in accordance with observations from selective pressure



**Table 6-5. Calculated breakthrough and statistical measures associated with the predicted PT-4 breakthrough times, cf. Tables 5-5 and 5-6.**

Test Section	KA2563A : S1	KA2563A : S4	KI0025F02 :P3	KI0025F02 : P6
Recovery (%) *	N/A**	99.64 %	99.4%	N/A
T <sub>5</sub> (hrs)	N/A**	34.25	33.9	270.68
T <sub>50</sub> (hrs)	N/A**	53.00	84.01	N/A**
T <sub>95</sub> (hrs)	N/A**	91.10	181.33	N/A**

\* Recovery (%) is calculated at the end of the simulation. More tracer can be recovered with longer observation times

\*\* Simulation was not run long enough to achieve results

build-up tests in borehole KI0023B. Each simulation was run long enough to allow for at least 95% tracer recovery (t<sub>95</sub>).

Table 6-5 presents the results of the simulated PT-4 tracer injections in terms of times for 5%, 50%, and 95% mass recovery. Figures 6-8 presents the calculated breakthrough curves for the four injections.

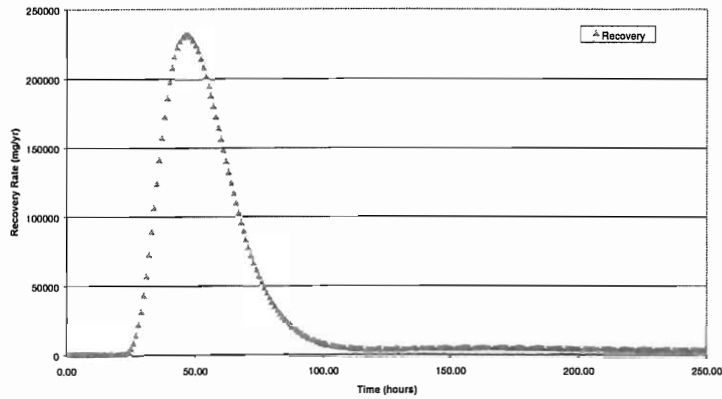
### 6.3.4 Conclusions

Simulations of cross-hole pressure interference and radially converging tracer tests have proved a useful contribution to reconcile hydraulic data with the current structural model. A comparison of the results of the analysis of hydraulic tests with the results of the simulations indicates that the northern terminations of the Type 2 features #21 and #22 need to be modified. It seems likely that both #21 and #22 terminate at, or immediately beyond Structure #20.

In addition, the results of PT-4 simulations will assist not only in revisions to the current geologic model, but also in the assessment of source and receiver sections to be used in future experiments.

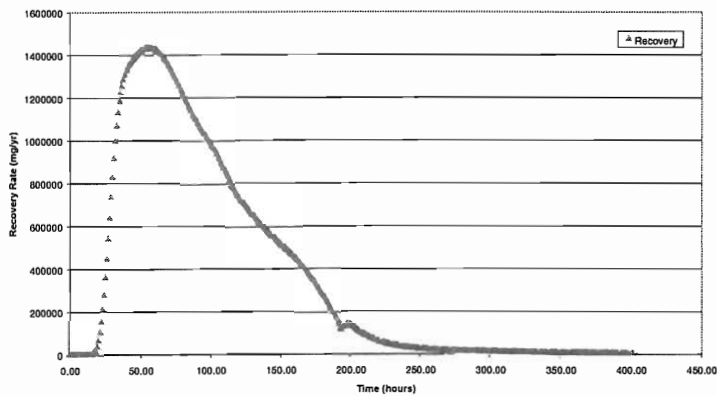
One set of disappointing results were the absolute drawdown in KI0023B:P6 (sink for PT-4). Simulation results indicate that a 2.5 l/min pumping rate is not supportable in this section (in the model) for longer periods without significant drawdown. This will need to be resolved as part of future modelling work.

PT4: Source in KA2563A: S4 -- Breakthrough Curve



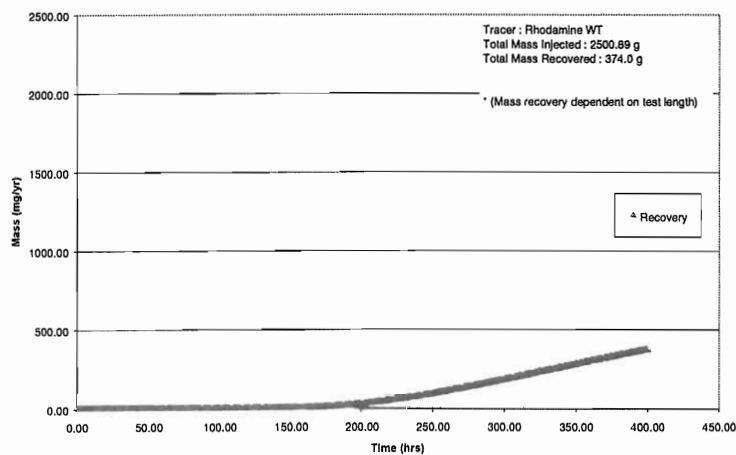
a)

PT4: Source in KI0025F02 Section P3: Breakthrough Curve



b)

KI0025F02 Packer Section P6: Breakthrough Curve



c)

Figure 6-8 Simulated breakthrough curves (mass flux in mg/yr vs. time in years) for the PT-4 injections; a) KA2563A:S4, b) KI0025F02:P3, c) KI0025F02:P6. No breakthrough was obtained at reasonable simulation time for injection in KA2563A:S1.

## **7. Hydraulic reconciliation of March '99 model**

### **7.1 Background**

This section provides a summary of work performed to reconcile the March '99 structural model with hydraulic data. The hydraulic data sets include 5 m double packer flow logs (KI0023B, KI0025F), POSIVA flow logs (KI0025F02, KA2563A), pressure build-up tests (KI0023B, KI0025F02), cross-hole pressure interference tests, flow and pressure responses collected during drilling, and tracer dilution tests. Particular emphasis has been put on the cross-hole pressure interference and dilution test results for the first three tracer Pre-tests (PT-1 through PT-3). The three Pre-tests have used as sources; Structure #13 (KI0023B:P4), Structure #21 (KI0023B:P6), and Structure #20 (KI0025F02:P5), respectively.

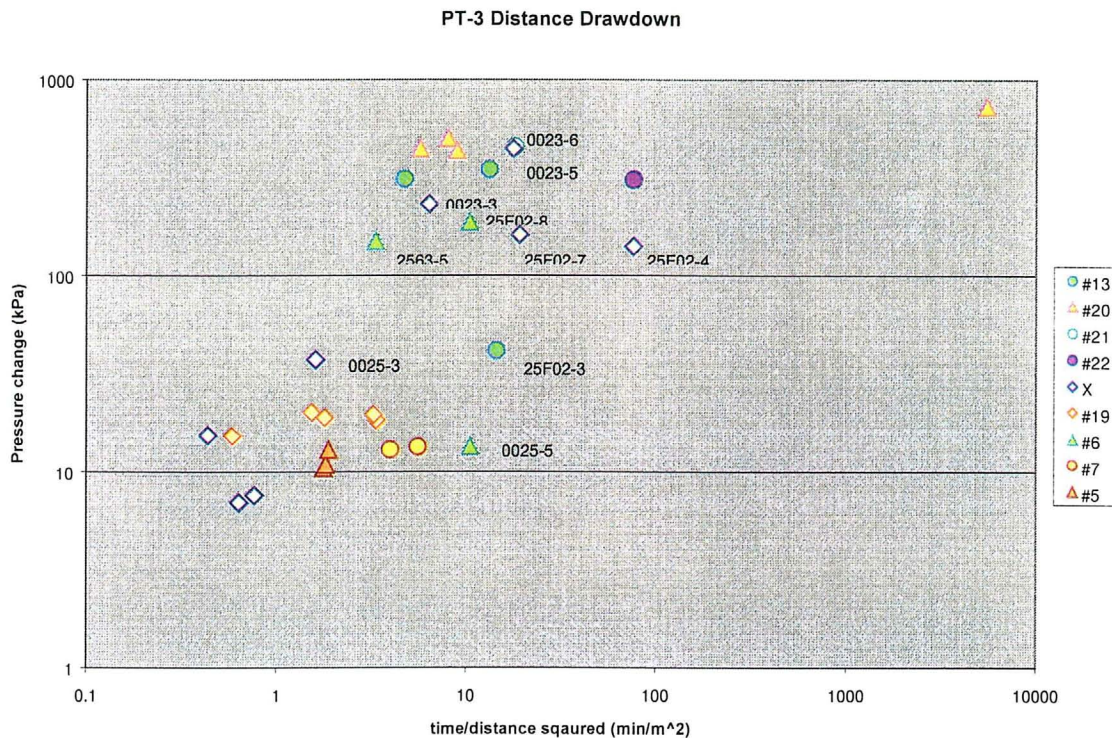
An important task for tracer test design is the identification of conducting features that connect major structures. The major goal of the TRUE Block Scale programme is been to look at tracer behaviour along pathways involving multiple conducting features. The sub-parallel orientations of the major features in the block has complicated the search for a network of features, hence particular emphasis has been placed on finding verifiable conductors that cross the major NW Type 1 trending conductive structures.

The TRUE Block Scale Technical Committee has decided to concentrate the tracer design activities on the region around two numbered Type 1 structures; Structures #20 and #13. Hermanson (in prep) in his draft report on the March '99 model, proposed two new Type 2 features that crosscut Structures #13 and #20, giving them the designations "#21" and "#22". The present review effort seeks a verification and visualisation of the hydraulic data to check the existence of these features and others that may be suitable for tracer testing.

### **7.2 Procedure and results**

The main tools for analysing pressure responses have been plots of drawdown versus distance, divided by the real distance between the observation point and the pumping source squared. The extent to which these plotted points lie on coherent type curves, or tend to cluster provides indications of the homogeneity of the system or the presence of multiple conductors. These plots are complemented by maps of drawdown for each pump test. Figure 7-1 shows an example of a distance-drawdown plot for the PT-3 test.

The results of the reconciliation study have shown that the March '99 structural model



provides a largely accurate description of the major conducting features in the TRUE Block Scale volume. A brief description of each important structure is given below. A

*Figure 7-1 Example of drawdown distance plot for the PT-3 pre-test, compare Appendix B:III.*

summary plot of the hydraulic data and the connectivity of the structures is shown in Figure 7-2. This figure shows the boreholes as parallel features for convenience of plotting data. The length axis is adjusted so that the origin "0" is the location of Structure #20. This adjustment aligns the boreholes to allow a visual comparison of features and characteristics common to different holes.

Flow log anomalies and pressure build-up data are shown as bars with heights proportional to the inferred steady flows from those zones. The 5 m flow log data are shown as bar charts, and the locations of significant inflow or pressure response during drilling are shown with triangles below the line representing each hole. Each horizontal line on the chart represents a borehole. Packer locations are shown by squares, and heavier lines indicate the intervals that are being monitored. The March '99 structural model is shown in yellow, and inferred conductors from the recent data are shown as transparent grey overlays.

Structure #20 is the major conducting feature of the core of the block, and it appears in all boreholes except KA2511A, which lies about 80-m above the borehole array. The current pre-test results provide further validation of the location and transmissive nature of Structure #20.

Structure #13 is distinct from, but connected to Structure #20. The pressure responses indicate strong connections between boreholes KI0023B and KA2563A. The connection becomes weaker in KI0025F02 as the pressures responses are later in time

Summary of Flow and Pressure Responses  
(March '99 Structural Model in Yellow)

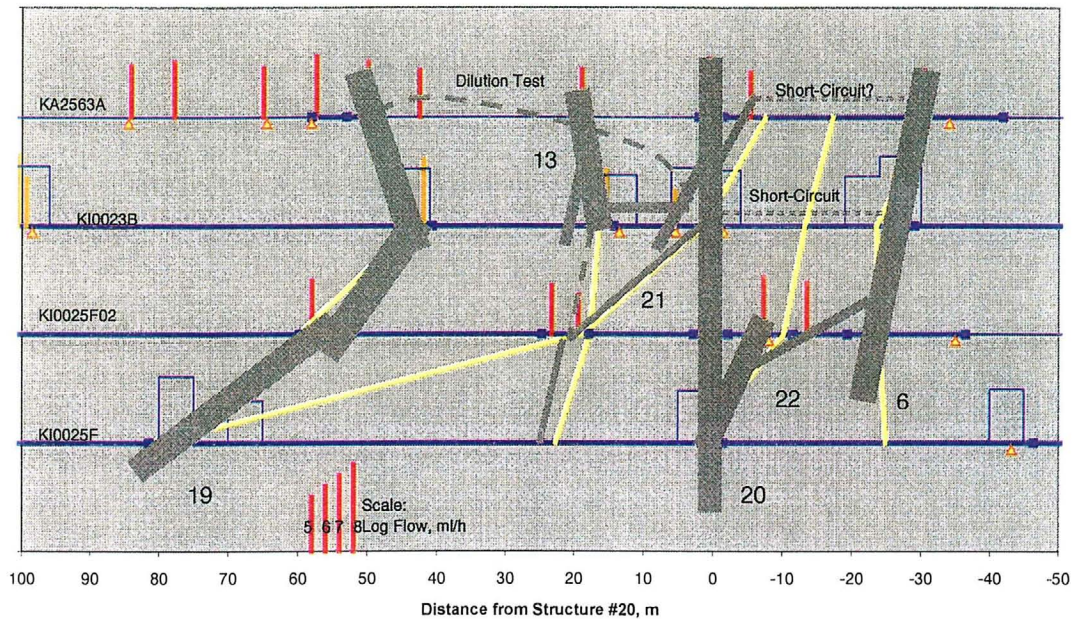


Figure 7-2 Reconciled hydraulic and structural model of the TRUE Block Scale volume. Simplified representation with boreholes aligned and intersecting structures normalised to the position of Structure #20. Grey shaded lines show hydraulic structures. Yellow lines indicate structures in March '99 Structural model, cf. Figure 7-3.

and lower in magnitude. The responses of KI0025F02:P3 are very important for the hydraulic model. The March '99 structural model also has Structure #21 intersecting in this interval. It is significant that this section responds weakly to all three Pre-tests (Appendix B), and even more weakly to pumping in Structure #13 than to Structures #20 and #21. An alternate explanation for the low drawdown in KI0025F02:P3 is a boundary effect. A boundary effect that would cause a reduced drawdown would imply a constant-pressure rather than a no-flow boundary. Constant-pressure boundary effects imply that the interval contains a second conductor with higher storage and conductivity than Structure #13 such that it provides a stronger flow than we would expect from Structure #13 alone. We can discriminate between these two possible explanations, poor connection versus boundary effect by checking the tracer dilution data. If the connection is poor, we should see low-flow results in tracer dilution test from this interval, while a boundary effect would show stronger dilution. Table 5-2 shows the tracer dilution test results for PT-1, from which we may conclude that there is a Structure #13 connection and the low drawdown may be a boundary effect. All things considered, Structure #13 may largely disappear hydraulically between KI0023B and KI0025F02, cf. Figure 7-3.

One difficulty in verifying Features #21 and #22 has been that they appear very close to other major zones/structures in the boreholes. One test of the existence of Feature #22 was to examine the drilling records of KI0025F02, which should separate #22 from #20 by several metres. The investigation of drilling records did affirm the existence of a structure at the assumed location of #22, and showed that hydraulically it is closely tied to Structure #20. Structure #22 does not appear to extend very far from Structure #20, as there are no intersections of this feature observed in KI0023B or KA2563A. Structure #22 also extrapolates to intersect Structure #19 in KI0025F in the March'99 structural model, cf. Section 4.1. There is however no hydraulic evidence for this extension of Structure #22.

In the pressure interference responses of the pre-tests, Structure #22 (KI0025F02:P6) behaves as an integral part of the Structure #20 network. This feature is also interpreted to act as part of the bridge from Structure #20 to Structure #6. The feature does not extend to the northwest, as there appears to be no flow anomalies along the projections of the structure in KA2563A or KI0023B.

The pressure interference data and the tracer dilution data offer somewhat contradictory evidence for Feature #21. The tracer dilution data for Pre-test PT-2 show a clear connection between KI0023B:P6 and KI0025F02:P3, cf. Table 5-3. The pressure interference tests do not indicate a strong hydraulic connection between KI0025F02:P3 and other proposed Structure #21 locations. The most striking aspect of the pressure behaviour of KI0025F02:P3 is its generally low-pressure response, cf. Appendix B. When discussing Structure #13 above, this low-pressure response was explained as a possible boundary effect where Structure #21 was acting as a very permeable boundary that reduced the pressure responses to pumping in Structure #13. By this logic, Structure #21 should be more transmissive than Structure #13 and pumping in Structure #21 at KI0023B:P6 should produce stronger drawdowns in KI0025F02:P3 than pumping in Structure #13, as was done in Pre-test PT-1.

Unfortunately for clarifying the hydraulic structure, PT-2 produces only slightly stronger drawdowns in KI0025F02:P3 than PT-1 did, Appendix B. There are clearly connections between KI0025F02 and Structure #20, but these do not support a very direct connection along a possible Structure #21.

One could look for another candidate intersection of Structure #21 in KA2563A:S5. This zone contains a conductor at the right location, but sharing the piezometer interval with Structures #6 and #7 may smear its pressure responses. KA2563A:S5 does show strong drawdown, but the behaviour is consistent with the responses of other parts of Structure #6.

In summary, the evidence for Feature #21 mainly comes from geology and the tracer dilution test results. The dilution tests performed as part of PT-2 support a pathway along the proposed feature, whereas the hydraulic pressure interference data do not suggest a strong hydraulic pathway.

Another structure, which has no designated number, was also identified in the adjacent interval to the one containing Feature #22 in borehole KI0025F02. This feature appears to connect Structure #22 with Structure #6, cf. Figure 7-3.

Structure #6 as presented in the structural model appears validated, however, the strength of the connections may be exaggerated by a short circuit in the KI0023B:P7 interval. This interval contains both Structures #20 and #6, and dilution tests performed under both ambient and pumped conditions confirm the presence of a short-circuit along the borehole, cf. Section 5.2.5.

Section KA2563A:S5 contains two significant conductors at 157.6 and 182.6 m. The shallower interval is part of Structure #6. The deeper interval is has not been identified with any numbered conductor, but it may be part of the Structure #20 system as it is separated from the main trace of Structure #20 by only 6 metres. However, the two structures at L=182.6 m are associated with two subhorizontal structures (225/11 and 244/15), but could still potentially connect to Structure #20 at L=188.7 m. If the 182.6 m conductor is part of the Structure #20 system, then it may be acting as a short circuit similarly to what has been found KI0023B:P7. It should however be noted that the transmissivity of the structures involved are significantly smaller (10-50 times). Given a head difference of 5 m, the resulting "leakage flow" is about 0.2 l/h, which should be compared with the 10 l/h flow calculated for the KI0023B:P7 short circuit. Consequently the effect of this short-circuit, if it does exist, will be significantly lower than the one in KI0023B:P7.

It is recommended that KA2563A:S5 should be a target for dilution tests to measure the flow rate under both natural and, if possible, pumped conditions. If this section has a significant flow, it may be desirable to install a packer at about 170 m in KA2563A.

Performed short-term pressure interference tests using KI0025F02:P2 as a source provide further validation of Structure #19 as a through-going, though somewhat isolated hydraulic structure. Structure #19 was not a target for the pre-tests other than to perform a tracer dilution test in KA2563A:S1 during PT-2 and an actual tracer injection in the same section during PT-4, cf. Chapter 5. The former test (PT-2) pumped Structure #21 in KI0023B and showed a water velocity change in KA2563A:S1. This zone also showed stronger interference responses than other sections containing the interpreted Structure #19. Given that a previous installation of the KA2563A packer system produced artefacts, ie. created connections between the innermost section and the central part of the block, it may be useful to review the piezometer installation.

Two other structures that might connect Structures #20, and Features #21 and #22 were identified from the interference responses. One was already mentioned above as a connection to Feature #22. The other one intersects KI0023B:P5 at about 75 meters depth and may connect Structures #13 and #20.



### 7.3 Conclusions

In conclusion, the reconciliation efforts have both validated and further refined the March '99 structural model. The reconciliation indicates a shorter lateral extension for both Structures #13 and Feature #22 than suggested by the March '99 model. The Type 2 Feature #21 is still uncertain. The hydraulic connections between #13 and #20 are well documented, but the exact locations of structures carrying water between these two structures are not known with great confidence. The definition of additional conducting features between Structures #20 and #6 suggests that the project may consider including optional tracer tests between these two structures.

An overlay of the March '99 model highlighting the parts of the interpreted structures and features which are interpreted active from a hydraulic and transport perspective are shown in Figure 7-3. It should in this context be emphasised that the overall geometry of the structures as presented in Table 4-1 and Figure 4-1 is retained as valid.

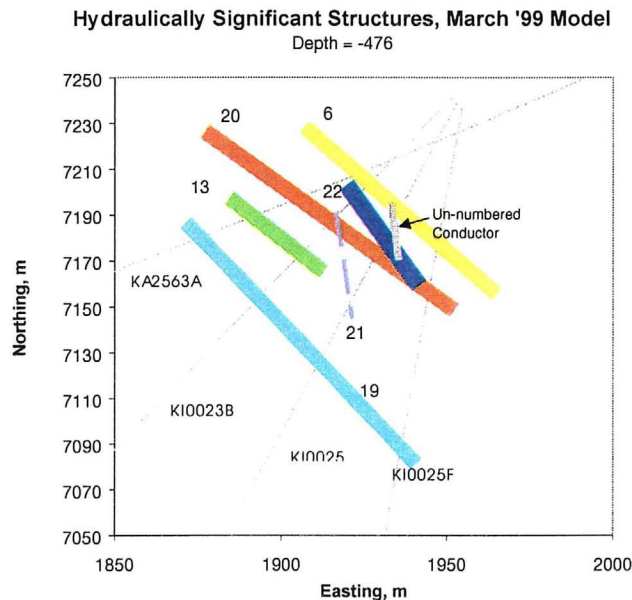


*Figure 7-3. Overlay on March '99 structural model showing the extent over which the interpreted structures and features are interpreted to be active from a hydraulic and transport perspective, cf. Figure 1-1 and Table 4-1 and Figure 7-2.*

With regards to a new borehole there are three major needs that can be addressed by a new borehole. There are the following:

- Verification of structures
- Optimisation of tracer test arrays
- Targeting of specific structures for inclusion in tracer tests.

Based on the structural-hydraulic reconciliation, it is proposed to locate a possible new borehole between KI0023B and KI0025F02. The objectives of this borehole would be to validate the structures, including Feature #21, between Structures #20 and #13, and to validate the features that connect Structure #6 and Structure #20, ie. Feature #22 and the newly defined conductor. The hole would be spaced from KI0025F02 in a way that optimises the performance of tests with sorbing tracers. The borehole should address the continuity of Structure #13 between KI0023B and KI0025F02 to study the nature of the structure, whether it is made up of multiple structures or a single heterogeneous conductor. Finally, the borehole could also potentially be positioned to target an intersection between Structures #20 and #22, or some other feature.

The reconciliation work supports tracer test design. Given the goals of finding pathways that traverse multiple conducting features, we may tentatively identify two regions that deserve particular attention. The first region may use parts of Structure #13, and the Type 2 Features #21, and #22. The second region between Structures #20 and #6 that uses pathways along Feature #22 and the new conductor in KI0025F02.

## **8. Premises for tracer tests**

### **8.1 General**

The preceding chapters have compiled the results of the modelling, desk-top and field studies which have led up to the formulation of this report. In the following sections the obtained results are discussed in terms of a number of selected key headers.

### **8.2 Validity of March'99 Structural model**

**The performed reconciliation work has verified the March'99 structural model but has also suggested some refinements to the model.**

The major contribution of the reconciliation work was to reduce the lateral extent of Structures #13 and #22, cf. Section 7.2. The Type 2 Feature #21 remains uncertain. In addition, new potential structures not included deterministically, but of importance for connecting Structures #20 with the Type 2 features #21 and #22, have been identified. Use of these structures in a tracer test context, and answering to resolving our Hypothesis 1, calls for verification using a new exploration borehole, cf. Section 8.5.

In addition the performed reconciliation also identifies the area between Structures #20 and #6 as an optional target region for tracer tests.

### **8.3 Feasibility of block scale tracer tests**

**The most important take-home message from the performed Pre-Tests and PT-4 is the fact that multiple breakthroughs have been demonstrated for the network proposed for future tracer tests.**

The breakthroughs all represent pathways invoking multiple structures. In addition, two of the four breakthroughs show a recovery of 75-80 % (projected to full recovery had the test been prolonged). In short, the prospects for future tracer tests are good.

In addition, the performed pre-tests have complemented the list of combinations of sink and sources for future tracer tests, cf. Section 4.3 and Chapter 5. In reality only a few sink intervals are considered feasible which were also used during the PT-1 through PT-4 tests. The tests indicated a previously unidentified short-circuit in KI0023B:P7 which could potentially affect future tests. A series of pre-PT-4 tests indicated that the identified short-circuiting can be managed and overruled when employing KI0023B:P6 as a sink interval. Additional tests can show to what extent the short circuit will affect the use of alternative sink sections, which could possibly result in tracer loss.

The performed reconciliation work has also identified a possible additional short-circuit in section KA2563A:S5, which is interpreted to contain Structure #6 and a second conductor which may be associated with Structures #20 or the Type 2 Feature #21. The existence and role of this possible short-circuit should be further investigated.

## 8.4 Feasibility to distinguish intersection effects

A generic and a site-specific study has been performed to assess the possibility to distinguishing the contribution and effect of fracture intersections from the overall heterogeneity in a fracture network, cf. Section 6.2. Various assumptions and hypotheses regarding the nature of the intersections (FIZ) have been tested in the context of a channel network model. A procedure of multiple tracer test geometries in the vicinity of the FIZ is proposed. It is shown that effects of FIZs are more likely to be captured in the case where the distance from the neighbouring pump and injection sections is short. However, it has been shown that even with a very high conductance contrast between the FIZ and the surrounding features, it is not possible to distinguish the FIZ from the effects of the heterogeneity in the structures which are making up the FIZ. In the study, the effects of heterogeneity within the FIZ itself were not studied. A heterogeneity within the FIZ itself, which cannot be ruled out, would most likely make it even more difficult to distinguish the FIZ .

**The performed model study show that intersection effects can prove to very difficult, if not impossible, to distinguish from that of intra-structure heterogeneity.**

This finding calls for moderation of success expectancy with regards to the stated hypotheses 2a and 2b, the latter which calls for field experiments targeted on intersections effects. It should be emphasised that we see no reason to withdraw the posed hypothesis. The nature and material properties of fracture intersections are components in the evaluation of the planned tracer tests. With the help of collected field data in combination with tests of hypotheses in our computer models, we still hope to contribute valuable findings related to this issue within the framework of the project.

## 8.5 Assessment of experimental array

The Pre-tests have consisted of three pre-tests, PT-1 through PT-3, each making use of a separate sink in a given structure, #13, #21 and #20, respectively, cf. Chapter 5. In the sections prioritised for dilution tests, we have conducted 28 separate tracer dilution tests using 14 different test sections and three selected sink sections. Of these dilution tests 16 (57%) show a significant increase in flow under pumped conditions compared to ambient conditions.

**The prospects for using the array for tracer transport tests are consequently promising.** This has also been shown in the tracer transport tests performed as part of pre-test PT-4, cf. Section 8.3.

However, as pointed out in Sections 5.3 and 7.3, there are **arguments for drilling an additional exploration borehole**. These are 1) to facilitate shorter distances between sink and source points (shortest at present is about 16 m), this to facilitate performance of tests with sorbing tracers, b) improvement of our structural-hydraulic model with regards to the nature and extent of Structure #13, and the Type 2 Features #21 and #22, and their siblings, c) provide additional injection/abstraction points.

In addition, the present tracer test array suffers from the following drawbacks identified from the Pre-test data;

- 1) A short-circuit exists in Section P7 in KI0023B which connects Structures #20 and #6. High flow rates have been measured in this section which can potentially limit the usage of alternative sink sections within the array, cf. Section 5.3.1. *Remediation calls for extraction and reinstrumentation of the present equipment, cf. Section 8.6.*
- 2) A flowing structure in KI0023B:P5 which may provide connection between Structures #20 and #13 can presently not be used. *Remediation calls for extraction and reinstrumentation of the present equipment, cf. Section 8.6.*
- 3) The interpreted intercept of the Type 2 Feature #22 in KI0025F presently lies underneath a packer. *Remediation possible and relevance of this interpreted intercept can be tested by a small shift of the multi-packer array before deciding to undertake the actual remediation/optimisation.* Part of Project Plan. Recommended undertaking.
- 4) Section KI0025F02:P3 includes both Structures #13 and #21. A separation of the two structures would potentially improve the understanding of the two structures and may add an additional injection point for tracer. *Remediation possible.* Part of Project Plan. Recommended undertaking. Structures not well separated. The role of near section intercept between the two structures should be reviewed.
- 5) Section KA2563A:S5 may have a short-circuit similar to the one in KI0023B:P7. The nature of this short-circuit should be explored using existing data and, if possible, with complementary tracer dilution tests.

**It is recommended to explore the listed remediation measures in KA2563A, KI0025F and KI0025F02.**

**Further it is recommended to drill a new borehole to answer the wish list defined above. It is also recommended to drill and characterise the borehole before starting up the tracer tests.**

The geometry of this new borehole is not decided at present but should be collared in the I-tunnel and should ideally be oriented close to KI0025F02 and should have an inclination different from the existing boreholes. The latter to provide a spread in the vertical direction of the new intercepts relative to the old ones. The length of the borehole is tentatively set to between 100-120 m. It is expected to carry out drilling and the necessary characterisation work (BIPS and POSIVA flow logging) in 4-5 working weeks.

## **8.6 Risks associated with attempted KI0023B salvage**

Soon after its emplacement, section P3 in of the KI0023B instrumentation collapsed. The problem was diagnosed and following detailed evaluation and planning and a series of materials tests, a salvage attempt was performed in the Spring of 1998. It was possible to pull the system out about 17 m at which it got stuck. During the salvage a pulling force of < 2000 kg (4600 kg identified as the average force of failure for the weakest point of the system) was applied but it was not possible to move the system past the point where it got stuck. It was thereafter decided to terminate the salvage attempt and reposition the system at its original location. It was identified that a brute force pull might have jeopardised the future use of the whole site.

The reinstatement of the system was successful, and the system is now functioning well with the exception of the failed section P3. It should be mentioned that the preferential sink section (P6) including Structure #21 is located in this borehole. The access to the innermost sections P1 and P2 and associated packers is restricted because of the collapse of the central tubing in section P3..

During the last year requests have been put forward to obtain POSIVA flow log data from this borehole to support the construction of structural and hydraulic models. In addition, as indicated in Section 8.3, requests for remediation of the multi-packer system have been proposed. Hence a need to revisit the plans for salvage of the borehole instrumentation.

Tentative contacts have taken place with drilling contractors and drilling supervisors. In addition contacts have taken with the manufacturer and installer of the system. In summary, the following statements have been obtained from the manufacturer;

- The sticking point is presumably in the section P3, somewhere between L=70 to 93 m given the noted mobility of 17 m. However, the sticking point can in principle be anywhere along the borehole!

The primary risk when pulling the system out is that the system may be torn apart as a consequence of using too much force;

- it is impossible to say where the system would break. A break would most likely occur at one of the tubings - but which one? The performed materials tests indicate that a deformed coupling may be stronger than an non-deformed coupling. This means that the failure could be anywhere between the sticking point and the tunnel. Since friction loss is least near the tunnel, it is expected that the tubing would fail nearer to the tunnel than to the problem area. Then, if one tries to push the system down the hole, one may get a buckling of the tubing between the sticking point and the tunnel, which would really be a mess.
- If the steel tubing fails, one has to pull until all of the nylon lines break. The lines will form a mess of “spaghetti” ahead of the tubing, which will act as a elastic sponge, making it difficult to apply much force to the system in any attempt to push the rest of the array down.

Tentative contacts with people in the drilling circuit has indicated that there are no (Swedish) precedence to the problem faced. Given the above information, the current approach is consequently directed towards a primary option which includes reaming of the hole with a thin-wall drill-bit and drilling tube to swallow the existing system. It should be understood that there is a risk of the reaming diverging from the original borehole trajectory. A feasibility study has been initiated to further explore the possibilities for retrieving the system.

**Given the above statements it is advocated not to start up a new salvage attempt on KI0023B before;**

- a) a satisfactory base data set has been collected from the site as part of the Tracer Test Stage**

**and**

- b) it has been firmly demonstrated that a remediation is imperative to reach the full project objectives**

## 9. Tracer tests

### 9.1 Objectives

The primary objective of the Tracer Test Stage is to provide us with the data from which we can “increase understanding, and the ability to predict” “transport in a fracture network” in a block scale, ie. over a length scale of 10–50 m. In addition we to “assess the importance of tracer retention mechanisms (diffusion and sorption) in a fracture network”. Embedded in the latter objective is a goal to assess to what extent the way retention processes manifest, will change with scale.

The proposed specific objectives for the planned tracer tests within the Tracer Test Stage are;

- 1) To assess and quantify the parameters which control radionuclide retention in a fracture network in the block scale

Comments :

Can we from the available information build an overall understanding of retention in a network. If we can show that there is no fundamental difference between retention in network and a single feature, or alternatively if we can show the essential elements in scaling of retention phenomena from a single feature to a network of multiple structures, these are potentially important contributions to modelling of transport in fractured media.

In the analysis the experience and data collected from the TRUE-1 field and laboratory experiments are utilised. This includes assessment of the effects of fracture intersections in relation to the overall heterogeneity experienced in the studied network. Design calculations has shown that the latter may be very difficult in the field. The performed design calculation also shows that the results are relatively insensitive to different modelling assumptions . This also makes it difficult to analyse this issue in a modelling context. An added comment to objective #1 is that the difficulty of make distinctions between the FIZ and the in-plane heterogeneity, whether in the field or in our models, may make it necessary to retain the notion of channels (also allowing for heterogeneity along them), the channels being constrained by the underlying fracture network, and accounting for all types of heterogeneity in the network.

All these aspects considered, the role of the fracture intersections in the overall heterogeneity can still be potentially important and should be part of our assessment.

This task also includes an assessment to what extent a deterministic address as used in TRUE Block Scale is satisfactory, or whether use of background fracturing, representing less well identified structures, is warranted. In this context it should be noted that background fracturing is accounted for beyond the representation of interpreted deterministic structures. It is assumed that the background fractures are much less permeable than the deterministic ones..



- 2) To assess the predictive capability of developed block scale transport models and characterisation tools for predicting transport of sorbing tracers, and to evaluate which model assumptions are most appropriate and important.

Comments :

To what extent can hydraulic data be used for predicting conservative transport, and to what extent can conservative transport data, in combination with (imported/site-specific) laboratory data (diffusivity/sorbitivity), be used to predict transport of sorbing tracers. An associated issue is how these parameters scale, ie. the question of upscaling flow and retention parameters. Several assumptions can be made regarding the link between flow and transport parameters. Different assumptions should be used for predictions and compared to the experimental results.

This objective may be subdivided into the role of the underlying structural model and the process model and its parameters at the studied scale. In addition the procedure of integration of laboratory and field measurements (including detailed scale results from other experimental sites) should be addressed in this context.

N.B. Retention includes effects of both diffusion and sorption.

## **9.2 Scope and components**

In the presented Project Plan a staged approach, very much like the one developed for the TRUE-1 experiments is proposed. The actual tracer test phases (A through C) are preceded by a remediation and optimisation phase.

### **9.2.1 Remediation and optimisation phase**

Following the recommendations in Section 8 this is what is foreseen within this phase (in sequential order);

- 1) Remediation of KI0025F. The remediation is preceded by a test outlined in Section 5.3.2.
- 2) Remediation of KI0025F02 (assessment of plausibility pending!)
- 3) Remediation of short-circuit in KA2563A. This activity calls check of plausibility and test as outlined in Section 8.5.
- 4) Drilling and characterisation of a new borehole (subsequently denoted KI0025F03)

Ideally, the drilling should be started after the activities in KI0025F and KI0025F02 are completed, so as to collect drilling responses in the remediated boreholes. The drilling responses, together with the BIPS and POSIVA flow log, data will expediate design of

the multi-packer system. However, given time constraints and the present stature of the structural model, parallel activities may have to be accepted.

A multi-packer system is available for the new borehole allowing a total of 15 lead-throughs.

### **9.2.2 Tracer tests - Phase A**

The primary objective of this phase is to test alternative sink sections in the new borehole and collect complementary tracer dilution data required as a consequence of the performed remediation activities. In addition to the preferred sink section in KI0023B:P6 (#21), three other sinks will be explored. On the basis of the dilution results, the preferred sink for the future tests will be identified, and used for a new set of injections similar to the ones performed as part of Pre-test PT-4, cf. Section 5.2.6. Focus is put on multi-feature pathway tests. The results of Phase A will constitute the platform for selecting the part of the array where tests over shorter distances will be performed.

During these tests conservative tracers are used exclusively. Among tracers foreseen to be used are the dye tracers, metal complexes reported in Section 4.6.

The Phase A tracer tests are preceded by blind model predictions using stochastic continuum, discrete feature and channel network models. These models will be updated using the reconciled March '99 model and existing hydraulic and transport data.

The developed models are subsequently used to evaluate the data from the Phase A tracer tests. This activity also includes a calibration effort.

The activities are regulated by quality plan documents in accordance with SKB standards.

### **9.2.3 Tracer tests - Phase B**

It is foreseen that the sink section preferentially used during Phase A is also used for the remainder of the Tracer Test Stage. However, alternate sinks may be used for specific purposes. Compared to the Phase A experiments, the Phase B tests feature test times of longer duration which can facilitate investigations of both long (50-100 m) and short flow paths (5-15 m), and the address of single feature as well as multi-feature pathways. The results are also used to assess intersection effects. Study of tracer retention is made through the use of Helium and possibly some weakly sorbing tracers. The results will form the basis for the design of the Phase C tests, which are focused on tracer retention. It is foreseen that in reality there will be a smooth transition between Phases B and C, and that pumping in the selected sink is continued without interruptions to provide for a sustained stable flow field, long pathways and study of retention.

All three model concepts are used to evaluate the data from the Phase B tracer tests. This activity also includes a calibration effort.

The activities are regulated by quality plan documents in accordance with SKB standards.

### **9.2.3 Tracer tests - Phase C**

In this phase of the Tracer Test Stage the focus is on retention. Hence the transport pathways are foreseen to be short (5-15 m) with varying range of transport times. Both single feature and multi-feature pathways are addressed. Retention is addressed full out with helium and the available suite of radioactive sorbing tracers. The latter include a selection of the weakly sorbing tracers utilised in the TRUE –1 experiments (Winberg et al., in prep). The tracers in question,  $\text{Na}^+$ ,  $\text{Ca}^{2+}$ ,  $\text{Rb}^+$  and  $\text{Ba}^{2+}$ , have also been tested extensively in the laboratory (Byegård et al., 1998).

The tracer tests are preceded by blind model predictions of selected tests using the developed models. In addition the semi-analytical evaluation framework for reactive transport utilised in the evaluation of the TRUE-1 experiments will be employed (Cvetkovic, et al., 1999, Winberg et al., in prep). The strategy for making use of available modelling tools is not decided at this point. The models used for predictions should all be updated using the Phase B data and associated updated models.

All four model concepts are used for evaluating the data from the Phase C tracer tests.

The activities are regulated by quality plan documents in accordance with SKB standards.

### **9.2.4 Evaluation and reporting**

The evaluation and reporting of the Tracer Test Stage is integrated with the overall reporting of the TRUE Block Scale project.

### 9.3 Schedule

A tentative schedule is presented in the Project Plan for the Tracer Test Stage (v. 1999-07-21). In this plan the time frames allocated for the identifies phases are presented in Table 9-1.

**Table 9-1 Tentative scheduling of TRUE Block Scale Tracer Test Stage in accordance with Project Plan (v. 1999-07-21)**

Remediation phase	July 19 '99 to Oct 01 '99
Phase A (incl. Predictions)	Aug 2 '99 to Feb 22 '00
Phase B	Jan 03 '00 to May 26 '00
Phase C (incl. Predictions)	May 29 '00 to Dec 08 '00
Evaluation/reporting (of project)	Nov 20 '00 to Dec 31 '00

## **10. Conclusions**

In the following section the important results of the Detailed Characterisation Stage are reviewed and some general conclusions are drawn;

### **10.1 Issues and Hypotheses**

An important component in the planning of the future Tracer test Stage has been the identification of important issues/questions, hypotheses formulated as plausible answers to the issues, to be tested by the filed tests. The issues are related to a) the conductive geometry of the studied fracture network, b) heterogeneity of the network, including the role of fracture intersections zones and intra-structure heterogeneity, and the possibility to differentiate the two, c) characteristic differences between breakthrough curves in a single fracture as opposed to that observed for a flow path involving a fracture network.

Of the three issues it is acknowledged that the expectancy of successful address of the hypothesis related to heterogeneity should be low given the geometry of the borehole array, and the interrelation between suitable sink and source sections for tracer tests.

### **10.2 Structural-hydraulic model**

The structural model has been refined during the stage with special emphasis on the rock volume planned to be used for tracer tests. The resulting model identifies two northwesterly structures, #20 and #13, as the dominant structures in this volume. Performed hydraulic testing has significantly reduced the hydraulic importance of the structure formerly identified as Structure #9. Instead, two NNW features, #21 and #22, supported by structural and hydraulic data are interpreted to account for the observed connectivity between Structures #13 and #20. The lateral extent of the various structures have been assessed on the basis of the hydraulic information. In addition, an additional NNW structure has been interpreted based on the hydraulic data, for which structural support is required. A new borehole is advocated for the purpose of verifying the reconciled March'99 structural-hydraulic model.

## 10.2 Instrumented array

On the basis of the performed verification tests focused on Structure #9, the instrumentation of boreholes KA2563A and KA2511A has been optimised for the purpose of performance of tracer tests. The focus is put on the fracture network made up of the NW structures #20 and #13, and the NNW features #21 and #22, interpreted to provide the connectivity between the former two structures.

## 10.3 Tracer test results

A series of pre-tests have been performed with the purpose of providing tracer dilution data which can cater to identification of suitable injection points for tracer. In addition tracer injections have been performed at four points while pumping in section KI0023B:P6. The results of the latter tests show breakthroughs from all four sections over an experimental time of approximately 20 days. The longest flow path from KA2563A:S1 (#19) showed very low recovery. Of the remaining three, one flow path from KA2563A:S4 (#20) showed a recovery of about 50%. The remaining two, from KI0025F02:P3 ((#13,#21) and KI0025F02:P6 (#22) show recoveries in excess of 75%. The latter two are expected to show essentially full mass recovery, had the tests been prolonged. The test results show that successful tracer tests can be performed in multi-structure flow paths in fracture networks in the block scale over distances of 15-40 metres. The noted mass recoveries also show that well controlled tests with radioactive sorbing tracers are feasible. It was recommended to drill another borehole to provide shorter transport paths within the studied fracture network.

## 10.4 Modelling

During the performed stage, a site scale fracture network model has been devised which incorporates the structural model of the TRUE Block Scale rock volume. The model has been used to ia. produce boundary conditions for models focused on the interior of the investigated block, including the volume designated for future tracer tests.

In addition, a stochastic continuum model has been developed which has been conditioned using existing transmissivity data, steady state head and transient drawdown data.

The developed PathWorks channel network model has been used to scope the potential for investigating fracture intersection zones (FIZ) using tracer tests and also to predict. The model was conditioned on the PT-1 through PT-3 tests and was subsequently used

to predict the PT-4 tracer test. A comparison between the predictions and the results of the field tests show both under- and overestimation of travel times. The same is also true for mass recovery.

## **10.5 Outlook on Tracer Test Stage**

A general conclusion is that the Detailed Characterisation Stage has constituted an important step in reconciling the observed hydraulic responses of the studied system with the developed structural model. The important message is that the majority of the important hydraulic responses can be explained by the underlying structural model.

Further, the feasibility of performing high quality quantitative tracer tests with an acceptably high mass recovery has been demonstrated in the results of the performed Pre-tests. The noted high mass recoveries also show that tests with radioactive sorbing tracers are feasible in the investigated fracture network.

## REFERENCES

- Byegård, J., Johansson, H., Skålberg, M. and Tullborg, E-L. 1998 : The interaction of sorbing and non-sorbing tracers with different Äspö rock types. Sorption and diffusion experiments in the laboratory scale. . Swedish Nuclear Fuel and Waste Management Co. SKB Technical Report TR-99-18.
- Carlsten, S. 1998 : Results form borehole radar measurements in KA3573A, KA3600F and G-boreholes. Swedish Nuclear Fuel and Waste Management Co. Äspö Hard Rock Laboratory Progress Report HRL-98-16.
- Cvetkovic, V., Selroos, J-O., and Cheng, H. 1999 : Transport of reactive solute in single fractures. *J. Fluid. Mech.*, vol. 318, pp. 335-356.
- Dershowitz, B., Foxford, T., and Eiben, T. 1998 : PAWorks Channel Network Model with LTG solute transport. User documentation version 1.5
- Winberg, A. (ed) 1996 : Descriptive structural-hydraulic models on block and detailed scales of the TRUE-1 site. Swedish Nuclear Fuel and Waste Management Co. Äspö Hard Rock Laboratory International Cooperation Report ICR 96-04.
- Winberg, A. 1997 : Test plan for the TRUE Block Scale Experiment. Swedish Nuclear Fuel and Waste Management Co. Äspö Hard Rock Laboratory International Cooperation Report ICR 97-02.
- Winberg, A. (ed) 1999 : TRUE Block Scale Project – Scientific and technical status – Position report prepared for the 2<sup>nd</sup> TRUE Block Scale review meeting. . Swedish Nuclear Fuel and Waste Management Co Äspö Hard Rock Laboratory International Progress Report IPR 99-07.
- Winberg, A, Andersson, P., Hermanson, J., Byegård, J., Cvetkovic, V., and Birgersson, L., (in prep) : Final Report of the First TRUE Stage. Swedish Nuclear Fuel and Waste Management Co. SKB Technical Report TR-00-XX.



## **APPENDICES**

**Appendix A Calculated shortest distances along multi-feature pathways, March'99 Structural Model**

<b>Shortest pathway lengths along TRUE Block Scale features, March '99 Structural Model</b>								
<b>Intersections</b>				<b>Lengths (m)</b>				<b>Total(m)</b>
<b>Feature</b>	<b>Borehole</b>	<b>Feature</b>	<b>Borehole</b>	<b>13</b>	<b>20</b>	<b>21</b>	<b>22</b>	
13	KI0023	to	20	KI0025	19.1	42.6	27.9	<b>89.6</b>
	KI0023		21	KI0025	19.1		76.5	<b>95.6</b>
	KI0023		22	KI0025	94.1		58.8	<b>152.9</b>
	KI0023		20	KA2563	19.1	11.8	29.4	<b>60.3</b>
	KI0023		21	KA2563	19.1		42.6	<b>61.7</b>
	KI0023		22	KA2563	94.1		116.2	<b>210.3</b>
	KI0023		20	KI0025F02	19.1	16.2	19.1	<b>54.4</b>
	KI0023		21	KI0025F02	22.1		1.5	<b>23.6</b>
	KI0023		22	KI0025F02	94.1		91.2	<b>185.3</b>
20	KI0023		13	KI0025	44.1	38.2	63.2	<b>145.5</b>
	KI0023		21	KI0025		1.5	110.3	<b>111.8</b>
	KI0023		22	KI0025		38.2	4.4	<b>42.6</b>
	KI0023		13	KA2563	114.7	38.2	63.2	<b>216.1</b>
	KI0023		21	KA2563		1.5	14.7	<b>16.2</b>
	KI0023		22	KA2563		35.3	42.6	<b>77.9</b>
	KI0023		13	KI0025F02	75.0	38.2	63.2	<b>176.4</b>
	KI0023		21	KI0025F02		1.5	29.4	<b>30.9</b>
	KI0023		22	KI0025F02		35.3	26.5	<b>61.8</b>
21	KI0023		13	KI0025	32.4		26.5	<b>58.9</b>
	KI0023		20	KI0025		41.2	1.5	<b>42.7</b>
	KI0023		13	KA2563	30.9		27.9	<b>58.8</b>
	KI0023		20	KA2563		11.8	1.5	<b>13.3</b>
	KI0023		13	KI0025F02	1.5		29.4	<b>30.9</b>
	KI0023		20	KI0025F02		17.6	1.5	<b>19.1</b>
22	KI0023		13	KI0025	44.1		107.4	<b>151.5</b>

	KI0023	20	KI0025		2.9		48.5	<b>51.4</b>
	KI0023	13	KA2563	105.9			107.4	<b>213.3</b>
	KI0023	20	KA2563		45.6		39.7	<b>85.3</b>
	KI0023	13	KI0025F02	75.0			107.4	<b>182.4</b>
	KI0023	20	KI0025F02		23.5		39.7	<b>63.2</b>
13	KI0025	20	KA2563	44.1	50.0		64.7	<b>158.8</b>
	KI0025	21	KA2563	32.4		42.6		<b>75.0</b>
	KI0025	22	KA2563	44.1			116.2	<b>160.3</b>
	KI0025	20	KI0025F02	44.1	23.5		61.8	<b>129.4</b>
	KI0025	21	KI0025F02	32.4		1.5		<b>33.9</b>
	KI0025	22	KI0025F02	44.1			91.2	<b>135.3</b>
20	KI0025	13	KA2563	38.2	41.2	26.5		<b>105.9</b>
	KI0025	21	KA2563		44.1	13.2		<b>57.3</b>
	KI0025	22	KA2563		2.9		54.4	<b>57.3</b>
	KI0025	13	KI0025F02	1.5	42.6	26.5		<b>70.6</b>
	KI0025	21	KI0025F02		42.6	1.5		<b>44.1</b>
	KI0025	22	KI0025F02		2.9		27.9	<b>30.8</b>
21	KI0025	13	KA2563	38.2		82.4		<b>120.6</b>
	KI0025	20	KA2563		11.8	113.2		<b>125.0</b>
	KI0025	13	KI0025F02	1.5		82.4		<b>83.9</b>
	KI0025	20	KI0025F02		16.2	108.8		<b>125.0</b>
22	KI0025	13	KA2563	51.5			4.4	<b>55.9</b>
	KI0025	20	KA2563		114.7		58.8	<b>173.5</b>
	KI0025	13	KI0025F02	22.1			4.4	<b>26.5</b>
	KI0025	20	KI0025F02		67.6		58.8	<b>126.4</b>
13	KA2563	20	KI0025F02	114.7	23.5		61.8	<b>200.0</b>
	KA2563	21	KI0025F02	38.2		1.5		<b>39.7</b>
	KA2563	22	KI0025F02	114.7			91.2	<b>205.9</b>
20	KA2563	13	KI0025F02	75.0	50.0		64.7	<b>189.7</b>

	KA2563	21	KI0025F02		11.8	30.9		<b>42.7</b>
	KA2563	22	KI0025F02		45.6		27.9	<b>73.5</b>
21	KA2563	13	KI0025F02	1.5		47.1		<b>48.6</b>
	KA2563	20	KI0025F02		17.6	14.7		<b>32.3</b>
22	KA2563	13	KI0025F02	76.5			116.2	<b>192.7</b>
	KA2563	20	KI0025F02		25.0		45.6	<b>70.6</b>
13	KI0023	20	KI0023	19.1	1.5	29.4		<b>50.0</b>
	KI0023	21	KI0023	19.1		26.5		<b>45.6</b>
	KI0023	22	KI0023	95.6			107.4	<b>203.0</b>
20	KI0023	21	KI0023		1.5	1.5		<b>3.0</b>
	KI0023	22	KI0023		35.3		41.2	<b>76.5</b>
13	KI0025	20	KI0025	32.4	42.6	26.5		<b>101.5</b>
	KI0025	21	KI0025	32.4		80.9		<b>113.3</b>
	KI0025	22	KI0025	44.1			58.8	<b>102.9</b>
20	KI0025	21	KI0025		42.6	107.4		<b>150.0</b>
	KI0025	22	KI0025		2.9		2.9	<b>5.8</b>
13	KA2563	20	KA2563	36.8	11.8	27.9		<b>76.5</b>
	KA2563	21	KA2563	38.2		35.3		<b>73.5</b>
	KA2563	22	KA2563	114.7			116.2	<b>230.9</b>
20	KA2563	21	KA2563		10.3	10.3		<b>20.6</b>
	KA2563	22	KA2563		45.6		45.6	<b>91.2</b>
13	KI0025F0 2	20	KI0025F02	1.5	16.2	26.5		<b>44.2</b>
	KI0025F0 2	21	KI0025F02	1.5		1.5		<b>3.0</b>
	KI0025F0 2	22	KI0025F02	75.0			91.2	<b>166.2</b>
20	KI0025F0 2	21	KI0025F02		16.2	26.5		<b>42.7</b>

	KI0025F0 2	22	KI0025F02		20.6		27.9	<b>48.5</b>
--	---------------	----	-----------	--	------	--	------	-------------

**Appendix B – Drawdown vs time divided by distance squared for the Pre-tests PT-1 through PT-3**

